SURFACE ENERGY OF CERAMIC MATERIALS

DCIC

DEFENSE CERAMIC INFORMATION CENTER

A Department of Defense information analysis center

A focal point in acquiring, evaluating, and disseminating authoritative, timely information about ceramic materials of interest to the Department of Defense, other Government agencies, their contractors, and their suppliers

DCIC REPORT 69-2
JUNE, 1969

103

DISCLAIMER NOTICE

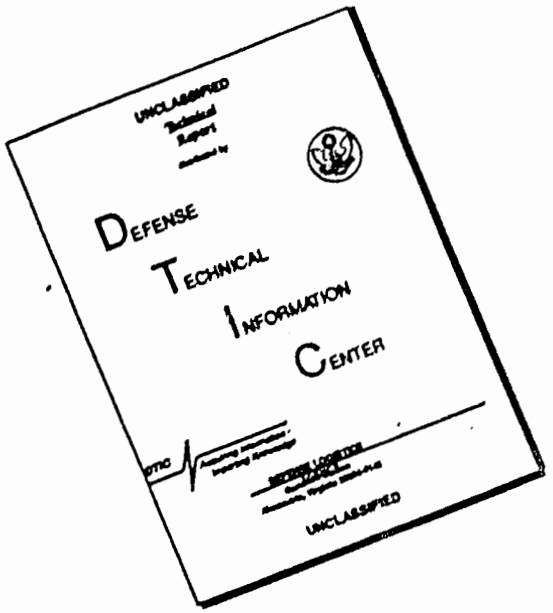

THIS DOCUMENT IS BEST QUALITY AVAILABLE. THE COPY FURNISHED TO DTIC CONTAINED A SIGNIFICANT NUMBER OF PAGES WHICH DO NOT REPRODUCE LEGIBLY.

DCIC

DEFENSE CERAMIC INFORMATION CENTER

MISSION

The Center collects, interprets, and disseminates technical information about ceramics for Department of Defense needs.

SCOPE

The Center's coverage and acquisitions, selected primarily on the basis of material composition, includes borides, carbides, carbon (graphite), nitrides, oxides, sulfides, silicides, and selected intermetallic compounds and glasses in the form of monophase and polyphase ceramic bodies, coatings, fibers, composites, and foams.

The subject fields include applications, property and performance data, processing and fabricating methods, testing methods, and fundamental aspects of processing and behavior of these materials.

SPONSOR

Air Force Materials Laboratory
Materials Support Division (MAAM)
Wright Patterson Air Force Base, Ohio

SERVICES

The services of the Center include answering technical inquiries, providing technical advisory services, and publishing data compilations, critical technical reviews, and news of recent developments.

QUALIFIED USERS

U. S. Government agencies, their contractors, suppliers, and others in a position to assist the defense effort.

ADDRESS

Defense Ceramic Information Center
Battelle Memorial Institute
Columbus Laboratories
505 King Avenue
Columbus, Ohio 43201
Telephone: Area Code 614, 299-3151
Extension 2758

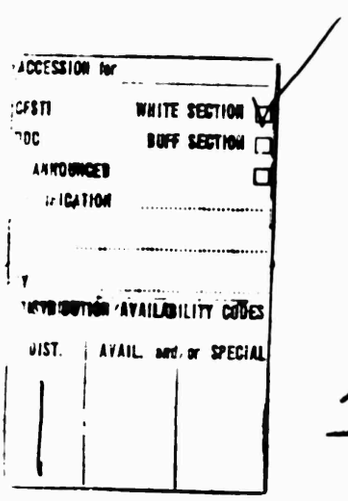

NOTICES

This document is approved for public release and sale; its distribution is unlimited.

[redacted]

DCIC Report 69-2
June, 1969

SURFACE ENERGY OF CERAMIC MATERIALS

Prepared by

Jules J. Duga

for the

Defense Ceramic Information Center
Battelle Memorial Institute
Columbus Laboratories
505 King Avenue
Columbus, Ohio 43201

ABSTRACT

The concepts, experimental techniques, and theoretical analyses of the surface energy of solid ceramic materials are reviewed with the aim of condensing a large mass of unrelated data into a concise form for comparison and evaluation. It is shown that various experimental methods can be applied to the measurement of surface energy, but, that each of these has certain limitations which are often unstated. Furthermore, it is shown that theoretical analyses and empirical correlations, while sometimes rather imprecise, can be used to approximate surface energies, particularly as functions of temperature. While a few materials have been discussed in considerable detail (such as MgO, Al_2O_3 and some alkali halides), a review of the literature notes that there is a great paucity of information on the surface energies of many solids of interest. Improvements and extensions of experimental and empirical techniques are suggested that will help to fill the voids in the present understanding of ceramic solid surfaces, and specific analyses of experimental methods are forwarded. It is shown in the report that the proper use of thermodynamic techniques offers considerable potential for the measurement and interpretation of solid surface energies of a large number of materials that are poorly understood at present. In addition, the further development of thermodynamic methods presents an opportunity to investigate solid surface energies of non-brittle materials, thus overcoming one of the basic limitations of the use of mechanical methods.

FOREWORD

This special report was prepared for the Defense Ceramic Information Center (DCIC) by Dr. Jules J. Duga, Associate Advisor, Physical Chemistry and Solid State Materials Division, Department of Chemistry and Chemical Engineering, Columbus Laboratories, Battelle Memorial Institute.

The author wishes to acknowledge the contributions from the following individuals: B. R. Emrich of the Air Force Materials Laboratory for his support and encouragement; Prof. J. A. Pask, University of California; Prof. Hayne Palmour, III, North Carolina State University; Dr. A. R. C. Westwood, Research Institute for Advanced Studies; and Dr. S. M. Wiederhorn, National Bureau of Standards, for their contributions to the literature search; and W. H. Duckworth and C. L. Downey of Battelle's Columbus Laboratories for their advice and editorial comments.

DCIC is operated by Battelle's Columbus Laboratories under U.S. Air Force Contract No. F33615-67-C-1472. The program is administered by the Information Branch (MAAM), Materials Support Division, Air Force Materials Laboratory, Wright-Patterson Air Force Base, Ohio.

TABLE OF CONTENTS

TABLE OF CONTENTS
(Continued)

LIST OF FIGURES

LIST OF FIGURES
(Continued)

LIST OF TABLES

LIST OF TABLES
(Continued)

I. INTRODUCTION AND SUMMARY

The surface energy of a solid is an important factor in many phases of science and technology, not only for itself but also through its marked influence on other physical properties. Since the earliest work of Griffith, in which the now famous "Griffith criterion" for crack propagation (i.e., for surface formation) was expounded, many researchers have attempted to use his concepts in describing the nature of fracture in brittle, semi-brittle or ductile materials. Moreover, numerous modifications to basic Griffith theory have been developed to account for deviations from the perfect cases, which are more easily treated.

During the past few years, efforts on the study of solid surface energies have increased, particularly as a by-product of basic research on fracture. While the preponderance of recent literature on the subject of solid surface energy is still devoted to considerations of the fracture process, the study of surface energy is increasingly being extended to numerous other areas of investigation. One of the most obvious applications lies in the theory of adhesion and the development of adhesive joints, which have tremendous potential, for instance, in airplane and automotive construction, in the fabrication of habitable dwellings, and in spontaneous cold-welding of components in high vacuum environments, such as outer space. Surface energy is an important factor in all studies of friction, lubrication, and wear; of coatings; of glass-to-metal seals; and many other areas of product development. Similarly, in process development the surface energy of a material will contribute, in part, to mechanisms of filtering, wetting, catalysis, sintering, epitaxial growth, any kind of joining or bonding, and crystallite and colloid morphology, including the size and shape of ultra-fine particles in smokes and other particulate pollutants. Furthermore, the role of the surface energy is a critical determinant in any surface treatment, such as cleaning, polishing, activation, or the like. The design of coupling agents for composite structures is an area of particular current importance in which surface energy is basic.

Inasmuch as the solid surface energy is a significant factor in many different fields of research and technology, and, in addition, since there is no collected work known to this writer which organizes the subject in any detail, the present state-of-the-art report was commissioned.

The concept of surface energy, from its basic definition through a discussion of general factors that affect measured values, is covered in some detail, and the relations between surface energy and other materials properties are explored.

From an experimental point of view, the report describes various techniques that have been devised for the determination of surface energy. These may be broadly classed in two categories: mechanical and thermodynamic. In the former, primary consideration has been given to the Griffith criterion for crack propagation and the extensions of this to a multitude of experimental arrangements. The fracture of a material is accompanied by the creation of fresh surfaces, and the simplest concepts show that the energy required to effect fracture is merely the product of the surface energy and the area of the newly exposed faces. This theory, with modifications, has been applied to the determination of surface energies in brittle materials, but is seen to be insufficient in materials with significant plasticity. Techniques based on the Griffith criterion have included single crystal fracture and crack propagation, determination of total stored elastic energy prior to failure in polycrystalline masses, measurements of total area created in crushing, the energy to effect drilling, and others.

Aside from the applications to single-crystal materials, most of these mechanical methods result in erroneous values of surface energy, generally too large as a result of not having corrected for plasticity, kinetic energy of resulting particles, friction effects, and the like.

Other mechanical methods have been devised for specific materials classes, such as the spontaneous bending of thin wafers of compound semiconductor crystals. In this case, a lack of inversion symmetry in the (111) direction of the crystal lattice serves to expose different "compositions" on opposite crystal faces, and a corresponding difference in surface tension produces a bending moment that may be interpreted in terms of these tension differences. In addition, analyses of unit cell dimensions of extremely fine particles provide a measure of the degree to which surface tensions act as body forces on the bulk of the sample, and the technique is found to apply where there are large surface area/volume ratios. Other determinations of surface energy have been made through the observation of the stretching of a heated fiber under its own weight or an applied force. It is presumed that gravitation effects will tend to elongate a fiber while surface tension forces tend to reduce the length. From the balance of forces that results, an estimate of the surface tension, as well as the effects of adsorbed impurities, may be ascertained.

Each technique is described in sufficient detail to provide familiarity, and each is criticized for its ranges of applicability and the reliability of the results obtained.

The crack propagation experiments are believed to be the most direct method of determining solid surface energies. Their major drawback lies in the range of temperatures over which they may be applied. Wherever dislocation maneuverability becomes appreciable, surface energy measurements are grossly affected, and complicated correction factors must be applied to the analysis. Hence, additional techniques must be supplied for the determination of surface energies over a wider temperature range. To this end, various methods are reviewed that involve the interaction between solids and liquids, these falling into the general category of thermodynamic techniques. The method showing the greatest potential for further development involves the determination of the critical surface tension for wetting of a solid. This method, originally applied to the wetting of low-energy organic materials, has been modified for certain high-energy solids and suggests that similar critical surface tensions can be measured. There are, however, two major difficulties in the interpretation of data. First, one must recognize that the critical tension for wetting is different from the solid surface energy by an amount equal to the spreading pressure of the candidate liquid on the solid, a term which may be difficult to evaluate. Second, it has been shown by various investigators that thermodynamic techniques will generally provide only a partial answer to the problem, this being due to the different types of interactions that are possible between dissimilar materials. In this case, it is necessary to determine critical tensions using various classes of liquids for a given solid, and the analysis tends to become quite involved.

In spite of these difficulties, thermodynamic techniques (including heats of immersion, heats of solution, solubility rates, and the like) offer considerable promise through their applicability to materials at elevated temperatures. While the most reliable mechanical methods may be applied only to complete brittle materials, the thermodynamic methods can, in principle, be utilized up to the melting point of the specimen.

The theory of solid surface energies is discussed from essentially two points of view, with different degrees of sophistication in each. The most detailed work on first-principles calculations of surface energy is considered, where much of the effort has

been directed toward materials which crystallize in the simple cubic structure, such as the alkali halides. Calculations are highlighted in which consideration is given to the electrostatic forces between ions, the effects of surface relaxation, and deformation of the lattice due to thermal oscillations. In addition to the detailed formulation given for the alkali halides, simpler approaches have been used for the estimation of surface energies of several chalcogenides and oxides.

Various techniques have been proposed for the estimation of surface energy of solids based upon correlations with other physical properties. While one method suggests comparison of surface energies with mechanical properties such as hardness, recrystallization temperature, and elastic modulus, to name a few, other methods are based on the comparison with thermodynamic and structural data, including heats of formation, critical temperatures, crystal structure, and the like. To make full use of these correlative approaches, it is necessary to obtain information on the surface tensions of molten ceramics and their temperature dependencies. To this end, the scope of the report is expanded to include such data on the liquid state, where applicable.

The report includes tabulation of surface energies for many different materials (with many common minerals), and reports most measured values, with appropriate comments regarding the reliability of the results. In addition, data on several different types of glasses are combined in separate tables, although no major effort is expended to evaluate this information.

Finally, recommendations are made regarding the direction in which future research should be directed to the determination of surface energies of ceramic materials.

II. SCOPE

While the surface energy is an important parameter in a number of different fields of interest, as indicated in the previous section, certain limitations must be placed on the scope of materials to be considered in this present review. Firstly, we shall be concerned only with ceramic materials (i.e., nonmetallic inorganic materials). A number of research programs have been devoted to the determination of surface energies of metals, many through the use of scratch-smoothing, grain-boundary grooving, sintering, and similar techniques. A complete analytical compendium of the solid surface energies of metals is definitely needed, but this subject is beyond the scope of this report.

Furthermore, much work has been done on organic materials, particularly by Zisman[1] and his co-workers, but this subject is similarly omitted from this review. However, some of Zisman's techniques are applicable to ceramic materials and consequently, this report will consider some of the organic materials with which he has been concerned, but solely for illustration.

Secondly, little space will be given to the discussion of the surface tension of molten ceramics or glasses. It is well-recognized that the surface tension of glasses and slags has important technological implications, including the applications to glass molding, enameling, glass-to-metal seals and other areas; however, the material presently available is quite voluminous (with many major contributions from the Russian literature) but so unrelated that no detailed review is possible at the present time. To collect the data without some semblance of a connecting thread would be inconsistent with the aims of the present report. Such a compilation will be left to future reviews*.

There are, to be sure, several materials that are expected to fall within the scope as defined here and for which no values of surface energy are available except in the liquid state (primarily alkali metal compounds). The inclusion of such data here will be seen to be consistent with the scope of the report when discussions on correlation techniques begin.

There will, in addition, be some reference to the work on selected molten ceramic systems, particularly where it is believed that the use of critical contact angle data will provide information relative to the surface energy of certain solids. Several glass systems suggest themselves as being suitable for this application, and mention of these and their role in the determination of solid surface energies will be made at the appropriate places.

Two very important aspects of the surface-energy determinations have also been omitted from this report: namely, surface preparation techniques and surface area determinations. The first of these constitutes a major report in itself, being comprised of complicated procedures and analytical techniques. The preparation of a surface for detailed structural, physical and chemical studies is not necessarily directed toward the attainment of a clean surface so much as it has the aim of obtaining a characterized surface. Although clean surfaces are highly desirable in fundamental studies of interface reactions, the characterized surface provides a more direct means of analyzing effects at real interfaces.

*There are several early reviews on the surface tension of molten glasses, as noted by Parikh[2]. The reader is referred to these [3,4] for general details.

Surface area determinations have similarly been omitted from detailed consideration here, although it is necessary to have such information available. This is particularly true in those cases where fine particle distributions are required in surface energy measurements, such as by solubility rates and heats of immersion. Quite generally, the surface area can be measured by adsorption techniques, usually employing nitrogen gas where interactions other than physical adsorption are generally negligible. Surface measurement methods have recently been reviewed by Kantro et al.[5]

III. THE CONCEPT OF SURFACE ENERGY

III-1. Basic Definitions and Distinctions

There are several ways to view the concept of surface energy, depending upon the degree of detail required and whether interest is theoretical or practical. For a basic qualitative picture, we may first consider a perfect crystal in an evacuated chamber in equilibrium with its own vapor. The atoms in the bulk of the crystal are surrounded on all sides by other bulk atoms and are in an equilibrium configuration that can be readily determined by well-known x-ray techniques.

At the surface of this perfect crystal, such an arrangement is not generally maintained. The surface atoms interact with only half as many atoms as do bulk atoms and, as a consequence, the surface lattice is somewhat distorted; a certain energy must be applied if this distortion is to be eliminated. The solid surface energy is the energy required to restore the bulk lattice configuration at the surface of a perfect crystal. It is always greater than zero.

A similar concept is surface tension (the force tending to reduce the area of a surface in equilibrium with its vapor), more commonly considered in discussions of the properties of liquids. Under certain conditions, surface tension and surface energy are equal, although a rigorous thermodynamic treatment is required to delineate the conditions of equivalence clearly. One of the more important conclusions of such a treatment is that not only can the surface energy and surface tension be different, but the surface tension can be negative[6] (in anisotropic cases). Specific examples of the difference between surface energy and surface tension of solids will be given in Section V-1.

The details of the argument regarding the differences between surface energy and surface tension of solids are not necessary to this review. Perhaps the most critical review and exposition has been given by Johnson[7], with further discussion by Gregg[8]. In the rest of the text, little distinction will be made between tension and energy. In general, this decision will not affect the interpretation of experimental techniques and measurements. Where confusion might arise (for example, in the discussion below regarding the thermodynamics of surfaces and interfaces), surface tensions will be denoted by Γ while surface energies are given as γ. Where the two are equivalent, particularly with liquids, γ is used.

III-2. Factors Affecting the Ideal Surface Energy

In the preceeding paragraphs, we considered only the case of nearly perfect crystals that might be studied in the laboratory and neglected the more "practical" types of morphologies encountered in ceramic technology. The reasons for this are rather straightforward; it is generally easier to measure, interpret and analyze the experimentally observed behavior of simple, pure structures rather than become involved in a number of additional variables that are often poorly specified. In fact, throughout this report major emphasis has been placed on high-quality well-characterized materials rather than on the so-called "engineering" materials.

In view of this situation, we should consider, in rather broad terms, the nature of the differences to be expected between the types of information obtained with pure single crystals as opposed to polycrystalline masses and other material conditions, particularly with regard to experimental observation. First, as will be discussed later, the surface energy of a crystal is not a unique quantity but varies rather widely for different crystal orientation. Hence, in a polycrystalline material with many different crystal faces exposed, the measured surface energy will be a weighted average of the spectrum of values realizable for the specific material.

Further complicating the theory of a heterogeneous sample face are the contributions from exposed grain-boundary traces, where the grain-boundary energy is difficult to isolate, although it is usually intermediate between the surface energies of the juxtaposed faces at the boundary; however, exceptions to this are quite important.

Various extrinsic factors also affect the ideal surface energy, the most common of which is the adsorption of extraneous phases from a surrounding atmosphere. For example, a freshly cleaved surface will rapidly reduce its surface energy by adsorbing gaseous species. Such contamination is one of the factors that can prevent easy "repair" of a fresh break by simply remating the exposed fracture surfaces (surface rearrangement due to surface tension also makes repair difficult).

In addition, "real" materials pose an important impurity problem. In certain systems, these impurities are surface active, that is, they tend to concentrate at surfaces and interfaces (grain boundaries) and lower the surface energy. While high-purity materials may be available in the laboratory, processing steps can introduce impurities in the final product, and significant differences in surface energy can result. Furthermore, as mentioned above, in all materials (of both scientific and technological usage) atmospheric impurities reduce the practical surface energy, not only through adsorption but often through chemical reaction.

We also note that temperature affects the solid surface energy of any body, both intrinsically and extrinsically. The intrinsic value of surface energy is temperature dependent, partly because of configurational changes caused in the crystal lattice. Secondly, an extrinsic factor arises in consideration of the equilibrium adsorbate pressures, also temperature dependent. As the temperature increases and the degree of surface coverage decreases, a "cleaner" surface is exposed, which has a higher surface energy than the "dirty" surface.

III-3. Relation of Surface Energy to Other Material Properties

From purely qualitative reasoning, it appears that the surface energy of a solid could be correlated with other physical properties if we give a more detailed description of the energy concept. Some of these correlations are introduced below.

Since the analysis of fracture mechanics is important in the measurement of surface energy (as will be discussed in Section IV), it is necessary to consider the conditions necessary for an applied force to propagate a crack. Quite simply, the basic Griffith criterion for crack propagation stems from an energy-balance relationship in which the energy required to extend a crack is balanced by the increased energy of the two fresh surfaces created. Griffith considered the two-dimensional case of an idealized elliptical crack in an isotropic elastic material. By calculating the rate of decrease

in strain energy associated with the growth of the crack under stress and equating this to the rate of increase of surface energy, he derived the relation

$$\sigma = \sqrt{\frac{4E\gamma}{\pi c}}, \tag{1}$$

where σ = minimum applied stress required for crack growth
E = Young's modulus
γ = surface energy
c = length of ideally grown crack

Similar treatments have been given to ellipsoidal cracks, surface cracks, and the discrete nature of the crystal structure. In general, it is found that

$$\sigma = k\sqrt{E\gamma/c}, \tag{2}$$

where the geometry factor, k, can vary between 0.8 and 1.3.

A major limitation of such straightforward models is associated with the value chosen for c, which can be interpreted in different ways. In a review of the brittle behavior of glasses, Mould[9] discussed the effect of stress concentration on the propagation of a crack and showed that for a surface crack of depth, c, and tip radius, ρ, the maximum stress, at the tip, is greater than the applied stress by a factor of $2\sqrt{\frac{c}{\rho}}$. It follows that the minimum applied stress for growth, σ, and the ultimate stress, σ_m, are related by

$$\sigma = \frac{1}{2}\sigma_m\sqrt{\rho/c}\ . \tag{3}$$

This is equivalent to Equation (1) if

$$\frac{\sigma_m\sqrt{\rho}}{2} = \sqrt{\frac{4E\gamma}{\pi}}\ . \tag{4}$$

Several researchers investigating fracture in ceramic materials have concluded that the definition of the tip radius, ρ, affects the determination of γ. A major limitation of fracture energy measurements and their application to surface energy determinations relates to the uncertainty of assigned values of ρ, which, in turn, relates to considertions of partial plasticity, effective values of ρ, and similar perturbations. In a recent review, Stokes[10] delved into questions associated with the definition of brittleness, semibrittleness and ductility, and discussed dislocation mobility and maneuverability in various crystal systems. Major corrections to the values of ρ are necessary whenever a material is sufficiently ductile to result in a plastically deformed zone around the crack tip. Otherwise, such zones (and the corresponding work to produce these zones) result in a larger apparent value of the surface energy.

In most materials with a brittle-to-ductile transition, it has been observed that the transition temperature can depend on the experimental conditions, particularly the magnitude of impulse or strain rate imparted to the specimen. For sufficiently small impulses, a material can behave in a ductile, plastic manner, while large impulses (at the same temperature) will produce catastrophic failure. It is therefore important to

recognize that fracture-surface energy measurements and interpretations must consider the relative ductility at particular temperatures. As will be seen in later comparisons of data, for KCl, for instance, plasticity effects are readily observed in various materials and these are reflected in the values of surface energy that result.

At this point, we should also consider the concept of surface energy as it applies to the thermodynamics of wetting and adhesion, inasmuch as experimental tools related to these phenomena have been proposed. One of the more complete, yet straightforward, descriptions of these interface characteristics has been forwarded by Sharp and Schonhorn[11], who use the following approach.

In an equilibrium closed system of a liquid, L_2, in contact with a plane surface of an isotropic solid, S_1, (completely insoluble in L_2) and with the saturated vapor V_2^o of the liquid, the Young-Dupre equation may be written as

$$\Gamma_{S_1V_2^o} - \Gamma_{S_1L_2} = \Gamma_{L_2V_2^o} \cos\theta. \tag{5}$$

where the Γ's are surface tensions between the phases denoted by the subscripts and θ is the liquid-solid contact angle. For an equilibrium situation, the surface tensions are replaced by free energies, which yields:

$$\gamma_{S_1V_2^o} - \gamma_{S_1L_2} = \gamma_{L_2V_2^o} \cos\theta, \tag{6}$$

where the γ's are the surface free energies.

From purely qualitative considerations, if the new solid surface is completely devoid of adsorbed species, it follows that the maximum reversible work of adhesion takes the form

$$W_{adh} = \gamma_{S_1^o} + \gamma_{L_2V_2^o} - \gamma_{S_1L_2}, \tag{7}$$

where the first two terms refer to the new surface created by a complete separation of the interface and the last term represents the work "lost" when the interface is destroyed. Eliminating $\gamma_{S_1L_2}$ from Equations (6) and (7) permits writing the combined expression

$$W_{adh} = (\gamma_{S_1^o} - \gamma_{S_1V_2^o}) + \gamma_{L_2V_2^o}(1 + \cos\theta). \tag{8}$$

We note here that a smaller work of adhesion, W'_{adh}, results if the solid retains an adsorbed layer of the vapor V_2, whence

$$W'_{adh} = \gamma_{L_2V_2^o}(1 + \cos\theta). \tag{9}$$

If, now, one assumes a reversible work of cohesion of the liquid that is merely the work required to create two new liquid surfaces (without molecular surface rearrangement), we have

$$W_{coh} = 2\gamma_{L_2V_2^o}. \tag{10}$$

It now follows that for $\theta = 0$ (that is, complete spreading of a drop on a solid surface), then $W_{adh} - W_{coh} = \gamma_{S_1}^{o} - \gamma_{S_1 V_2}^{o}$ and the work of adhesion is greater than the work of cohesion of the liquid.

Sharpe and Schonhorn extended the argument to the case in which the liquid of the above example is allowed to solidify (without introducing interfacial stresses) and again concluded that the work of adhesion is always greater than the work of cohesion of the weaker of the two materials.

The line of reasoning developed here assumes that the conclusions are valid when solidification occurs after joining the materials. These authors also argue, without specific substantiation, that the same results will obtain if there is solidification before joining. In that case many additional parameters must be considered in detail.

From this treatment, it can be deduced that where there is intimate contact between two dissimilar, distinct and immiscible solid materials, the joint so formed will always fail cohesively, rather than by a breaking of the interfacial bond. Bikerman's qualitative statistical model[12], as well as detailed studies on van der Waals forces in gases tend to support this thermodynamic conclusion. However, the application of this conclusion to real systems requires that many other factors be included, such as miscibility, compound formation, surface texture, interfacial strains, and others.

It has been shown that if the liquid, L_2, spreads on a solid, S_1, then the work of adhesion is greater than the work of cohesion. Conversely, Sharpe and Schonhorn[11] point out that if the work of adhesion of L_2 to S_1 is greater than the work of cohesion of L_2, then L_2 must spread on S_1. From above we can write

$$W_{adh} - W_{coh} = \gamma_{S_1}^{o} - \gamma_{L_2 V_2}^{o} - \gamma_{S_1 L_2} = S, \tag{11}$$

where S shall be considered as the (initial) spreading coefficient.

In the study of the spreading of organic liquids on various substrates, Zisman[1] observed that, for a homologous series of liquids, a linear relation could be established between the contact angle and the liquid surface tension, such that

$$\cos \theta = a - b\, \gamma_{LV}^{o}, \tag{12}$$

provided that $\gamma_{LV}^{o} > \gamma_c$, a critical surface tension, the significance of which will be pointed out below. The contact angle vanishes for $\gamma_{LV}^{o} = \gamma_c$, and we can then write

$$\cos \theta = 1 + b\,(\gamma_c - \gamma_{LV}^{o}). \tag{13}$$

If the term $\Gamma_{S_1}^{o} - \Gamma_{S_1 V_2}^{o}$ in Equation (8) is disregarded, and $\cos \theta$ is eliminated between Equations (8) and (13), a quadratic relation results:

$$W_{adh} = (2 + b\gamma_c)\gamma_{LV}^{o} - b\gamma_{LV}^{o\,2}, \tag{14}$$

which, following Zisman, shows a maximum in W_{adh} when

$$\gamma_{LV_o} = \frac{1}{b} + \frac{\gamma_c}{2} \quad . \tag{15}$$

Zisman concluded that experiments on determination of γ_c, the critical surface tension for wetting, can be used to determine maximum adherence, even if the solid surface energy is not known. The applications of Zisman's techniques and arguments will be pointed out in the following section.

Before leaving the thermodynamic arguments and definitions, one final point or critique should be emphasized. Throughout the above discussions, the thermodynamic relations among the various surface energies and the considerations of different surface phenomena, including wetting, spreading, contact angles, adhesion, etc., are assumed to be quite general and applicable to the study of interactions between all different types of materials. That such may not be the case has been argued quite strongly by Weyl[13] and Fowkes [14, 15], where they have suggested that the total surface energy should be divided into various components. Different types of interactions are well known to contribute to the total surface energy of a given material, depending upon the nature of that material. Van der Waals forces, Coulombic forces, metallic bonding, hydrogen bonding, dispersion forces, and the like can each contribute (to one degree or another) to the total surface energy, and similar forces contribute to interfacial interactions between contiguous dissimilar materials. The basic argument suggests that, in a system where two materials interact, consideration should only be given to forces common to both materials. That is to say, for example, that dispersion-force contributions might well be included in a discussion of the interface between a metal and a polymer, but that the metallic component of the metal bonding should be disregarded, inasmuch as there is no counterpart in the other partner. Hence, one should re-evaluate the conclusions regarding so-called general rules of wetting and spreading.

As a consequence, some basic questions might arise in the ensuing discussions of experimental techniques for the determination of the solid surface energy, inasmuch as some of them use, as a tool, the interaction between two dissimilar materials. It is possible, of course, to circumvent some of these difficulties or, in fact, to turn them into advantages by the proper choice of a number of different materials.

IV. EXPERIMENTAL TECHNIQUES

IV-1. Summary of Experimental Techniques

In general, the available techniques for measuring solid surface energy are divided into two broad classes: mechanical and thermodynamic. But it must be pointed out, as will be shown in the following text, that the values obtained by different methods will not necessarily be the same. Moreover, the use of two different thermodynamic techniques can yield different results. This can be demonstrated by the following argument.

It was shown earlier that the total surface energy of any material is a result of partial surface energies arising from different types of interactions. Furthermore, the available evidence indicates that when two materials interact by surface forces, only similar components of the surface energy contribute to the total interfacial energy of the system. These concepts can now be applied to two examples of experimental methods for determining the surface energy of solids; the extreme mechanical case of a crack propagated in a completely brittle material, and the thermodynamic case of a solid brought into contact with a sessile drop of a high-energy (nonspreading) liquid.

In crack propagation, the freshly created surfaces were in contact with each other in the same material. Since the total surface energy of each of these two surfaces must be equal, it follows that the surface energy calculated from the experimental data must represent the total surface energy of the solid.

On the other hand, if the surface energy of the solid is considered as the sum of individual contributions, say $\gamma_S = \gamma_S(1) + \gamma_S(2) + \gamma_S(3) + \gamma_S(4)$, and the surface energy of the liquid is comprised of only two components, say, $\gamma_L = \gamma_L(2) + \gamma_L(4)$, then the interfacial energy determined by the sessile drop technique will only be $\gamma_{SL} = \gamma_{SL}(2) + \gamma_{SL}(4)$. This argument shows that the sessile drop or other thermodynamic methods require not only a detailed study of the solid surfaces in question, but also a detailed study of the liquids used as the experimental tools.

Returning to the mechanical techniques for surface energy determination, crack propagation methods have been shown to be most suitable for brittle materials; but additional terms enter the analysis when ductility becomes significant at elevated temperatures. Part of this difficulty can be overcome by using high strain-rate methods, although kinetic energy of the separated parts (in a double cantilever experiment) should be included in the calculations. These comments generally apply to other mechanical methods.

While the thermodynamic techniques seem to offer the greatest potential for application to all types of solids over wide temperature ranges, there are limitations above and beyond those pointed out immediately above. The proper choice of liquid systems with which to work (as in sessile drop experiments) is generally difficult, particularly for high-temperature applications. Even small amounts of impurities (especially the so-called "surface-active" impurities) must either be avoided or taken into account to realize the near-equilibrium conditions required. Furthermore, if the substrate dissolves or the liquid diffuses into the solid to an appreciable degree, the thermodynamic analysis will be invalid, at least in the present state of development. Some of these

restrictions are not quite so severe when solubility and/or heat of solution methods are used to assess the solid surface energy.

Table 1 summarizes the more common experimental techniques for determining solid surface energy, and points out the areas of applicability and the major difficulties encountered in using them. As the following discussions will show, each method suggested for the determination of surface energy has several restrictions that must either be eliminated or accounted for in the evaluation of experimental parameters. Where extraneous factors affect the measured quantities, the necessary correction factors can be so large they practically swamp the factors sought, and problems inherent in subtracting large numbers to obtain small differences arise.

One of the better reviews of the early techniques for determining surface energies was given by Partington[16], where some discussion was directed toward historical data and the evolution of the significance of the surface energy. Although the data included by Partington are not nearly as well defined as those available from later work, his review provides a reasonable perspective for viewing later results.

More recently, Bikerman[17] investigated the measurement of solid surface energies and drew the conclusion that nothing provides reliable values of this devious quantity, provided that it does indeed exist. It is of interest here to note two of Bikerman's quotations. First, it will be shown in the following sections that cleavage techniques appear to result, when properly interpreted, in values of the surface energy of brittle solids that agree reasonably well with theoretical values. Of this, Bikerman notes that "...it appears that the fracture methods ... not only yield improbable results but are devoid of any theoretical foundation....." Second, after discussing other experimental techniques, Bikerman closes with the comments "...this review does not answer the question whether surface energy analogous to that existing in liquids exists in solids but, in the literature, no experiment could be found which would necessitate an affirmative answer. Perhaps the reader of this review will be able to invent such an experiment...".

In many respects, one has to agree with the attitude taken by Bikerman regarding the state of the art of measurement and interpretation of surface energies of solids. The techniques described below all leave something to be desired. Moreover, it should become apparent that the actual experiments depend critically on the definition of surface energy and, therefore, the interpretation of each experiment can be open to question.

While Benson et al. made their major contributions in the theoretical calculation of surface energies (particularly of the alkali halides), their recent review article[18] goes to some length in describing various experimental methods that may be used to determine surface energies.

Techniques have been proposed to measure surface energy other than those discussed in this review, including adherence tests, which are purported to be reliable. As a word of caution, this reviewer points out that extreme care must be used in the application of adherence tests to the determination of the surface energy, inasmuch as it is presumed that complete characterization of the physical and topographical nature of the pertinent surfaces and interfaces is available. It is the opinion of this writer that no simple tests of adhesion have been developed to the point where fundamentally reliable information can be extracted from the experimental operation.

TABLE 1. SUMMARY OF PRINCIPAL EXPERIMENTAL TECHNIQUES FOR DETERMINING SURFACE ENERGY

Method	Advantages	Limitations
Mechanical		
(1) Crack propagation	Measures total surface energy; can determine effect of adsorbate pressure and/or coverage; best applied at low temperature	Analysis applies strictly only to completely brittle materials; inapplicable at elevated temperatures; interpretative difficulties arise with plastic flow, crack branching[126], polycrystalline material
(2) Strain energy release	Essentially same as (1). Somewhat more applicable to polycrystalline bodies, giving averages.	Same as (1); difficulty in separating transgranular from intergranular components
(3) Crushing	Same as (1)	Must include kinetic energy terms in analysis; complicated contributions from size dependence; "frictionless" apparatus required
(4) Drilling	Same as (1)	Same as (3)
(5) Bent wafer	Accurate determination of surface tension difference; simple calculation of adsorbate effects.	No absolute values; only applicable to materials with particular features
(6) Fiber stress	High-temperature determinations of ductile materials; believed to measure total surface energy; can be used for adsorbate effects; generally applicable to amorphous structures	Analysis questionable; spurious contributions from grain-boundary sliding in crystalline materials
Thermodynamic		
(7) Contact angle	Can be used at elevated temperatures and on ductile materials; nondestructive	Analysis results in only partial surface energy; complicated choice of several homologous liquids required; "homologous series" poorly defined; solubility and compound formation possible
(8) Heat of immersion	Same as (7)	Same as (7); contributions from many different surfaces; edge and corner effects; difficult temperature measurements, especially at elevated temperatures
(9) Heat of solution	Avoids final interface contribution if dissolution is complete	Same as (7); size effect enters calculations; totally destructive
(10) Dissolution	Can determine magnitude of size effect	Same as (7); difficulties in recovering undissolved fraction for particle size analysis

IV-2. Mechanical Methods

IV-2.1. Crack Propagation

As discussed in the reference to the Griffith criterion, brittle fracture provides one of the more popular experimental techniques for determining the surface energy of solids. While many authors refer to the early work on mica by Obreimov[19], the more recent developments by Gilman[20] set the stage for increased activity in solid surface energy experiments. The method of Gilman will be reviewed, including extensions derived by Westwood et al[21].

The system studied consists of a specimen of cross-section dimensions, w and 2t, with a crack of length, L, as shown in Figure 1. A force, F, is applied to the two halves of the crystal, which can then be treated as two cantilever beams, and the force required to propagate the crack is measured. Gilman neglected elastic anisotropy in the analysis, with the exception of the choice of elastic moduli values.

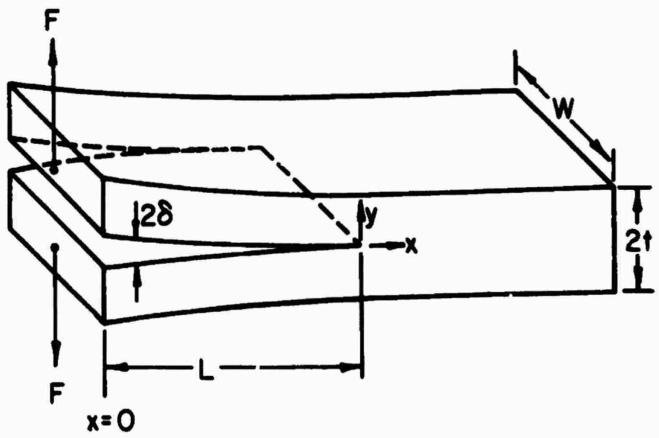

FIGURE 1. SCHEMATIC DRAWING OF THE CLEAVAGE OF A CRYSTAL[20]

With the physical model described in Figure 1, the cantilever beams have a moment of inertia $I = wt^3/12$. Applying the force, F, at x = 0 results in a bending moment M(x) = Fx in each beam and a strain energy, U, in each beam,

$$U = \frac{1}{2EI}\int_0^L M^2(x)dx = \frac{F^2L^3}{6EI} \quad . \tag{16}$$

Furthermore, the deflection, δ, of the beam (along the line y = 0, the so-called "neutral" plane in each beam) will be

$$\delta = \frac{Fx^3}{6EI} - \frac{FL^2x}{2EI} + \frac{FL^3}{3EI} + \frac{Ft^2(L-x)}{8GI} \quad , \tag{17}$$

where the first three terms are due to bending and the last is a contribution from shearing. E and G are the Young's and the shear moduli, respectively. Gilman argued that the contribution from shearing will usually be small enough that the last term of Equation 17 can be neglected and the deflection curve is taken as

$$\delta = \frac{F}{6EI}(x^3 - 3L^2x + 2L^3) \quad . \tag{18}$$

We must now consider the various contributions to the energy of crack propagation. As a crack propagates under the action of the force, F, the cantilever beams are put into motion, thus creating a kinetic energy term. The mass of an incremental volume in one of the cantilevers is $\rho wtdx$, where ρ is the density, and the beam moves with velocity $d\delta/dt$; thus the kinetic energy is $dT = \frac{1}{2}\rho wtdx(d\delta/dt)^2$. The total kinetic energy of the cantilever is

$$T = \frac{\rho wt}{2}\int_0^L \left(\frac{d\delta}{dt}\right)^2 dx \quad . \tag{19}$$

Now $d\delta/dt = (d\delta/dL)(dL/dt) = (d\delta/dL)v_c$, where v_c is the crack velocity. Substitution and integration yield

$$T = 12\,(v_c/v_s)^2\,(L/t)^2U \quad , \tag{20}$$

where $v_s = (E/\rho)^{1/2}$ = velocity of sound. For specimens where L/t is about 10, the kinetic energy is small compared with the strain energy unless the crack velocity exceeds about $v_s/100$.

If, now, we turn to the energy balances that obtain during the slow reversible extension of a crack, the work done (dW) when a crack increases its length (dL) must be equal to the increase in strain energy (dU) plus the energy of the newly created surfaces (dS), i.e., $dW = dU + d\gamma$. Since $dW = Fd\delta_o = (F^2L^2/EI)dL$ and $dU = (F^2L^2/2EI)dL = dW/2$, if $dS = \gamma wdL$, it follows that

$$\gamma = 6F^2L^2/Ew^2t^3 \quad , \tag{21}$$

which is the equation derived by Gilman for the measurement of surface energies. This is expected to be a minimum value, measured under reversible conditions, and should provide a direct determination of the intrinsic surface energy. When cracking is accompanied by irreversible phenomena (including plasticity near the crack tip), the measured value should reflect these additional factors and would be larger.

Gillis[22], and Westwood and Hitch[21] discussed the Gilman approach in some detail, noting that difficulties in interpretation arise for certain values of L/t. In partially ductile materials, large values of L/t give rise to plastic deformation terms that increase the apparent surface energy. Furthermore, for small L/t shearing forces are more pronounced at the crack tip, and erroneous surface energies again result.

Again assuming the geometry of Figure 1, but now following Westwood and Hitch's methods, the deflection at the crack opening is taken to be

$$\delta_o = (FL_o^3/3EI) + (\alpha FL_o t^2/4GI) \quad , \tag{22}$$

where the second term (omitted in the preceding discussion) represents the contribution from shearing forces. The factor, α, is a constant determined by the boundary conditions in the vicinity of the crack tip, and, as before, G is the shear modulus. Following the same arguments concerning the energy balance at the instant of crack propagation, it follows that

$$\gamma w = \frac{F}{2}\frac{d\delta_o}{dL} \quad . \tag{23}$$

Taking the derivative of Equation (22) and combining that with Equation (23) yields

$$\gamma = \frac{6\,F^2L^2}{Ew^2t^3}\left[1 + \frac{\alpha E}{4G}\left(\frac{t}{L}\right)^2\right] , \tag{24}$$

or

$$\gamma = \frac{6F^2L^2}{Ew^2t^3}\,(1 + C_s) , \tag{25}$$

where the correction term, C_s, includes contributions from end effects and shearing forces. For $\alpha \approx 0.1$ and $L > 3t$, C_s is $<<0.01$ and, as in Gilman's report, may be neglected. However, for very short cracks ($L < t$), C_s becomes quite important in the analysis. Westwood and Hitch's work on KCl shows that the proper interpretation of the data requires that C_s be considered.

If, now, one refers to γ_A as an "apparent" surface energy ($6F^2L^2/Ew^2t^3$), then Equation 24 can be rewritten as

$$\gamma_A^{-1} = \gamma^{-1} + \left(\frac{\alpha E}{4\gamma G}\right)(t/L)^2 \tag{26}$$

Plotting γ_A^{-1} vs. $(t/L)^2$ should then permit a direct measurement of γ^{-1} and, from the slope of the line, the value of α. The value of γ so calculated is that which would be expected from elementary beam theory.

In other work, Westwood and Goldheim[23] showed that with long beams, erroneous values of γ can be resolved (at least qualitatively) in terms of the plastic relaxation at the crack tip, even for the reasonably ductile materials they investigated.

A somewhat more detailed calculation of crack velocities and crack accelerations has been given by Berry[24], in which the surface energy may be determined from the relations:

$$V_L = \frac{v_s\tau}{2L\sqrt{3}}\left(1 - \frac{L_{cr}}{L}\right)\left(1 + \frac{2L_{cr}}{L}\right)^{1/2} \tag{27}$$

$$a_L = \frac{v_s^2\tau^2}{12L^3}\left(1 - \frac{L_{cr}}{L}\right)\left(\frac{5L^2_{cr}}{L^2} - \frac{L_{cr}}{L} - 1\right) \tag{28}$$

where

v_L = crack velocity

a_L = crack acceleration

v_s = velocity of sound in the medium

L = length of crack at time, τ

L_{cr} = critical crack length = $\left(\frac{E\gamma w^2 t^3}{6F^2} \right)^{1/2}$.

The other symbols were defined earlier. In an application of these relations, Wiederhorn[25] has shown that rather precise values of the surface energy may be obtained under a variety of experimental conditions.

In the preceeding discussion, qualitative consideration has been given to the effect of adsorbed impurities on the measured value of surface energy. That adsorption should play such a significant role is clearly pointed out for the case of mica ($K_2O.3Al_2O_3.6SiO_2.2H_2O$), which was the material originally studied by Obriemov[19]. While investigations of cleavage in vacuum have resulted in surface energies in the range of 2400 to 5000 dyne per cm[26, 27, 28], similar experiments in selected atmospheres[26, 29, 30] show considerably reduced values of surface energy (180 to 375 dyne per cm). All of these measurements were performed at 25 C and clearly show the effects of adsorption on surface energy.

In addition, it should be noted that the values measured in selected atmospheres vary among themselves, where these differences may be associated with the type of species adsorbed. As was discussed earlier, the interaction between dissimilar species will depend upon partial surface energies, and the interaction of mica with water vapor (yielding a measured surface energy of 180 dyne per cm) is significantly different from that with hexane vapor (γ_s = 271 dyne per cm.).

IV-2.2. Calculation from Elastic Constants

Later discussion will be devoted to the theory of surface energies and various methods of calculation, but some of the criteria for crack propagation should be considered here, with the analysis given by Gilman[31]. Gilman's argument rests on various criteria for predicting cleavage planes in different (metallic and non-metallic) systems. Some have agreed that the cleavage planes are those with closest packing, or that bound unit cells, or that cut the fewest chemical bonds; the approach taken here is that cleavage will occur on planes having minimum surface energy.

In the preceding analysis of cleavage cracks the force necessary for crack propagation depended primarily on two materials constants: the elastic modulus and the surface energy. Attempting to relate these two factors, Gilman assumes that the stress between two surfaces can be approximated by a sine function

$$\sigma(w) = \sigma_0 \sin \frac{\pi w}{A} \ , \ 0 \leq w \leq A \ , \tag{29}$$

where A is a "range" or relaxation distance of the attractive forces. Assuming small displacements ($\sin \pi w/A \approx \pi w/A$) and Hooke's law, we have

$$\sigma(w) = E\left(\frac{w}{w_o}\right) = \sigma_o \frac{\pi w}{A} \ , \tag{30}$$

where w_o is the lattice constant perpendicular to the plane.

Thus,

$$\sigma_o = \frac{EA}{\pi w_o} \ , \tag{31}$$

and

$$\sigma\,(w) = \frac{EA}{\pi w_o} \sin \frac{\pi w}{A} \ ,$$

If we now integrate this stress function over the entire range of application (0 to A), the resultant surface energy becomes

$$\gamma = 1/2 \int_0^A \sigma(w)\, dw$$

$$= \frac{EA}{2\pi w_o} \int_0^A \sin \frac{\pi w}{A}\, dw \tag{32}$$

$$= \frac{E}{w_o} \left(\frac{A}{\pi}\right)^2 \ .$$

Thus, the cleavage planes should be those with minimum elastic stiffness normal to these planes, maximum separation distance, and minimum relaxation distance for the attractive forces between them.

In the subsequent tabulation of surface energies, several values will be found quoted as being "calculated from elastic constants". It is the evaluation of Equation (32) that results in these entries.

IV-2.3. Strain Energy Release

While cleavage methods as outlined above are reasonably straightforward for studies on single crystals, the method is difficult to apply to polycrystalline, non-crystalline, or porous structures.

Davidge and Tappin[32] developed methods to determine the surface energies of a group of different brittle "irregular" materials that require a measure of the total

energy released when a pre-notched specimen is completely broken. In essence, the methods are three separate but related types of measurement with three interpretations. The specimen geometry for the three methods is shown in Figure 2, where a three-point bending apparatus with appropriate recording instrumentation is employed. A typical load/deflection curve is shown in Figure 3.

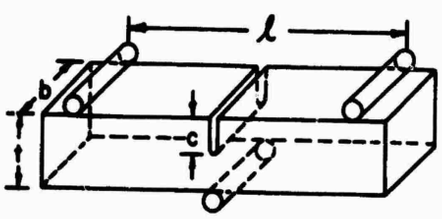

FIGURE 2. SPECIMEN GEOMETRY STRAIN-ENERGY RELEASE

ℓ = span; b = breadth; c = crack depth; t = thickness.

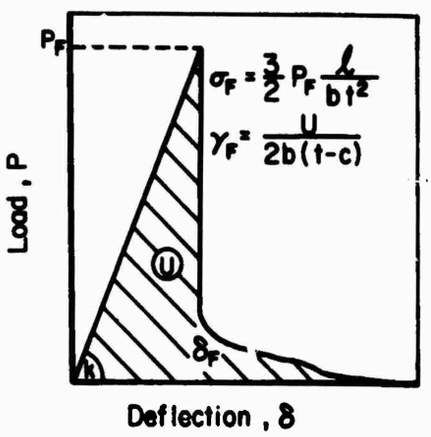

FIGURE 3. A TYPICAL LOAD/DEFLECTION CURVE FOR DETERMINING STRAIN-ENERGY RELEASE RATES

P_F = fracture load; δ_F = fracture deflection; k = specimen stiffness, σ_F = fracture stress; U = strain energy; γ_F = surface energy.

The strain energy release rate, dU/dA, where A is the new surface area generated, may be either calculated or determined experimentally. The former involves the stress distribution computed around the specimen notch while the latter derives dU/dA directly from load/deflection curves.

Analytical Approach. For small values of c/t (see Figure 2), the effective surface energy, γ_G, determined by this method is given by

$$\gamma_G = -\frac{dU}{dA} = \frac{(1-\nu^2)\,\pi\sigma_F^2 c}{2E} \tag{33}$$

where

ν = Poisson's ratio

σ_F = Fracture stress = $3F\ell/2bt^2$

E = Young's modulus.

Aside from specific numerical constants, Equation (33) is essentially the original Griffith criterion.

For crack depths where $c/t > 0.1$, various mathematical treatments are available[33], with their form being such that the surface energy may be expressed as

$$\gamma_G = \frac{(9\,(1-\nu^2)\,F^2 \ell^2 f(c/t)}{8Eb^2(t-c)^3}\ , \tag{34}$$

where f(c/t) is a dimensionless parameter and is plotted in Figure 4. For this correction factor to be interpreted properly, the reader should refer to the original publications, in which the details are explicitly defined.

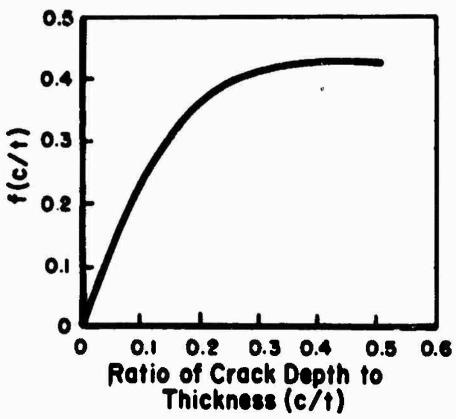

FIGURE 4. VARIATION OF CRACK DEPTH-TO-THICKNESS RATIO CORRECTION FACTOR, f(c/t), WITH CHANGING RATIO[33]

Compliance Method. The effective surface energy determined by this method, γ_C, should be the same as γ_G from above. The load/deflection curve may be represented as $F = k\delta$, where k is the specimen stiffness. The stored energy at the moment of fracture is then $U = F^*\delta^*/2$ or $k\delta^{*2}/2$. We now see that, for fracture at a fixed deflection, we have

$$\gamma_C = -\left.\frac{\partial U}{\partial A}\right|_\delta = -\left.\frac{\partial U}{\partial k}\right|_\delta \left.\frac{\partial k}{\partial A}\right|_\delta = -\frac{\delta^{*2}}{2}\left.\frac{\partial k}{\partial A}\right|_\delta \ . \tag{35}$$

The specimen stiffness, k, must be measured as a function of the initial crack area, $A = 2bc$. For each notch depth, $(\partial k/\partial A)_\delta$ may be obtained from the slope of the crack area-stiffness curve (Figure 5) at the appropriate value of A. Using these values with the experimental values of δ^* will give a series of γ_C values.

Work of Fracture. For the case of catastrophic failure (which will be better defined below), it is desirable to use deeply notched specimens, so that the total stored energy in a weakened structure will be small compared with the surface energy. In this case, controlled fracture proceeds as in Figure 5. The work of fracture is given quite simply as

$$\gamma_F = \frac{U}{2b(t-c)} \tag{36}$$

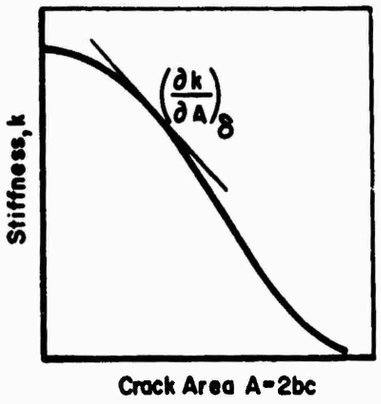

FIGURE 5. GENERAL FORM OF THE CURVE OF STIFFNESS, k, VERSUS CRACK AREA, A[32]

Solid surface energy can be found from $(\partial k/\partial A)_\delta$

In their studies on alumina and an unspecified glass, Davidge and Tappin[32] have shown that the analytical and compliance approaches provide self-consistent measures of the surface energy, and are in reasonably good agreement on the value of γ_I. On the other hand, the surface energy determined from the work of fracture is not as well-defined, there being a dependence on the ratio c/t.

The needs for techniques which are applicable to "rough" materials have been given general consideration by Nakayama[34], who compared various energy conditions and predicted the nature of failure. Again taking the case of three-point bending of a specimen of dimension ℓ, w, t, the energies stored at the time of fracture are calculated to be

$$\text{(a)}\quad U_s = \frac{\ell w t S^2}{18E}$$

$$\text{(b)}\quad U_a = \frac{4w^2t^4S^2}{K\ell^2} \qquad (37)$$

$$\text{(c)}\quad U_o = U_s + U_a \ ,$$

where

U_s, U_a = elastic energy stored in specimen and apparatus, respectively

S = specimen tensile strength

K = apparent spring constant of apparatus

U_o = total stored energy.

For effective fracture energy of γ_{eff}, the energy required to cause separation in the test piece (with cross section over A) is $U_\gamma = 2A\gamma_{eff}$. Now the difference $\Delta U = U_o - U_\gamma$ is an approximate criterion of the mode of fracture. For $\Delta U > 0$, the failure is obviously catastrophic since the stress energy must be consumed by other forms, such as kinetic energy of the fragments. For $\Delta U < 0$, the stored energy is insufficient to cause complete fracture, and this is referred to as stable fracture.

Nakayama showed different modes of failure, illustrated by the three curves of Figure 6, and discussed the conditions under which these obtain. For completely catastrophic brittle failure, the load/deflection curves (or, better, the load/time curves under constant deflection rate) are of the form shown in Curve A of Figure 6. While the total energy supplied to the system can be calculated, no reliable estimate of γ_{eff} is possible, because of the kinetic energy of the fragments.

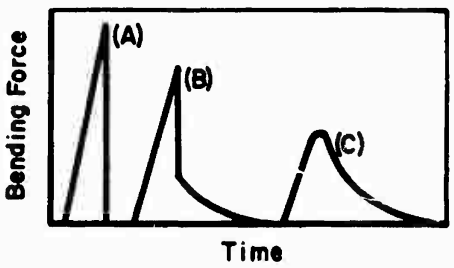

FIGURE 6. SCHEMATIC LOAD-TIME CURVES REPRESENTING (A) CATASTROPHIC, (B) SEMISTABLE, AND (C) STABLE FRACTURES[34]

On the other hand, the introduction of an artificial crack reduces the tensile strength, S, and thus U_o, and a stable or semi-stable crack can be propagated, as in Curves B and C of Figure 6. Then, the total external work, U_c.

$$U_c = v \int_0^{\tau_c} f d\tau \quad , \tag{38}$$

can be computed, where v is the speed of the overall deflection, τ_c the time for fracture completion, and f is the bending force. This method has produced results that are in essential agreement with the results of other techniques.

IV-2.4. Crushing

While Berdennikov[35] and Kuznetsov[36] have considered crushing as a way to determine surface energy, a more nearly complete treatment of the problem has been forwarded by Johnson et al.[37,38,39] in which experiments on the crushing of quartz, rock salt, and a number of minerals and ores was carried out. The results reported in this latter study seem questionable, but the method itself merits some brief discussion, particularly regarding the difficulties that arise.

In an ideal crushing experiment, a steady force or a sudden impact is applied to the sample, the heat evolved is measured in a completely adibatic system, and the total surface area of sample is determined after each step of comminution. Alternatively, rather than measure the heat evolved, it is possible, in principal, to determine the amount of energy dissipated in, say, a falling weight, that effects the crushing and to translate this energy directly into the surface energy of the resulting fragments.

Either method is grossly oversimplified, since the total energy dissipated in several ways, none of which is simple to calculate or account for. For examples, there are frictional losses in most apparatus used for the transfer of energy to the specimen;

in all but the most completely brittle materials, there are energy losses associated with plastic and elastic deformation of the material, as well as in the apparatus, and in unconfined systems, there is a contribution from the kinetic energy of the fragments.

The degree to which these uncertainties affect the results can be surmised from a single comparison of Johnson's data with that reported by other investigators. While the analysis of data was fairly crude, it can be seen that the surface energy experimentally determined from crushing techniques is approximately 1000 times larger than the (albeit inaccurate) theoretical figures quoted by Johnson. Clearly, considerable development is necessary before this technique can be regarded as a promising candidate for surface energy determinations.

IV-2.5. Bent-Wafer Techniques

Certain crystalline materials lack inversion symmetry in particular crystallographic directions. The most notable of these are the materials with the zincblende structure, particularly the III-V compound semiconductors such as InSb, GaAs An examination of the structure of these materials reveals that if these materials were split along a (111) plane, one resulting face would be all atoms of Group III and the other would be all atoms of Group V. Hence, a specimen of these materials that is cut so that it is bounded by (111) planes on opposite faces would show asymmetrical properties. Some of the earliest experimental evidence of the nonequivalence of the two faces was the work of Maringer[40] on the etching of (111) faces of InSb and on the resulting dislocation etch pits observed. More detailed observations on the etching behaviour was documented by Gatos et al.[41, 42, 43] and by Faust et al.[44] in several series of investigations on various materials with the zincblende structure.

A consequence of the dissimilarity in parallel faces is the spontaneous bending of thin wafers of these compounds. The different chemistry of the parallel surfaces gives rise to a different surface tension on each face, and the thin specimens will bend until a balance is achieved between the internal elastic energy and the applied bending moment; this configuration will be characteristic of the material and its dimensions. Cahn and Hanneman[45] undertook a detailed study of the surface energy of the III-V compounds and, with experimental data of Finn and Gatos[46], compared computed values of surface energy with the spontaneous bending observed and the resultant surface tension differences. It is expected that similar effects should be found for all materials which crystallize in the zincblende structure, including the III-V compounds of indium, aluminum, and gallium with arsenic, antimony, and phosphorus; as well as compounds from other groups in the periodic table, for example, compounds of beryllium, zinc, cadmium, and mercury with selenium, tellurium, and sulfur in Group VII.

It is interesting that the bent-wafer phenomenon can also be applied to the study of changes in the surface tension differences caused by adsorption of gases, effects of bulk impurities (particularly in very thin sections), and the influence of electronic effects associated with illumination and other excitation mechanisms.

One additional point of clarification should be added regarding the actual quantities contributing to the spontaneous bending of crystals having this structure. In principle, the bending is caused by a difference in surface tension rather than surface energy, and care must be exercised in the design of experiments which study this phenomenon. It has been demonstrated that, while the absolute surface energy of a material is always

greater than zero, the surface tension can be negative. A better understanding of the relationships between these two related quantities is required before experimental data can be properly interpreted.

IV-2.6. Fiber Stress

Most mechanical methods apply only to brittle or semi-brittle material. The fiber-stress technique applies specifically to ductile materials. In this technique for measuring the surface energy of solids, a fiber to be examined is held in a vertical position and a balance of forces is met in which the downward force (due to the weight of the fiber) is just balanced by the upward force (applied on the periphery) arising from the surface tension (Figure 7). Early experiments using this method was discussed by Udin et al.[47], with later contributions from Parikh[2].

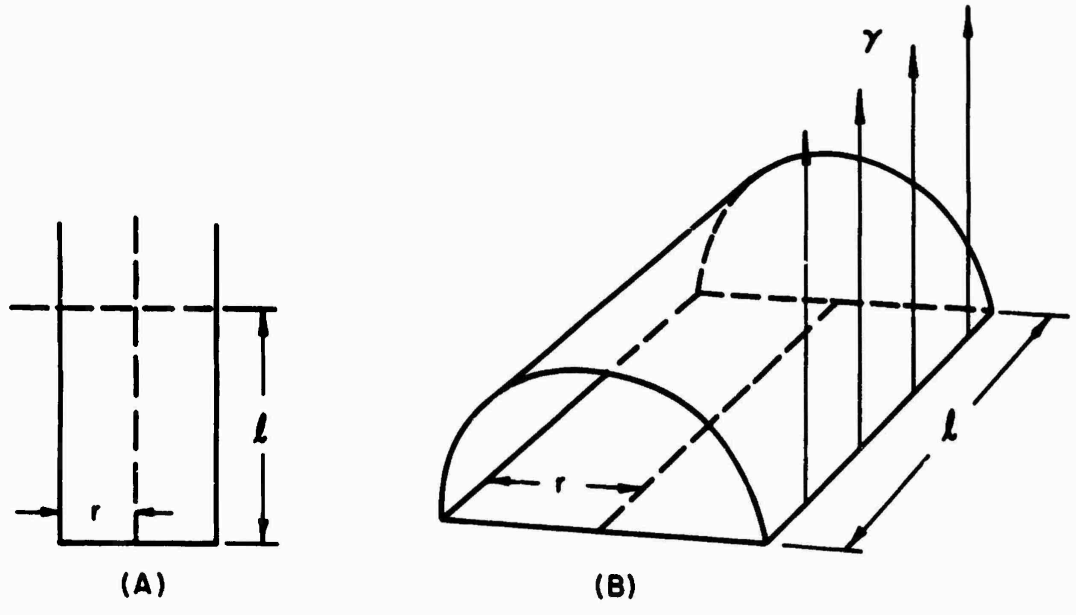

FIGURE 7. (A) FIBER ELONGATION AND (B) GLASS FIBER AS A CYLINDER OF VISCOUS MATERIAL[2]

According to Parikh's analysis, one considers the fiber stress along the axis of a cylinder to be given by

$$\sigma_x = \frac{2\pi r\gamma - w}{\pi r^2} \tag{39}$$

where

$2\pi r\gamma$ = upward surface tension force

$w = \pi r^2 \rho \ell g$ = gravitational force, downward.

The radial stresses are taken to be $\sigma_y = \sigma_z = 2\gamma/d = \gamma/r$. For the case of zero strain, $\sigma_x = \sigma_y = \sigma_z$, and

$$\frac{\gamma}{r} = \frac{2\pi r\gamma - w}{\pi r^2} \tag{40}$$

or

$$w = \pi r\gamma .$$

But

$$w = \sigma_o \pi r^2 \tag{41}$$

where σ_o is the stress at zero strain, so that we have

$$\sigma_o = \gamma/r. \tag{42}$$

Fibers of constant radius and different lengths can be suspended in a selected atmosphere at a given temperature and the length of fibers determined that neither contracts under the action of surface tension nor elongates under its own weight. If the radius and density of the material is known, the surface energy can be calculated directly.

Two limiting situations exist. For long fibers that tend to elongate under their own weight, the cross section should decrease continuously, increasing stress and finally causing ductile fracture. On the other hand, the short fibers should react more strongly to the surface forces that tend to reduce the area of the sample, and a sphere should result. In most practical cases, the movement is much too slow to be observed in a reasonable length of time.

As expected, Bikerman[17] takes a somewhat different view of this method, and criticizes its use, noting that "...there is no reason to suspect that surface properties of the solid have any influence on the phenomenon studied." Bikerman has presented several alternative derivations of the equations necessary to use fiber extension as a total determination of surface energy of thin wires and foils. However, he also details nine different objections to the method, each one of which is supposed to prove that the technique not only does not work but should never be expected to work. He omitted an important point from this critique, however, namely, the effects of creep and viscous flow (also omitted by Parikh). Whatever the relation between the weight of the fiber and the surface forces, no stable equilibrium is expected; in time, the fibers should either break under their own weight or reduce to a sphere. But while no stable equilibrium can be expected, a kinetic equilibrium might be defined in which the elongation caused by the weight of the fiber and the contraction associated with the surface energy are only two of the factors which will be active in the process. In addition to these, one must include terms associated with the diffusion of vacancies and other imperfections, dislocation migration, stress-concentration factors, inter- and inter-granular motion (except in amorphous or single crystal structures), and additional continuously operating variables that will influence the mass motion of the fiber. A concentrated effort on the kinetics of this motion should produce, at a given temperature, a more nearly exact and more rigorously defined value of the surface energy of the specimen.

It should be pointed out, in addition, that while the statement of the problem can be reasonably concise, it is not suggested that the solution of the problem is simple and straightforward. Further, and more important, the effective surface energy will not be constant during the experiment, but will depend, in part, on the composition of surface and the bulk. It is expected, indeed, that the presence of significant vacancy concentrations or other physical defects will affect the surface energy, so that second-order effects will contribute to the dynamic problem. Moreover, the presence of adsorbed species (where experiments performed in such a manner as to investigate the effect of such species on the surface energy) will complicate the problem further, inasmuch as the density of adsorption sites can be a function of the other variables of the system.

In summary, the reaction of a fiber to its environment can be used, in principles, as an experimental tool for determining solid surface energy, but the results must be analyzed and interpreted very carefully.

IV-2.7. Unit-Cell Measurements

The determination of unit-cell size by X-ray measurements on fine particles has been discussed by Nicolson[48] as a tool for the study of surface energies. Simply stated, it is assumed that the effective unit-cell dimensions are generally affected by impressed force fields (as observed in high-pressure experiments). For the case considered here, an increase in surface/volume ratios obtained from specimens with successively smaller size should manifest itself by an increased effective surface pressure per unit volume and the concomitant change in unit cell dimension would constitute a direct measure of the surface energy of the material.

It is apparent that the analysis of such an experiment implies that atomic arrangements are independent of position of atoms within a given particle; i.e., the surface "lattice" is essentially identical to the bulk lattice. That such is the case has been disproved in numerous LEED* studies, particularly of nonmetallic materials. Furthermore, considerable care must be exercised in making assumptions regarding the uniformity of the pressure across any crystal face in a fine particle, since it is shown in numerous examples that the surface energy is strongly orientation dependent. Finally, where surface tension effects determine the state of strain in fine particles, additional complications arise due to the fact that this term can be negative for selected crystalline faces.

At this point, it is not possible to ascertain the degree of reliability of data obtained through the use of this method, since there has not been, to this reviewer's knowledge, a detailed treatment of the theory of the measurement and its interpretation.

IV-2.8. Other Mechanical Techniques

Kuznetsov[36] reviewed a number of other techniques forwarded for the determination of the surface energy of various solids, particularly the alkali halides. Among these, the major emphasis has been on his own work using mutual grinding, abrading and drilling methods, as well as on the use of hardness as a correlative function. Much of this work is devoted to a semi-quantitative analysis of the weight and/or volume losses of materials that result from the techniques used and, with a few generalities

*Low Energy Electron Diffraction.

about crystal structure, lattice constants and other parameters, provides a highly simplified point of view. From a purely qualitative point of view, many of Kuznetsov's findings suggest areas for fruitful development, but, the analysis of the data (as presented) leaves much to be desired.

In general, Kuznetsov makes very simple assumptions regarding the products of the grinding, abrading or drilling methods, with the generalized comment that all contributions to stored and released energy can be associated with the production of new surfaces of crystallites, which are relatively uniform in size and shape. In some respects, his arguments resemble Nakayama's[34], described earlier, but lack enough detail to ascertain the limits of predictability. While Nakayama admits contributions from elastic and plastic deformation and attempts to correct for them, Kuznetsov appears to neglect such "spurious" contributions.

For completeness, many of Kuznetsov's results will be included in the tabulation of surface energy values in Section VI. However, the reader should realize that many of these are subject to more detailed analysis and might be unreliable (particularly where no other comparative data are available).

IV-3. Thermodynamic Methods

IV-3.1. Critical Angle for Wetting

As mentioned in discussing the thermodynamics of interface phenomena, Zisman[1] and his co-workers developed the concept of the critical angle for wetting and have used this to determine wetting conditions and associated phenomena. We shall consider here, in a little more detail, the nature of the approach and its application to inorganic materials as more recently pursued by Eberhart[57]. Using the relation defined in Equation 13, Zisman used a series of homologous liquid organics to determine the so-called critical surface tension, γ_c, of solid substrates. It is argued that the value of γ_c is a characteristic of the solid surface alone. Zisman considers γ_c to be an empirical parameter that varies with the solid surface composition in much the same way as one would expect for the surface energy γ_S^o, although no specific claim is made as to the identity of the two quantities.

More recently, Eberhart[49] discussed the application of this measurement to solids with high surface energies (it will be recalled that Zisman confined his considerations to materials with relatively low surface energies), comparing experimental determinations of γ_c with other values of γ_S. In reviewing the findings of others, Eberhart noted that the critical surface tension is of the same approximate magnitude as the solid-vapor interfacial tension, $\gamma_S^o - \pi_e$ where π_e is the spreading pressure of an adsorbed species. If this is the case, it is then only necessary to determine the spreading pressure in order to calculate the intrinsic surface energy directly from such contact-angle measurements.

One immediately encounters certain difficulties in interpretation and translation, however. The first of these comes from the definition of "homologous series of liquids" in the sense envisaged by Zisman. To use the technique with any degree of certainty,

the properties of the liquids in a service must be roughly similar or at least must vary in a well-understood manner. It would seem logical to choose binary or higher order liquid mixtures with well-behaved surface tensions in the region of miscibility. That is, the liquids should have a regular (not necessarily linear) variation in surface tension with composition. Further, no component of the liquid should interact to any measurable extent with the substrate material; obviously, compound formation at the interfaces and interdiffusion should be avoided or minimized. These restrictions are somewhat severe, particularly for measurements at elevated temperatures, and one cannot expect that the technique will apply readily to a large range of solid materials until further definitive research has been carried out. Even so, it appears at this writing that the method has distinct advantages and deserves additional attention.

Examples of the type of binary liquid melts that may be used as homologous series for the determination of solid surface energies, are shown in Figures 8 and 9. Where no interactions occur between the melts and the substrates, these curves show that a wide range of liquid surface tensions can be employed for high-temperature measurements on selected solids. Similarly, Figures 10 and 11 depict the variability in surface tensions available in ternary systems at high temperatures, where these can be most useful in examining the surface energies of refractory compounds.

Recently, Rhee[50] used the "homologous series" technique to measure surface energies of a number of refractory carbides and nitrides using molten metal as the contact liquid, but introduced a simple modification that might be extended to a number of different systems. Rather than choosing a series of liquid metals or metal alloys, Rhee elected to use a single metal and vary the temperature over a range where there is no significant difference in the reactions between liquid and solid surfaces. By plotting the contact angle as a function of temperature, a value is chosen for the critical angle for wetting (similar to Zisman's and Eberhart's method) as a function of temperature.

To lend support to Rhee's results, it is necessary to investigate, at least in a cursory fashion, the theoretical basis for his choice. The most important of Rhee's basic assumptions relates to the temperature dependence of the various surface energies and surface tensions that affect the contact angle. The somewhat arbitrary choice of a linear temperature dependence to all pertinent energies is made and the validity of the final values rests on this assumption. From the discussion given later regarding the Bruce technique[53] for estimating surface energies, it is reasonable to assume that the solid surface energy will be a linear function of temperature. This assumption does not apply so well to liquids, inasmuch as a 6/5-power dependence can be shown to obtain[54, 55]. However, it is more important to question whether the interfacial energy can be assumed to be reasonably linear.

In an attempt to analyse the behaviour of the interfacial energy of two materials, each of known surface energy, Berghausen et al.[56] have shown that

$$\gamma_{12} = f(\gamma_1, \gamma_2) = \gamma_1 + \gamma_2 - 2\Phi\sqrt{\gamma_1\gamma_2} \qquad (43)$$

where the γ's refer to the two separate materials and the interface, and the function Φ depends upon various intrinsic materials parameters. It can be seen here that if both γ_1 and γ_2 are approximately linear functions of the temperature (ignoring the 6/5-power dependence), then γ_{12} will also be a nearly linear function of the temperature, at least

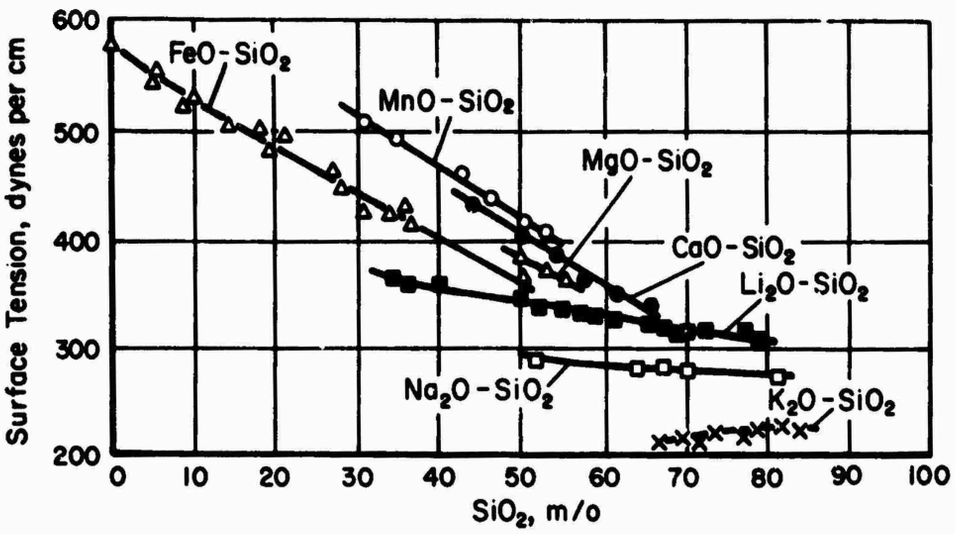

FIGURE 8. SURFACE TENSION VERSUS SILICA CONTENTS FOR BINARY SILICATE MELTS[51]

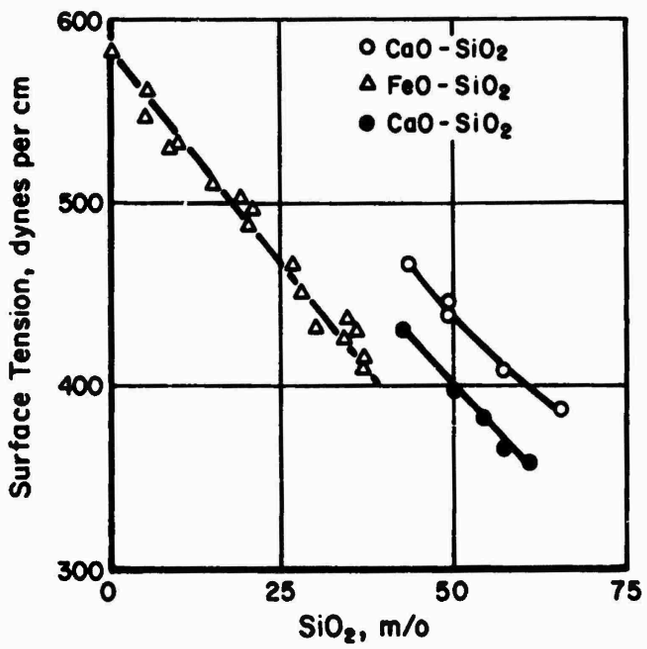

FIGURE 9. SURFACE TENSION VERSUS SiO_2 CONTENTS FOR $FeO\text{-}SiO_2$ AND $CaO\text{-}SiO_2$ MELTS[51]

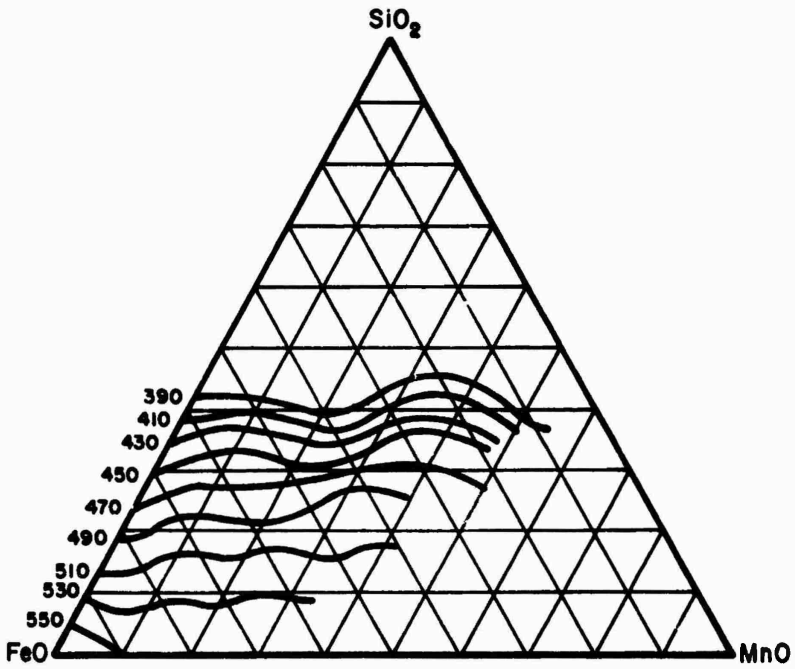

FIGURE 10. SURFACE TENSION IN THE SYSTEM FeO-MnO-SiO_2 AT 1400 C[52]

The surface tension isopleths are in dynes per cm.

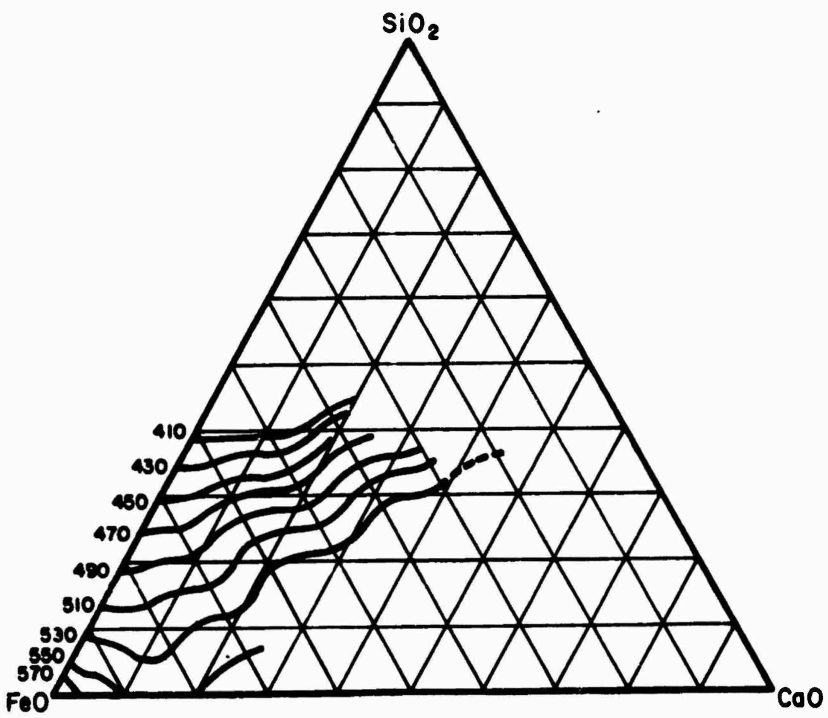

FIGURE 11. SURFACE TENSION IN THE SYSTEM FeO-CaO-SiO_2 AT 1400 C[52]

The surface tension isopleths are in dynes per cm.

over a small temperature range. It must be emphasized, of course, that Rhee's method applies strictly only over a small temperature range; for large ranges, reaction kinetics would probably invalidate the basic assumptions of the method.

A major advantage of this and similar techniques lies in the measurement of solid surface energies at temperatures where mechanical methods no longer apply. In particular, the fracture techniques required that the specimens fail by completely brittle fracture; difficulties in interpretation arose when plastic flow occurred in the vicinity of the crack tip. The present technique precludes such difficulties, and, in fact, the method is also essentially nondestructive. The only limitations encountered are those associated with an interpretation of the spreading pressure and the problems which would arise from high-temperature interactions. Well-defined data on the surface tensions of a number of liquid metals and alloys are available for a wide temperature range, it appears that this technique, if properly interpreted, provides the most direct and widely usable method for the determination of surface energies and their temperature dependence. Further detailed consideration should be given to the theoretical and experimental application of this method.

However, at this point, we should again refer to the arguments of Fowkes[14, 15] and Weyl[13] regarding the interpretation of interface phenomena and the contributions to total surface tension or energy as represented by the various possible interactions. Certainly, if these arguments are valid, the critical surface tension experiments outlined above would measure only a fraction of the total surface energy of the substrate material. To avoid this problem and obtain representative values of total surface energy, it would be necessary to use liquids that would cover the entire range of the various interactions. Again, it is difficult to determine all the various contributions at a given temperature. The greater the similarity between the substrate and the testing liquid, the greater is their tendency to interact. On the other hand, the more the liquid and solid are dissimilar, the less likely it is that the total surface energy can be measured. Obviously, considerable care is necessary in the selection of "tools" and the interpretation of results. More will be said about this later, when the results of Eberhart's studies are included in the discussion.

One additional note is of interest here, although it might seldom apply. It may be expected that, at sufficiently high temperatures, the weight of a sessile drop could deform the solid surface elastically. This will change the measured value of the contact angle slightly [see Lester[57]]. Generally, this effect is probably not significant unless a temperature is reached where the solid actually becomes quite viscous, as in a glass. The correction factor for most cases (particularly since contact-angle techniques do not measure total surface energy) is probably negligible.

IV-3.2. Heat of Immersion

A series of papers[58, 59] from the University of Cincinnati (1957-58) considered, in great detail, the calculation of many factors related to the interaction between dissimilar phases, with particular emphasis on adhesion, wetting, immersion, adsorption, and similar phenomena. The basic theory was summarized by Berghausen et al[56] and only the general content of these papers will be discussed here.

The general theme of these papers was the application of interaction integrals defined by Fowler and Guggenheim[60], in which the atomic structure of the subject materials was taken into account and the cohesive and adhesive energies were calculated by integration of the interaction energies over all space. While the form of the integral representations sets the stage for detailed calculations, a major drawback is that the forms of the energies are confined to only the simplest cases of van der Waals interactions and the treatment cannot be translated straightforwardly to other types of interactions between molecular species.

In addition, Berghausen et al made some extremely simplified assumptions for the sake of tractability, and thereby sacrificed much of the potential value of their results and methods. Be that as it may, Good et al[58] discussed the use of this theory in the determination of the surface energies of solids by measurement of the heat of immersion. Immersion primarily involves the replacement of a solid surface by a solid-liquid interface. The heat evolved in this process can be measured quite accurately with appropriate calorimeters and, with a knowledge of the surface area involved, the change in energy can be determined. With the use of appropriately defined functions of the van der Waals constants for the materials being studied, it was shown that the measured heat of immersion can be related to the surface tension of the liquid (which is directly measurable) and the surface energy of the solid alone, thereby eliminating the effect of the solid-liquid interface.

In principle, this technique offers considerable promise for determining surface energies of solids, rivaling the wetting methods. In fact, it can be shown (through rather laborious calculations) that there is a distinct relationship between these two "surface-thermodynamic" experimental procedures[60, 61]. It is anticipated that the immersion method might even be superior, in that lower-energy liquids can be used and a more flexible choice of liquids (especially organics) may be available.

There is one particular drawback, however, similar to the limitation imposed in the earlier discussion of wetting techniques, and this relates to the definition of the function used to describe interaction phenomena. In general, Berghausen et al[56] derived this function in terms of the van der Waals constants, which depend on such factors as polarizabilities, magnetic susceptibilities, interatomic or intermolecular spacing, crystal structures, and the like. Furthermore, it is assumed throughout the theory that the two species involved are completely immiscible. In the practical application of the theory the conditions imposed and the real situation conflict, for it can be shown that the assumptions necessary to evaluate the function are precisely the same conditions that lead to a basic breakdown of the theory. Specifically, in most cases where the function has been evaluated, polarizabilities, lattice constants, force constants, etc., must be assumed to be roughly equal for the two "dissimilar" materials, whereupon they are no longer as dissimilar as the derivation of the theory demanded. It is in just such cases that compound formation, interdiffusion, and (at least partial) miscibility are the rule rather than the exception, and the entire applicability of the theory is subject to question.

Moreover, as in wettability studies, there is also the question regarding the partial surface energies measured and the necessity of delving into several different materials systems as tools for the determination of the individual components of the total solid surface energy.

The heat of immersion technique also has a few drawbacks that critical wetting methods don't have. In the first place, fine particle dispersions must be used to take greatest advantage of the method. With greater area/weight ratios, the heats of immersion are measured more accurately and it would be expected that surface energy would be determined somewhat more accurately. However, it is also obvious that with large number of small particles, there are also increased edge and corner effects; thus the measured heat of immersion represent a more heterogeneous system than does a critical wetting experiment, and the interpretation of total heat of immersion must take this into account. While the "effective area" of the edge and corner effects can be separated by adsorption studies, the heat of immersion is totally integrated, and the weighting of the different components could present formidable analytical problems. Finally, difficulties are expected with the exposure of various crystalline faces, while the wetting angle experiments can conceivably be performed on selected single-crystal faces.

This discussion of the limitations of the theory is not meant to completely discourage consideration of the Berghausen technique and calculations, but merely to point out the immense difficulties to be expected in using heats of immersion as a tool in the quantitative measure of surface thermodynamic properties.

IV-3.3. Dissolution and Heat of Solution

Early experiments showed that both the vapor pressure and the dissolution rate of particles are functions of particle size, with the general result being that in a saturated solution, large particles tend to grow at the expense of smaller ones. From measurements of particle size and solubility, it is possible to calculate the surface tension (surface tension is one of the driving forces for dissolution and, indeed, is the major driving force with all other factors, such as composition, being equal). It has been shown[12] that the surface energy of a material can be determined from the relative rates of solubility for two particle sizes by the Ostwald-Freundlich equation:

$$\gamma = \left(\frac{r_1 r_2}{r_1 - r_2}\right) \frac{RT\rho}{2M} \ln \frac{S_2}{S_1} \qquad (44)$$

where

r_1, r_2 = particle radii

S_1, S_2 = solubility rates

R = gas constant

T = temperature (K)

ρ = density

M = molecular weight.

It should be emphasized here that this relation pertains only to solubility ratios. A related technique is based on the heat of solution as a function of surface area. There

is a major distinction between the two types of experiments and great care must be exercised in removing possible confusions. In most heat of solution experiments, the material under study is immersed in the solvent and is then permitted to dissolve completely. During the various steps in the heat of solution determination (where it is assumed that the sample materials are uniform, pure, and homogeneous) the initial introduction into the solvent results in the destruction of the solid-vacuum (or solid-air) interface and the creation of a solid-solvent interface. To this point, the experiment is similar to a normal heat of immersion procedure. However, as dissolution proceeds, the solid-solvent interface eventually disappears completely and the net result – as regards the history of the solid – is the complete destruction of both the original solid-vacuum interface and the intermediate solid-solvent interfaces. With the solvent, the total history involves the change in the solvent surface tension resulting from the change in composition. By comparing results of heat of solution determinations that differ only in the surface area of the initial solid, one may then determine the solid surface energy from the original solid surface areas, the temperature changes in the solvent, and the accompanying change in solvent surface tension.

The situation is slightly different in most experimental arrangements employed for dissolution experiments. Here it is often more convenient to use a saturated solution of the solid under investigation, to which are added additional solids of known particle-size distribution. The changes in particle-size distribution (the larger particles grow at the expense of the smaller) is then used to determine the solid surface energy. It should be noted, of course, that neither experiment takes specifically into account the variation in surface energy expected with particle size; such size dependence is averaged out.* Similarly, no account can be made for the presence of surface inhomogeneities, asperities, and the like.

IV-4. The Interpretation of Experimental Data

In the preceding discussion, various experimental techniques have been described that are suggested as means to measure the surface energy of ceramic materials. Whether these do, in fact, result in a true measure of the intrinsic surface energy of a material will generally depend upon a number of factors, some of which are environment-controlled and others that are specimen-controlled.

IV-4.1. Adsorbate Effects

Specifically, it has been shown, in the discussion of the effects of atmosphere on the measured surface energy of mica, that the presence of various adsorbates will result in different, though equally reliable, values of surface energy. Where experiments can be performed in selected atmospheres, it is desirable that one choose, as an added independent variable, varying pressures of adsorbates. It is then expected that a plot of measured surface energy as a function of adsorbate pressure should produce an extrapolated value that is independent of the interaction between the solid

*Balk and Benson[63] have shown that the determination of surface enthalpy of KCl by dissolution techniques yields values that are not strongly dependent on original particle size, at least for particles greater than 500 A in diameter. Their experiments showed that the heat of solution (ΔH, cal per mole) and the specific area (A, m^2 per g), could be related by the simple equation

$$\Delta H = 4200 - 4.2\,A$$

for $0 < A < 60 m^2$ per g. See also Section IV-4.3.

surface and the particular gaseous species. Furthermore, such controlled experiments can provide a measure of the different contributions to the total surface energy of the subject material.

IV-4.2. Liquid-Solid Interfacial Effects

As a further example of the effect of various liquids on the measured value of surface energy, we considered heat of immersion studies of a number of different materials. The surface energies determined by such methods are assembled in Table 2.

TABLE 2. PARTIAL SURFACE ENERGIES OF VARIOUS SOLIDS IMMERSED IN DIFFERENT LIQUIDS[61, 64]

Solid	Chemical Formula	Liquid Employed			
		Water	Ethanol	n-Heptane	Benzene
α-alumina	Al_2O_3	693	--	151	--
Amorphous alumina	Al_2O_3	454	--	85	--
Kaolinite	$Al_2O_3 \cdot 2SiO_2 \cdot 2H_2O$	292-352	155	52-89	--
Pyrophylite	$Al_2O_3 \cdot 4SiO_2 \cdot H_2O$	348	154	97-105	--
Barite	$BaSO_4$	490	--	--	140
Graphite	C	48	--	122.5	225
Calcium Montmorillonite	--	226-284	133-150	71-77	--
Sodium Montmorillonite	--	219-296	137	59-76	--
Silica (amorphous)	SiO_2	210	--	--	218
Aerosil	SiO_2	165	--	118	--
β-quartz	SiO_2	847	--	--	--
Zirconia	ZrO_2	600	--	--	190

As is obvious from the Table, the partial surface energy determined by immersion techniques is markedly dependent upon the particular liquid chosen. The observed trends can be understood qualitatively by reference to the chemical structure of the liquids employed, as shown in Figure 12. It will be recalled from earlier discussions that the interaction between like species was expected to consist of similar terms in the expression for the total surface energy or surface tension. Furthermore,

it is shown in the evaluation of the Guggenheim integrals[56, 58, 60] that the interaction between two different materials will increase as they become more nearly alike.

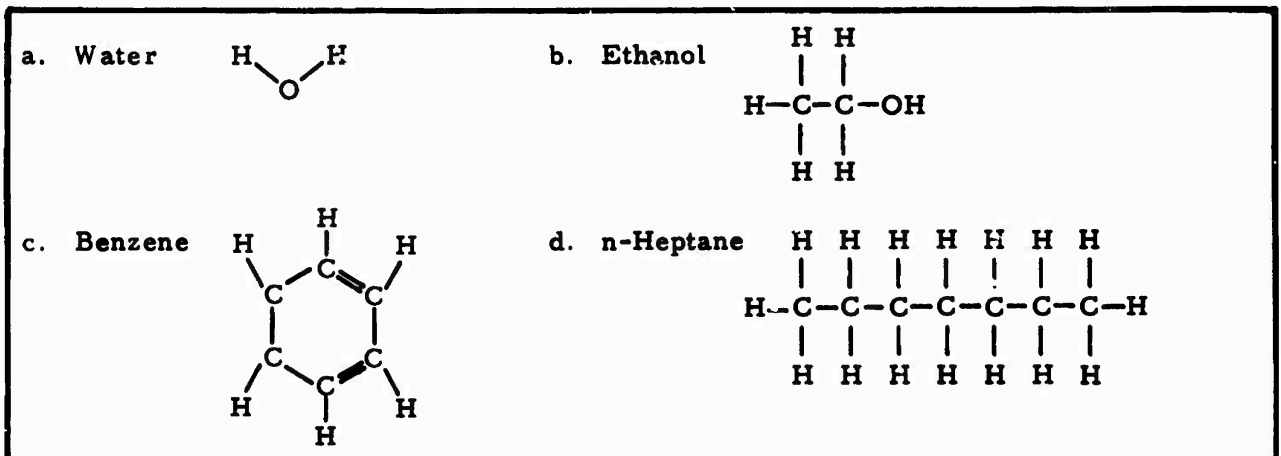

FIGURE 12. STRUCTURES OF LIQUIDS USED FOR IMMERSION STUDIES

As a further example of the manner in which the heat of immersion is influenced by the choice of liquid, refer to the data shown in Table 3, where the heats of immersion of rutile (TiO_2) are listed for various liquids. The data, taken from Zettlemoyer[61] have been obtained at 25 C with fine particles (5.8 m^2 per g, or a particle size of approximately 0.24 μ). The effect of the liquid molecular structure is pronounced.

TABLE 3. HEATS OF IMMERSION OF RUTILE IN VARIOUS LIQUIDS[61]

Liquid	Formula	Heat of Immersion, dynes per cm
n-Nitropropane	$CH_3CH_2CH_2NO_2$	664
n-Butyl aldehyde	$CH_3CH_2CH_2CHO$	556
Water	H_2O	550
Butyric acid	$CH_3CH_2CH_2COOH$	506
n-Butyl chloride	$CH_3(CH_2)_2CH_2Cl$	502
n-Amyl alcohol	$CH_3(CH_2)_3CH_2OH$	413
n-Butyl alcohol	$CH_3(CH_2)_2CH_2OH$	410
Ethyl alcohol	CH_3CH_2OH	397
n-Butyl iodide	$CH_3(CH_2)_2CH_2I$	395
n-Butylamine	$CH_3(CH_2)_2CH_2NH_2$	330
Heptane	$CH_3(CH_2)_5CH_3$	144
Octane	$CH_3(CH_2)_6CH_3$	140
Hexane	$CH_3(CH_2)_4CH_3$	135

These concepts will help to provide a degree of understanding to the general list of values of surface energy given in Section VI. In those materials that contain water molecules in their structure (for example, kaolinite, pyrophylite and the montmorillonites), the interaction with water is considerably greater than that with ethanol or n-heptane; that is, the use of water appears to measure a greater contribution to the total surface energy. Similarly, the presence of (OH) groups in ethanol suggests, at least pictorially chemical similarities and, hence, would measure a greater partial contribution to the total surface energy.

The strong interaction between graphite and benzene (Table 2) is quite obviously a consequence of the similarity in structure.

In spite of the apparent simplicity of this argument and the qualitative assertions which can be drawn, particular care must be exercised in attempting to infer too much from this approach. As the liquids and solids become more similar, there is a greater tendency for solution, diffusion, compound formation, and the like, and the initial prerequisites for determining surface energy are sacrificed. Materials which dissolve in water or show strong tendencies toward hydration would normally be expected to interact with water to a greater degree and the measured heat of immersion may then have little relation to the actual surface energy.

IV-4.3 Particle-Size Effects

Throughout much of the discussion, it has been sufficient to consider the surface energy of semi-infinite materials, recognizing only that difference from bulk structure which might occur at or near the surface. One should note, however, that the energy of the surface of a fine particle (which may have a large surface/bulk ratio) is not necessarily the same as the semi-infinite surface. DeBruyn[65] discussed the effects of the radius of curvature on the surface tension of liquids, and Hirschfelder et al.[66] calculated in detail the variation of liquid surface tension with droplet size. It has been shown that the surface tension may be expressed as

$$\ln \frac{\gamma}{\gamma_o} = - \int_r^\infty \frac{\frac{2z_o}{r^2}\left[1 + \frac{z_o}{r} + \frac{1}{3}\left(\frac{z_o}{r}\right)^2\right]}{1 + \frac{2z_o}{r}\left[1 + \frac{z_o}{r} + \frac{1}{3}\left(\frac{z_o}{r}\right)^2\right]} dr \qquad (45)$$

where

γ_o = surface tension for a semi-infinite specimen

z_o = depth of "surface layer".

and r = radius of curvature.

It is implied that z_o is independent of r in this calculation, which is not necessarily accurate. Care should be taken in the strict application of Equation (45) at large values of z_o/r. For small z_o/r, Equation (45) may be approximated as

$$\frac{\gamma}{\gamma_o} \approx 1 - \frac{2z_o}{r} , \qquad (46)$$

which is sufficiently accurate for qualitative interpretations. Figure 13 shows the effect of particle drop size on the surface tension of liquids as calculated from Equation (45).

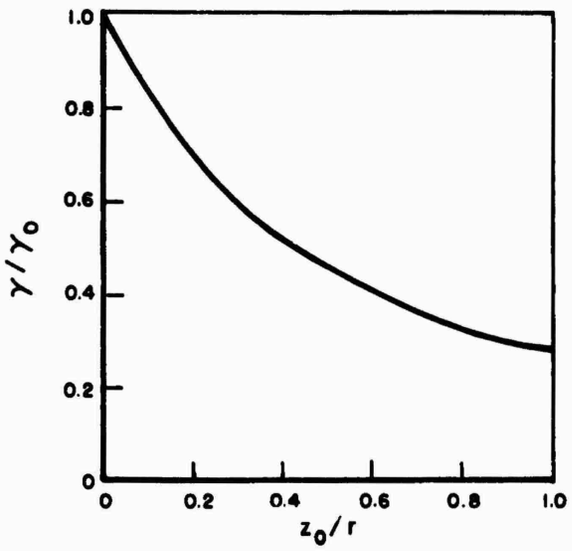

FIGURE 13. CALCULATED EFFECT OF PARTICLE SIZE ON THE SURFACE TENSION OF A LIQUID

The relation between liquid drop size and surface tension may be carried to consideration of similar effects in solid particles. Such dependence is inferred in the experiments on solubility of fine particles and also applies to variations in the surface energies of semi-infinite solids with small, but finite, asperities on the surface. The small radii of curvature of such asperities provide a locus of different surface energy on a material prepared by lapping or cutting. Furthermore, the size effect is one of the major driving forces in scratch-smoothing experiments, which are designed to measure either the surface energy or surface diffusion coefficients, as well as sintering rates. Hence, one should be concerned about the effect of particle size in the interpretation of surface energy experiments. It should also be seen that surface texture is expected to be significant in contact angle observations, a point reviewed by Marian[67].

IV-4.4. Grain-Size Effects

The next point to be considered is the influence of grain size on the measured value assumed to be the surface energy. The data on grain-size dependence are rather sparse, with the major effort having been directed toward Al_2O_3 and MgO, as shown in Figure 14. For the most part, the data suggest that measured surface energy increases with increasing grain size, although single crystal values are on the order of 1000 to 2000 dynes per cm for both alumina and magnesia. The above emphasis on

"measured" values clearly illustrates the importance of proper interpretation of experimental results. The total energy required to effect fracture is divided among several simultaneous events including transgranular and intergranular fracture, grain-boundary sliding, dislocation maneuverability, crack branching, and similar perturbing influences. It is thus expected that polycrystalline material would show higher apparent surface energies than single crystal specimens.

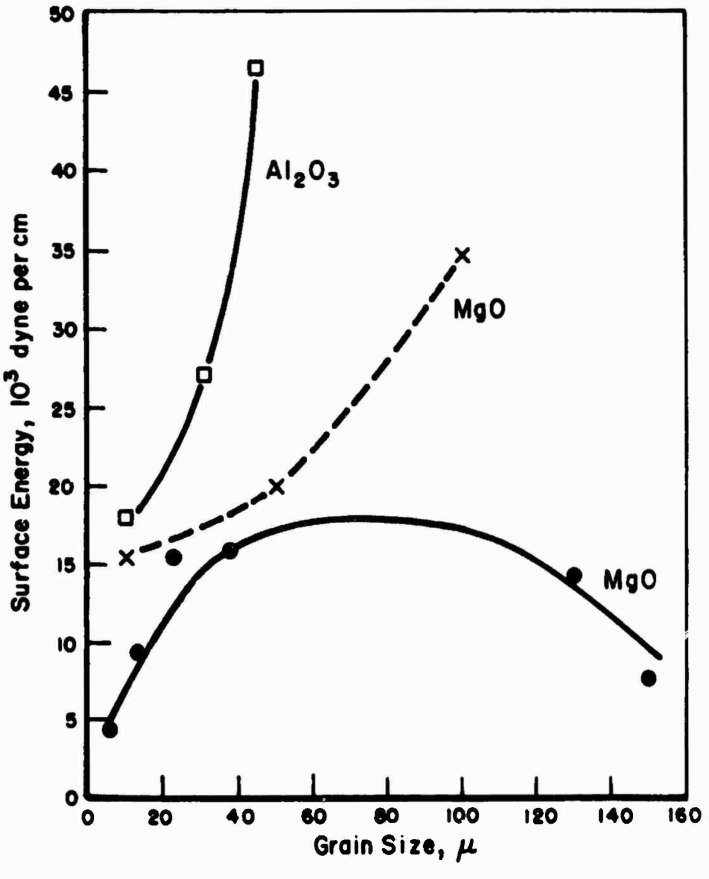

FIGURE 14. MEASURED SURFACE ENERGIES AS A FUNCTION OF GRAIN SIZE FOR Al_2O_3[68] and MgO[69]

The explanation of the trends as a function of grain size is not quite so straightforward. It is suggested that grain-boundary sliding effects would require less total energy dissipation in those cases where grain boundary densities are high (small grain side). Furthermore, more random crystallite distribution would be expected to provide easier paths for stress relief; hence, less energy is required to propagate a crack. In view of the complex analysis which is required to resolve the many questions associated with surface energy determinations on polycrystalline masses, it is suggested that the most meaningful data which is amenable to detailed studies will be obtained on single crystal specimens.

V. THEORETICAL CALCULATIONS

For the most part, earlier attempts to calculate surface energy of solids were channeled along three approaches. First, several authors went into great detail in the calculation and summation of the interaction forces between atoms and molecules in various crystal structures and developed elegant, though complicated, methods to evaluate the lattice sums and integrals involved. Second, there are semiempirical calculations based upon gross observables, with the inclusion of factors related to general thermodynamic principles and suitable averages to account for crystalline orientation effects. And third, there are estimates of surface energy based upon extrapolation and correlation of various data on other physical properties, such as characteristic temperatures, mechanical properties, diffusion coefficients, and the like. To re-derive the fundamental relationships that have been proposed in detail would lead us somewhat past the scope of the report and would require considerable space in background and supporting data. It is deemed sufficient, at this point, to bring out some of the highlights of different treatments and refer the reader to original sources for whatever minutiae of detail is desired.

For each area, one of the more important contributions to the field will be considered in order to orient the reader and set the stage for later discussions. It is not this reviewer's intention to imply that these papers are the most nearly complete, definitive, or all-inclusive of the many available (some of which are referenced in the text). Furthermore, it should be understood that heavy reference to any one of these three does not necessarily "endorse" the methods or conclusions of the individual authors; the discussion which follows merely illustrates the usage of the different methods and can provide some clue as to the degree to which such approaches are profitable.

V-1. The Atomistic Approach

By far the most exhaustive work on the calculation, from first principles, of the surface energy of solids was carried out by Benson and coworkers in a series of articles culminating with the definitive review recently published[18]. For the most part, Benson's work considered only the solid noble gases and NaCl-type crystals, although many of the principles evoked concern other systems as well, including the treatments of defect structures and the effects of impurities, anisotropies, inhomogeneities, physical defects, nonstoichiometry, and the like. (This is not to infer that the extension to include these other variables is straightforward and/or easy; the calculations are exceedingly complex, but the work of Benson sheds considerable light on the use of the method.) Benson includes, in the review paper, not only a compilation of his own work, but also a detailed discussion of the contributions made by other researchers, including the early work of Born and the later computations of Lennard-Jones and Dent[70], Shuttleworth[6], Huggins and Mayer[71], and Nicolson[49]. Comparisons of the calculated results of a number of contributors have been presented in concise form by Zadumkin and Khulamkhanov[72], with additional discussion by Walton[73].

To compute the surface energy of a crystal, it is necessary to define the interaction potential between a pair of particles, i and j, separated by a distance, r_{ij}.

Usually the total interaction must be considered as a sum of contributions from various types of forces, with the final expression containing characteristic constants that can be evaluated from other parameters such as compressibility, lattice spacing, etc.

The simplest interaction potential, ϕ_{ij}, used for the rare-gas crystals takes the Lennard-Jones form:

$$\phi_{ij} = \phi(r_{ij}) = c_{12} r_{ij}^{-12} - c_6 r_{ij}^{-6} \quad , \tag{47}$$

where the c's are adjustable coefficients. Early calculations on the NaCl-type crystals, recognizing the highly ionic character of the bond, used the coulombic and an unspecified inverse nth-power to express the potential, yielding:

$$\phi_{ij} = e_i e_j r_{ij}^{-1} + b r_{ij}^{-n} \quad , \tag{48}$$

where the e's represent electrostatic charge and b is an adjustable constant. Refinements were made to account for possible differences in interaction between (+, +), (-, -), and (+, -) charges on the ions.

A less approximate potential form,

$$\phi_{ij}^{o} = e_i e_j r_{ij}^{-1} - c_{ij}^{(6)} r_{ij}^{-6} - c_{ij}^{(8)} r_{ij}^{-8} + b_{ij} \exp(-r_{ij}/\rho) \quad , \tag{49}$$

has been used which includes not only the coulomb and exponential repulsion forces, but also the interactions due to dipole-dipole and dipole-quadrupole effects[6, 71].

In addition, ions at or near the surface of a crystal are subject to a finite electric field that arises from the loss of bulk crystal symmetry at the surface. The total potential energy for surface ions with dipole moments μ_i and μ_j will then be a modified form of Equation (49), namely:

$$\phi_{ij} = \phi_{ij}^{o} - e_i(\vec{r}_{ij} \cdot \vec{\mu}_j) r_{ij}^{-3} + e_j(\vec{r}_{ij} \cdot \vec{\mu}_i) r_{ij}^{-3} - 3(\vec{r}_{ij} \cdot \vec{\mu}_i)(\vec{r}_{ij} \cdot \vec{\mu}_j) r_{ij}^{-5} + (\vec{\mu}_i \cdot \vec{\mu}_j) r_{ij}^{-3} \quad . \tag{50}$$

Benson also notes that the total interaction energy is found by summing ϕ_{ij} over all pairs and adding an "elastic energy", $\mu_i^2/2\alpha_i$, where α_i is the ionic polarizability.

The results of Benson, et al., are found to depend largely upon the values chosen for various parameters of the bulk materials. In principle, it is possible to compute the surface energy of a particular material from the above expressions for the potential and the appropriate lattice sums. In addition, independent expressions containing the same coefficients may be derived for other characteristic physical properties of the materials under study. It is thereby possible to use readily measured or derived quantities (such as polarizability, modulus, sound velocity, etc.) to provide numerical values for the coefficients, and then to determine surface energy, which is not so easily measured.

A point stressed by Benson that is borne out by recent interpretations of LEED data[74], is that the surface structure of a perfect crystal in vacuum is different from that envisaged on a parallel plane in the bulk of the crystal. The discussion of this point considers the atomic processes which accompany perfect cleavage along a given plane.

If it is assumed that at the instant of fracture two new surfaces are formed, each having the same arrangement as in the bulk, then an amount of energy γ^{s0} is required. However, a spontaneous relaxation occurs on the new surfaces, which contributes to a decrease in the surface energy. The resultant surface energy at absolute zero is then conveniently expressed as

$$\gamma_0^s = \gamma^{s0} + \Delta\gamma^s \quad , \tag{51}$$

where the two terms correspond to the two steps outlined. $\Delta\gamma^s$ is, of course, a relaxation term and is negative in value. The $\Delta\gamma^s$ term is computed much like γ^{s0}, taking into account the different displacements of positive and negative ions at or near the surface.

One important point regarding surface distortion should be noted here. Benson assumed that the lattice distorts only in a direction normal to the bulk crystal, that is, the lateral spacing of the surface layer is no different from that in the bulk and the surface crystal plane has the same configuration as the corresponding bulk plane. Along the normal to this plane, ions of different sign are in slightly distorted positions, and the degree of distortion decreases with increasing depth into the bulk. This is essentially the same picture discussed by Weyl[75] in studies of adherence to MgO, where it is assumed that O^{--} ions protrude further from the nominal (100) plane than do the Mg^{++} ions, producing a permanent surface dipole.

On the other hand, Fowkes[76] allowed both normal and lateral displacements (this has been partially confirmed by LEED studies). However, Fowkes' treatment is almost entirely confined to a thermodynamic and phenomenological approach, so that the exact details of surface structure are irrelevant; it is only necessary to state that the structure is different.

The magnitude and importance of the surface distortion effect can be seen from the values of γ_0^s, γ^{s0}, and $\Delta\gamma^s$, taken from Benson and Yun's review[18] and listed for the (100) and (110) faces of the alkali halides in Table 4.

Benson's steps to include surface distortions are certainly in the right direction. The numerical calculations suggest that distortion must be considered to arrive at reasonable values of surface energy. While the treatment is incomplete, the essential features of the computations appear to suggest additional effort in this area. It is now necessary to extend the calculations to models which include lateral displacements (that is, a three-, rather than one-dimensional density change). It is anticipated that the proper interpretation of LEED data on clean surfaces will provide considerable impetus to these studies. It is important to note, moreover, that the positioning of stress or ions on the surface is not the only factor relating to the accuracy of the calculation. Benson and Yun[18] showed how the particular choice of interaction potential can effect final results markedly, and the need for a more thorough study of this aspect of the calculations is certainly indicated.

All of the above discussion centered about the problem of computing the surface energy at 0 K. For experimental results to compare better with theory, it has been necessary to extend these studies to finite temperatures. It is generally stated that the surface energy at any temperature may be expressed as a sum

$$\gamma(T) = \gamma_{pot} + \gamma_{vib} \ . \tag{52}$$

where the potential energy term, γ_{pot}, depends only on the bulk characteristics and corresponds to the static lattice energy, while the second term, γ_{vib}, is an explicitly temperature-dependent contribution. There is, of course, an implicit dependence of γ_{pot} on T because of the changing lattice parameter, so that we should write

$$\gamma^s(T) = \gamma_0^s + \left(\frac{d\gamma_0^s}{da}\right)\Delta a + \gamma_{vib}^s(T) \quad , \tag{53}$$

where the lattice parameter is denoted by a and γ_0^s is defined previously [Equation (51)]. Naturally, the contributions from the zero-point energy should be included, although these were omitted earlier.

TABLE 4. THEORETICAL SURFACE ENERGIES OF ALKALI HALIDE CRYSTALS AT 0 K

	(100) Face			(110) Face		
	γ^{s0}	$\Delta\gamma^s$	γ_0^s	γ^{s0}	$\Delta\gamma^s$	γ_0^s
CsBr	--	--	--	234.4	-34.8	200
CsCl	--	--	--	256.6	-37.7	219
CsF	211.2	-63.6	148	436.9	-96.1	341
CsI	--	--	--	207.1	-31.9	175
KbR	159.2	-36.4	123	326.5	-64.8	262
KCl	175.3	-34.0	141	367.3	-69.6	298
KF	225.9	-41.9	184	528.0	-105.2	423
KI	140.8	-27.7	113	279.1	-57.6	222
LiBr	226.2	-140.5	86	515.1	-234.8	280
LiCl	251.4	-144.7	107	599.2	-259.1	340
LiF	288.7	-146.4	142	962.3	-394.6	568
LiI	199.8	-126.4	73	424.6	-198.3	226
NaBr	192.2	-54.0	138	413.4	-109.2	304
NaCl	210.9	-52.7	158	469.7	-115.6	354
NaF	265.9	-49.5	216	711.7	-156.4	555
NaI	170.5	-52.5	118	348.8	-97.3	252
RbBr	150.5	-28.5	122	300.9	-55.3	246
RbCl	166.0	-28.4	138	337.3	-60.0	277
RbF	213.1	-42.3	171	473.2	-92.9	380
RbI	133.4	-29.8	104	259.0	-48.9	210

The vibrational energy term can best be computed by considering appropriate integrations or summations over the allowed vibrational states, and the calculations proceed with appropriate Debye weighting factors. The Benson calculations for some of the alkali halides and MgO were carried to 298 K for better comparison with experiment. A few of these results are somewhat tenuous, even allowing for approximation, because either surface distortion or lattice expansion factors were omitted. This will be discussed again in Section VI.

Previous discussion has alluded to the difference between surface energy and surface tension. The most detailed calculations of these differences have been reviewed by Benson and Yun[18]. The calculations will not be repeated here, but it is worthwhile

including, however, a comparison between the estimates given by various authors. As in the case of surface energy, there is a "bulk" contribution (Γ^0) to surface tension and a correction ($\Delta\Gamma$) due to surface relaxation. The resulting values of Γ^0, $\Delta\Gamma$ and $\Gamma = \Gamma^0 - \Delta\Gamma$ are compared in Table 5, along with the surface energy γ_0^s as computed by Benson and Yun[18].

TABLE 5. SURFACE TENSIONS (Γ) AND ENERGIES (γ) CALCULATED FOR ALKALI HALIDES AT 0 K

	(110) face,	Shuttleworth[6], (100) face			Nicolson[48], (100) face	Benson & Yun[18], (100) face			
	Γ°	Γ°	$\Delta\Gamma$	Γ	Γ	Γ°	$\Delta\Gamma$	Γ	γ_0^s
CsF	--	--	--	--	308	497	-126	371	341
KBr	442	341	-842	-501	250	330	-101	229	262
KCl	521	404	-779	-375	310	389	-125	264	298
KF	884	719	-929	-210	549	718	-223	495	423
KI	354	269	-581	-312	172	262	-71	191	222
LiBr	--	--	--	--	827	786	-195	591	280
LiCl	--	--	--	--	1025	948	-324	624	340
LiF	--	--	--	--	2287	1978	-1484	494	568
LiI	--	--	--	--	558	609	-63	546	226
NaBr	646	534	-868	-334	454	499	-113	386	304
NaCl	776	641	-771	-130	562	593	-155	438	354
NaF	1443	1214	-1034	180	1031	1149	-408	741	555
NaI	505	419	-724	-305	303	395	-54	341	252
RbBr	--	--	--	--	204	282	-90	192	246
RbCl	--	--	--	--	248	331	-109	222	277
RbF	--	--	--	--	427	600	-173	427	380
RbI	--	--	--	--	142	225	-49	176	210

V-2. Semi-Quantitative Structural and Thermodynamic Considerations

The detailed calculations outlined above can provide reasonably good estimates of the surface energies of a multitude of compounds covering a wide range of variables. In fact, there appears to be no limit to the extent of applicability of the method; given sufficient information (from experiments) and time for such calculations, the surface energies of all materials should be calculable, including ceramics, metals, organic compounds, etc. The major factor determining the accuracy of the calculations seems to be in the choice of potential functions and the constants associated with them. As stressed before, it is reasonable to assume that many different materials parameters can be computed and their experimental values can be used to adjust the necessary constants, thus giving credence to the computed values of surface energy.

While, in principle, the above technique should suffice for all applications, the calculations are quite time-consuming and a more direct, though perhaps less accurate, method might be preferred, especially for "quick guesses". There are semi-empirical methods that provide reasonable values of surface energy but which involve much simpler calculation. The methods, essentially due to Bruce[53], circumvent the detail of Benson but include, practically from the outset, a direct relationship between the surface energy and the other measurable parameters that are eventually required for the Benson approach.

The reasoning behind the Bruce approach is not particularly well defined, but many of the results are sufficiently accurate to merit considerations. At the outset, several basic definitions and boundary conditions must be stated.

The surface energy, γ_s, and surface enthalpy, ϵ_s, are usually related through

$$\epsilon_s = \gamma_s - T\frac{d\gamma_s}{dT} \quad . \tag{54}$$

Bruce points out that as $T \to 0$ K, $d\gamma/dT$ vanishes, so that $\epsilon_s^0 = \gamma_s^0$, the total surface energy at 0 K, which can be computed by the methods of Benson. Inasmuch as the surface energy (or surface tension) vanishes at the critical temperature, T_c (where the liquid-vapor separation is indistinguishable), it then follows that

$$\frac{d\gamma_s}{dT} \approx \frac{\epsilon_s^0}{T_c} = \frac{\gamma_s^0}{T_c} \quad . \tag{55}$$

It has also been found that the surface tension of a liquid at a temperature between the melting point and the critical temperature may be expressed as

$$\gamma_L^T = k(1-T/T_c)^n \quad , \tag{56}$$

with k and n as constants. [Further applications of Equation (56) will be considered again later.] If the effect of melting upon the surface energy is known, it should be possible to compute surface energy and surface tension at all temperatures, from absolute zero to T_c over both liquid and solid phases.

Bruce takes the point of view that the surface free energy can be described in terms of the bonding of atoms and that when energy is supplied to effect such breakage between two atoms, one half goes to each atom. Therefore, the bond energy, β, is taken to be

$$\beta = H_s/2cN \quad , \tag{57}$$

where H_s = molar heat of sublimation (ergs/mole), c is the number of bonds per molecule, and N is Avagadro's number. If b represents the number of bonds per cm^2 of the particular crystal face, then the total surface energy is

$$\gamma = \beta b \quad . \tag{58}$$

b can be determined from inspection of the surface lattice. We note that a perfect surface, similar in configuration to the bulk lattice, is assumed from these estimates. For the most part, this restriction is no more stringent than the assumptions regarding the initial calculation of γ_s^0.

Bruce now takes the point of view that Equations (54), (57), and (58) may be applied to the estimation of surface energy in the solid and that Equation (56) applies to the liquid. At the melting point, the latent heat of fusion (H_f) will contribute to a decrease in surface energy in the amount

$$-\Delta\gamma = \eta H_f/AN \quad , \tag{59}$$

where A is the surface area of a molecule and the parameter, η, is the ratio of free bonds to normal coordinate bonds in this surface.

It is now possible, in principle, to estimate surface energies over a wide temperature range, given the appropriate heats of sublimation and fusion. More precisely, the following "recipes" apply to a given system:

$$\begin{aligned}
&\text{(a)} && \gamma_s^0 = H_s b/2cN && T = 0\ K \\
&\text{(b)} && \gamma_s^T = \gamma_s^0 - \left(\frac{\gamma_s^0}{T_c}\right) T && T_m > T > 0 \\
&\text{(c)} && \gamma_s^{T_m} - \gamma_L^{T_m} = -\Delta\gamma = \eta H_f/AN && T = T_m \\
&\text{(d)} && \gamma_L^T = k(1 - T/T_c)^n && T_c > T > T_m
\end{aligned} \tag{60}$$

where

b = number of bonds per cm^2 of the plane considered
c = number of bonds per molecule
A = surface area of a molecule
η = ratio of free bonds to normal coordinate bonds
n = adjustable exponent, about 1.2.

The constant k can be evaluated by equating Steps (c) and (d) at $T = T_m$ and, using the definitions of Steps (a) and (b), may be written as:

$$k = \frac{H_s b}{2Nc} \frac{(1-T_m/T_c) - (2\eta c/bA)H_f/H_s}{(1 - T_m/T_c)^n} \tag{61}$$

Note that the factor b contains the lattice parameter at T = 0 K, while A contains a similar contribution from the lattice parameter at $T = T_m$.

Inasmuch as critical temperatures are unknown for many materials, Bruce pointed out that the ratio of critical temperature to boiling point, T_c/T_b, is approximately equal for different classes of oxides: for MO, $T_c/T_b \approx 1.52$; for MO_2, $T_c/T_b \approx 1.50$; and for M_2O_3, $T_c/T_b \approx 1.40$. No other such correlations have been noted thus far.

Comparisons of Bruce's data with previous work suggest that while agreements do not support the technique without qualification, the order-of-magnitude results indicate that as a rough approximation, the methods can be applied to a broad range of materials.

Bruce further considers the effect of crystallographic orientation on the surface energy of different crystal classes. Quoting Friedel et al.[77], the surface energy of a given (h, k, ℓ) plane is a function of h, k, and ℓ, the bond strength, β, and lattice parameter, a_0, such that, for different crystal systems, we have:

$$\gamma(hk\ell) = \frac{(h + k + \ell)\,\beta}{a_0^2\,(h^2 + k^2 + \ell^2)^{1/2}} \qquad \text{(simple cubic)} \tag{62}$$

$$\gamma(hk\ell) = \frac{(2h + k)\,\beta}{a_0^2\,(h^2 + k^2 + \ell^2)^{1/2}} \qquad \text{(face-centered cubic)} \tag{63}$$

$$\left.\begin{aligned} \gamma(hk\ell) &= \frac{2[2h\beta_1 + (h + k + \ell)\beta_2]}{a_0^2\,(h^2 + k^2 + \ell^2)^{1/2}} \qquad h \geq (k + \ell) \\ \gamma(hk\ell) &= \frac{2(h + k + \ell)(\beta_1 + \beta_2)}{a_0^2\,(h^2 + k^2 + \ell^2)^{1/2}} \qquad h \leq (k + \ell) \end{aligned}\right\} \text{(body-centered cubic)} \tag{64}$$

The γ's are surface energies near 0 K, and β_1 and β_2 refer to bond strengths between nearest and next-nearest neighbors, respectively. The equations apply when $h \geq k \geq \ell \geq 0$.

It can be readily seen that, for the simple cubic systems, (100) is the lowest surface energy, and we can then define the ratio

$$R(hk\ell) = \frac{\gamma(hk\ell)}{\gamma(100)} = \frac{h + k + \ell}{(h^2 + k^2 + \ell^2)^{1/2}} \quad , \tag{65}$$

which is independent of β and a_0. It is interesting to note from these expressions that the surface energy varies around a stereographic projection (lattice projection Figure 15) in the manner shown in Figure 16, where contours of constant surface energy (at 0 K) are drawn. Thus the surface energies at (111), (110), and (100) planes are in the ratio $\sqrt{3}$: $\sqrt{2}$: 1, as expected from the simple bond considerations.

Similarly, stereographic projections can be prepared for other crystal structures, that for the face-centered cubic being shown in Figure 17. Note that surface energy is a minimum on the (111) plane, and the indices of Figure 17 refer to the ratio $\gamma(hk\ell)/\gamma(111)$.

The projections are not quite so simple for the body-centered cubic structure, the added complication arising from the different bond strengths needed to describe the surface energy. Letting $\beta_1/\beta_2 = \tau$, we can rewrite Equation (65) to the form

$$\left.\begin{aligned} R(hk\ell) &= \frac{(2\tau + 1)\,h + k + \ell}{2(h^2 + k^2 + \ell^2)^{1/2}(\tau + 1)} \qquad \text{for } h \geq (k + \ell) \\ R(hk\ell) &= \frac{h + k + \ell}{\sqrt{2}\,(h^2 + k^2 + \ell^2)^{1/2}} \qquad \text{for } h \leq (k + \ell) \end{aligned}\right\} \tag{66}$$

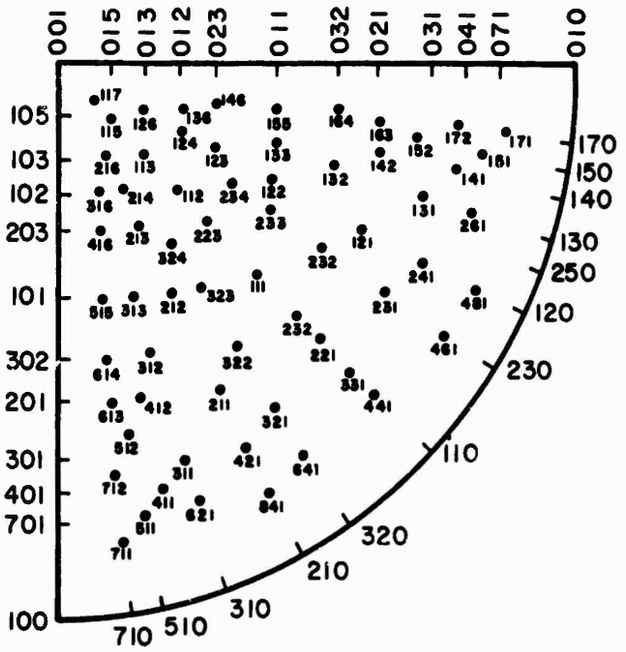

FIGURE 15. THE POSITIVE QUADRANT OF A STEREOGRAPHIC PROJECTION OF A CUBIC CRYSTAL WITH SOME PLANES INDICATED BY THEIR MILLER INDICES(53)

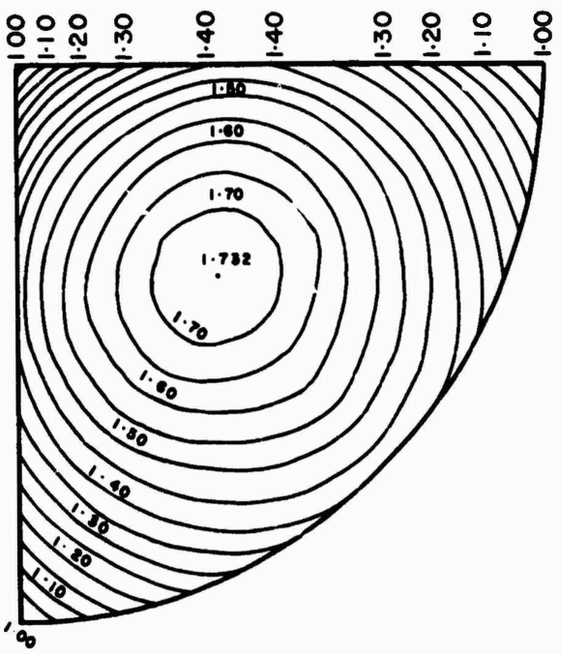

FIGURE 16. THE SURFACE ENERGY RATIOS FOR THE SIMPLE CUBIC SYSTEM PLOTTED ON A STEREOGRAPHIC PROJECTION(53)

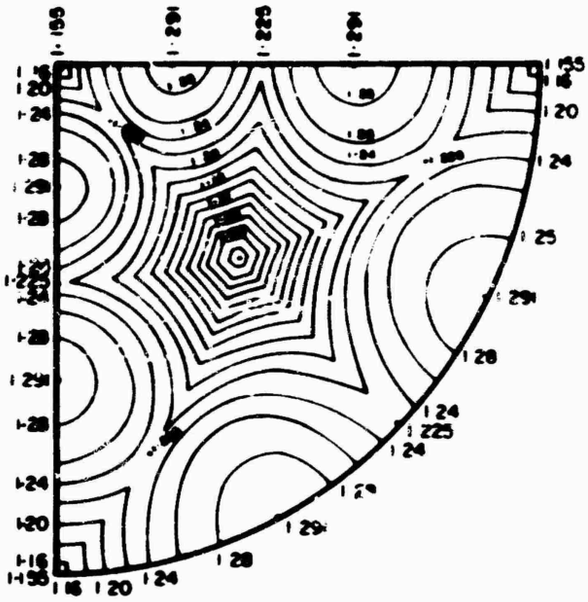

FIGURE 17. THE SURFACE-ENERGY RATIOS FOR THE FACE-CENTERED CUBIC SYSTEM PLOTTED ON A STEREOGRAPHIC PROJECTION[53]

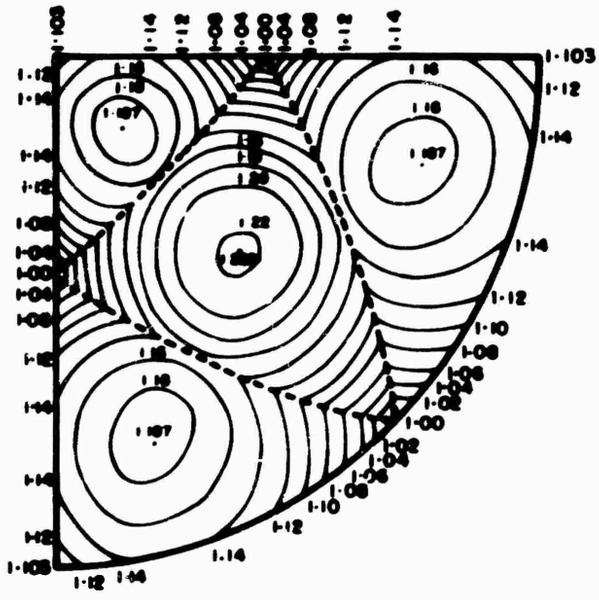

FIGURE 18. THE SURFACE-ENERGY RATIOS FOR A BODY-CENTERED CUBIC MATERIAL (α-Fe) PLOTTED ON A STEREOGRAPHIC PROJECTION[53]

The (110) plane represents the minimum surface energy and all R(hkℓ) are referred to this plane in the projection of Figure 18. For $h \geq k + \ell$, R(hkℓ) is independent of the ratio, -, and these areas appear in the three "corners" of the projection. However, the center portion where $h \leq k + \ell$ shows the effects of the differing bond strengths and produces "saddle lines" in the projection.

It is also expected that the ratios R(hkℓ) will be time-dependent for $T > 0$ K, since a mass arrangement should result from surface diffusion and, in effect, faceting. Such faceting effects proceed in the direction that produces the greatest density of low-energy surfaces. It is the very existence of ratios $R(hk\ell) \geq 1$, that acts as the driving force for this diffusion. Similarly, differences in surface energy, coupled with the high energies associated with cusps and other surface irregularities, provides the driving force for sintering or agglommeration.

The nature of the effect of temperature on surface energy of cations can be estimated as follows. Although surface diffusion and faceting is expected at all temperatures, there is a "threshold" temperature below which such mass motion is essentially arrested and above which sintering and similar reactions proceed at a measurable rate. This point is referred to as the "Tamman" temperature, T_T, and, for many oxides, is reported to range from 0.5 to 0.6 T_m. This value can vary over relatively wide temperature ranges. The T_T has no theoretical basis, being purely an empirical reference point, but it is sufficiently accurate to form the basis of reasonable speculations.

The rate of change of R(hkℓ) should be exponential with time for any given temperature, tending to unity in infinite time, so that

$$R_T = 1 + be^{-\lambda t} \tag{67}$$

where b and λ are merely constants for a particular material. Inasmuch as the rate should be infinitely slow for $T \leq T_T$ (for simplicity, we assume that R_T is constant for $T < T_T$, so that no significant surface diffusion and faceting occurs below the threshold temperature) and is infinitely fast at the melting point (where the anisotropies in surface energy vanish), we may then approximate

$$\frac{dR_T}{dt} = -k\left(\frac{T - T_T}{T_m - T}\right) \tag{68}$$

Since $R_T = R_0$ at $t = 0$, we may differentiate Equation (66) and substitute from Equation (68) to eliminate the factor b, whence.

$$R_T = 1 + (R_0 - 1)\exp\left[\frac{-k(T - T_T)t}{(R_0 - 1)(T_m - T)}\right]$$

Assuming a standard diffusion character to the mass motion we may let $k = Dk_r/r^2 = D_0 e^{-E/RT} k_r/r^2$, where D_0 is the diffusion coefficient; k_r is a statistical weighting factor E, the activation energy for diffusion; and r, the particle size. Taking reasonable figures for the various factors in Equation (66), Bruce computed the change in the ratio of surface energy to time for various particle sizes.

The results of this computation illustrates the nature of the changing driving forces for surface reactions and some of the rate-controlling constants that effect reactions.

Before leaving this section, two points deserve further mention because of their potential applicability in studies of surface energies and solid surface compatibility. First, in previous sections we suggested the possible use of surface-tension versus contact-angle measurements for the determination of critical surface tensions and, hence, solid surface energies, following the Zisman and Eberhart methods. Then, in the discussion of Bruce's work, we have come across the relation between surface tension of a liquid and its temperature dependence, as mentioned in Equation (56). It is therefore worthwhile at this point to digress to a short justification of the value of the exponent, n, in that equation.

Mitra and Sanyal[54] showed that the vapor pressure and surface tension of liquids may be related through

$$T \ln p = -a \gamma_L \left(\frac{M}{D-d}\right)^{2/3} + b \quad , \tag{69}$$

where p = vapor pressure

γ_L = surface tension

T = absolute temperature

D, d = densities of liquid and vapor, respectively

M = molecular weight

a, b = adjustable constants

It has also been shown[78] that the surface tension and density are related by

$$\gamma_L = C(D-d)^4 \tag{70}$$

where C is a constant. Using Equation (70) to eliminate (D-d) in Equation (69) yields

$$T \ln p + a\gamma_L^{5/6} = b \quad , \tag{71}$$

where the factor of M has been absorbed in the constants. By substituting from the integrated Clausius-Clapeyron equation

$$\ln p = C + d/T \quad , \tag{72}$$

T ln p can be eliminated, which leaves:

$$\gamma_L^{5/6} = A - BT \quad . \tag{73}$$

From this, it follows that Equation (56), with an exponent of 1.2, is based on better than purely empirical observations. These relations will be important to measurements of critical surface tension over a wide range of temperatures. Further considerations of the relations among liquid surface tension, heats of vaporization and temperature have been forwarded by Bowden[55] and his results can provide good estimates of this difficultly measured parameter.

The second point which should be mentioned here relates to the change in surface tension that occurs upon melting or solidification (as well as in other changes of state).

The Sharpe and Schonhorn[14] analysis of the thermodynamics of wetting, spreading, and adhesion showed that wetting is not a reciprocal process; that is, if material A will wet material B, then B will not wet A, and conversely. For example, to produce good adhesive bonds between polyethylene and epoxy resins, it is necessary to set the epoxy at its curing temperature, and then heat polyethylene to the softening point in order to promote adhesion (since the liquid epoxy will not wet the solid polyethylene). In the Sharpe and Schonhorn analysis, it is implicitly assumed that wetting in any solid-liquid system could be effected (if necessary) by interchanging the roles of the solid and liquid at a given temperature, but this is obviously impossible in all but the most specialized applications. Even given such a situation, their analysis presumes that the surface energy on curing does not change significantly. The earlier discussion on the contribution to surface energy made by the term at the melting point tends to overrule a strict application of the Sharpe and Schonhorn approach, and cautions against the indiscriminate use of their conclusions. This is particularly important in consideration of the role of surface energy differences when designing experiments to overcome intrinsic difficulties in promoting adhesion between dissimilar materials.

These observations are of great importance where attempts to achieve strong bonds between materials use deposition techniques to effect contact. Here we have a case where "solidification after contact" is carried out, rather than the mating of two solid materials. It should be recognized that the change in surface energy of the solidifying material might promote thermodynamic instabilities at the interfaces and the particular components might not adhere to each other well without the use of an intermediate phase.

V-3. Correlation Techniques

Several authors have attempted to calculate the solid surface energy of various solids through the use of correlations with other physical parameters. Quite often, these are based more on qualitative observations than on fundamental scientific investigations. However, it should be pointed out that this is not a criticism of the use of such techniques, inasmuch as the study of solid surface energies needs assistance wherever it can be found.

Considerable work has been done on the surface tensions of liquid metals and correlations with other physical observables, with perhaps the most nearly complete work being that of Siuta and Balicki[79]. Similarly, Sikorsky[80, 81] and Courtney-Pratt[81] have studied solid metals, reporting on the relations between physical properties and a form of practical adhesion. Perhaps the most extensive work with ceramic systems stems from the work of Livey and Murray[82].

Livey and Murray considered the qualitative effects of lattice energy, surface polarization, molar volume, heat of formation, diffusion, and other properties on the solid surface energies of a number of oxides, carbides and alkali halides. They showed that while bulk lattice energy certainly relates to surface energy (particularly in

elemental materials), there may be some difficulty in associating bulk and surface energies in compounds, especially where there are the added effects of lattice distortion and surface "non-stoichiometry". In addition, polarization effects at the surface add a new dimension to the computations, as shown earlier by Benson et al.[18]; simple extrapolation is not possible.

Furthermore, it is expected that the general rules of correlation should be tempered by the fact that the types of shielding and polarization effects expected in metal oxides of the form, say, MO, would be different from those found in oxides of the type M_2O_3, MO_2, etc. Moreover, as one goes through a series of "homologous compounds", intrinsic trends might not be justified as factors of correlation when considered individually, and extrapolation must be done carefully within one class of materials.

The results and techniques of Livey and Murray[82] are quite important in that this is one of the few articles of the correlative type which seems to deal honestly with the limitations of the empirical methods. Throughout their discussion, it is apparent that full consideration must be given to the interactions between different types of contributions to the total surface energy.

Sikorsky[80, 81] takes a somewhat different approach in the correlation between surface energy and mechanical properties of various solids, notably metals. The coefficient of adhesion is taken to be the ratio of the force necessary to pull apart two specimens divided by the force employed in bringing them into intimate contact. In some cases, it is necessary to effect a twist of the joints in order to break oxide layers, smooth out asperities, and the like. This coefficient of adhesion is then correlated with such factors as hardness, recrystallization temperature, and associated metallurgical properties, as well as with liquid surface tensions of the metals. The cross-correlations then permit the assessment of surface tension with respect to the mechanical properties of the solids.

Although such correlations may serve as another method or approach for the estimation of the surface energy of selected solids, it is not felt that there is sufficient merit in the method to justify extensive use. For example, the use of hardness as an intrinsic parameter may lead to large discrepancies, since the hardness will depend not only on the surface characteristics but also on bulk properties of the subject material. The hardness of a nearly perfect single crystal is somewhat different from the hardness of the same material in the form of a highly worked, polycrystalline mass. Furthermore, the recrystallization temperature is expected to be a function of diffusivity, crystal structure, defect concentration and other intrinsic factors that will also determine, to a certain extent, the value of surface energy. Consequently, by attempting to cross-correlate between two uncertain correlations one only multiplies the uncertainty.

Two major factors resulting from researches of Bondi[83] should be pointed out here inasmuch as they contribute to two distinct aspects of the present report: the correlations between surface tension and other physical measurables, and the use of "homologous" series of liquids for the determination of solid surface energies. In the first place, Bondi shows how the surface free-energy density and the cohesive energy density may be correlated for a number of different classes of molten specimens. As can be seen from Figure 19, the data for these different materials classes is somewhat incomplete, although more further experiments might extend the ranges of applicability of the Bondi correlation, particularly for the oxides (Class III). It is most important to

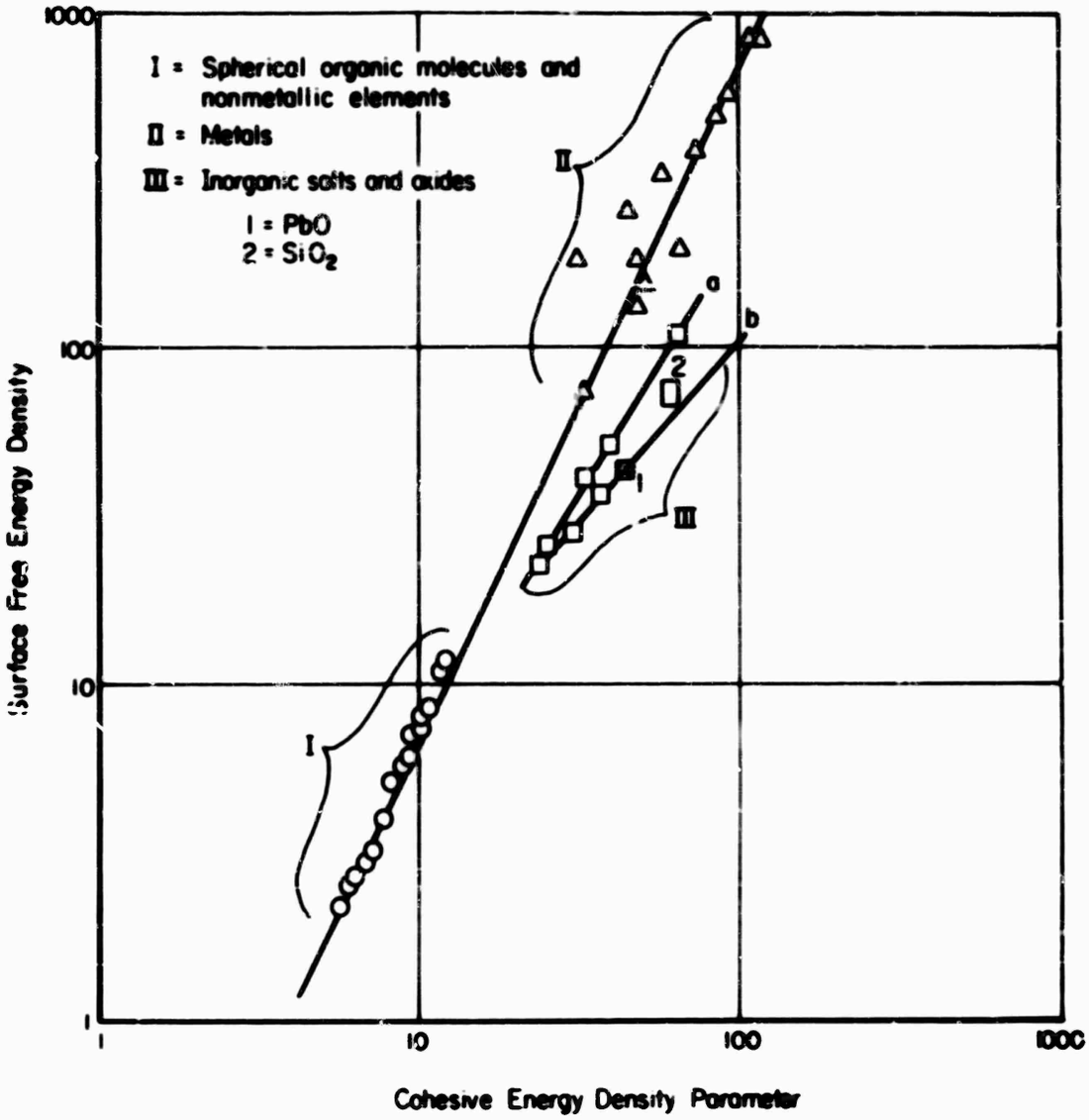

FIGURE 19. CORRELATION BETWEEN SURFACE FREE ENERGY DENSITY, ΔF_S, AND THE COHESIVE ENERGY PARAMETER, δ_V, FOR VARIOUS TYPES OF SOLIDS[48]

Surface free energy density is given by $\Delta F_S = \gamma / V_L^{1/3}$,

where γ is the surface tension and V_L is molecular volume.

The cohesive energy density parameter is given by $\delta_V = \Delta E_{vap} / V_L^{1/2}$,

where ΔE_{vap} is the heat of vaporization.

point out, however, that reasonable correlations do indeed exist and even with the limited data presently available, one may be able to determine order-of-magnitude estimates of surface energy for unknown materials.

Secondly, Bondi collected data on the effects of alloying (in the liquid state) on the surface tension of what might be considered a homologous series in the sense defined earlier. As discussed earlier, it is necessary to establish a series of liquid systems that do not interact with a substrate of unknown surface energy in order to define the critical surface energy for wetting, which is relatable to the solid surface energy. With such a series, the solid surface energy might be determined under conditions and at temperatures where mechanical techniques are not valid. Hence, data of the type shown in Figure 20 can be employed for such determinations.

Naturally, one must be cautious about defining the temperature of the experiments, for both the solid surface energy and the surface tension of the liquid mixtures vary with temperature. Again referring to Bondi's work, we see, in Figure 21, the manner in which the surface tension can vary with temperature in mixtures. While the form of the temperature dependence in pure liquids has been shown to be quite regular (sometimes linear, but believed to be related to the 6/5 power), it is seen from Figure 21 that in mixed systems, the variation can be quite erratic. This is thought to be associated with eutectic compounds or unique properties of the selected liquid mixtures. Hence, one must know in considerable detail the nature of the liquid mixtures before attempting use them in the determination of solid surface energies. A similar argument must be ·od in attempting to employ the methods suggested by Rhee[50], where compound ·rmation or enhanced diffusion can occur at a particular temperature.

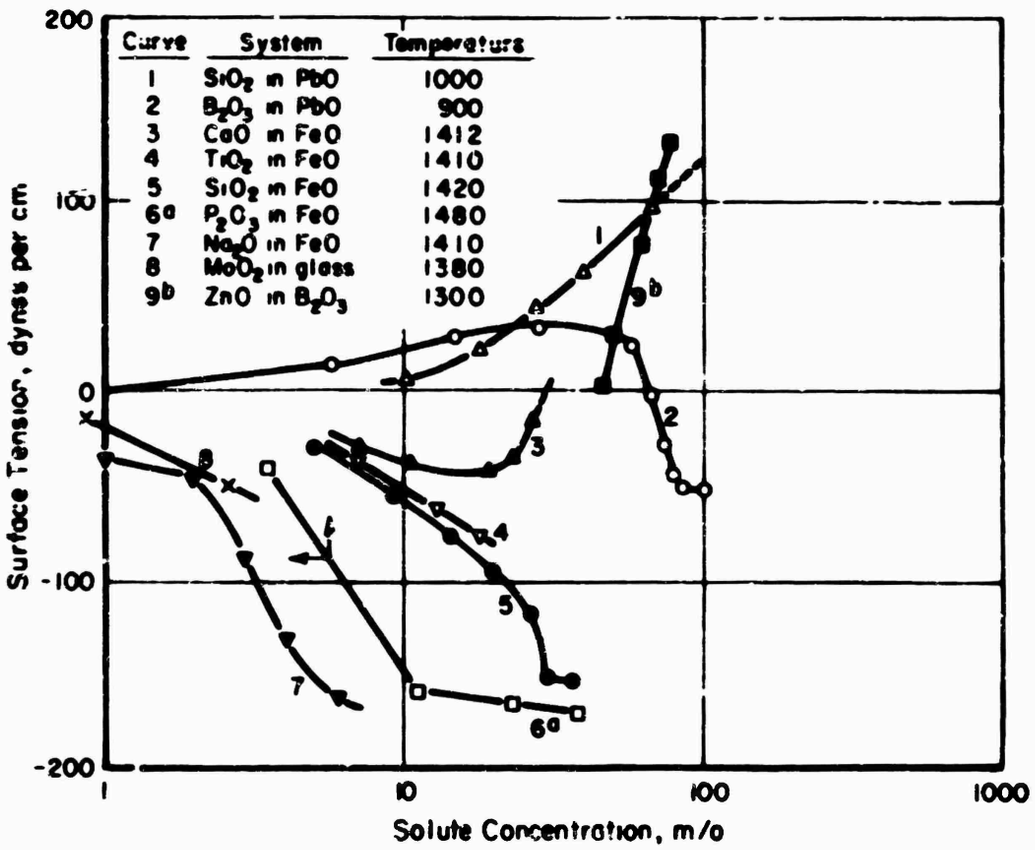

FIGURE 20. CHANGE IN SURFACE TENSION OF FUSED METAL OXIDES BY ADDITION OF VARIOUS OTHER METAL OXIDES[48]

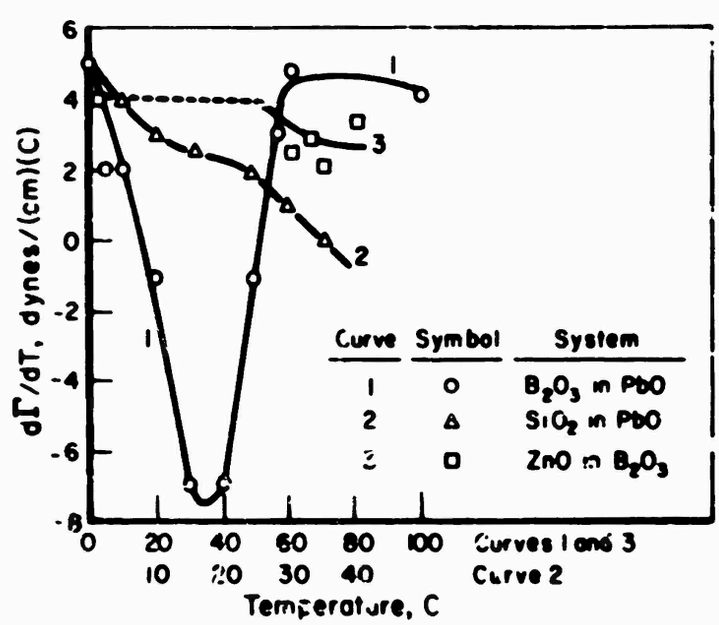

FIGURE 21. TEMPERATURE COEFFICIENT, dΓ/dT, OF THE SURFACE TENSION OF MIXTURES OF FUSED METAL OXIDES

VI. SOLID SURFACE ENERGIES

VI-1. The Surface Energy of Crystalline Solids

Several aspects of the measurement, interpretation, and theory of surface energies of solid materials have been discussed to provide a framework for understanding the experimental and theoretical values collected in the following tables. From the outset, it is well to point out where the major gaps will be encountered, since only relatively few materials have been investigated and the understanding of the present data is not uniform. The following tables list most reported data, including some that must obviously be in error. Erroneous data is included to illustrate the drawbacks of certain experimental and/or theoretical techniques, but is not meant to be a criticism of the technique as such. Such an exposition should provide a better feel for the applicability of a given method, and will suggest areas for more research.

The tables list the values of surface energy (for both liquid and solid, where applicable), the temperature of measurement, the method used, the condition of the material, and appropriate remarks. There are a number of gaps in the information, partly because the description is incomplete in the original source. In many cases, the values stated by the original authors have not been correlated with other calculations or experiments, and it is difficult to assess the reliability of such results.

The surface energies of most materials have been neither measured, calculated, nor subjected to much speculation; hence, there is little information on this important quantity. In addition, while a few techniques have been developed whereby estimates may be made by the combination of other physical data, there are two major pitfalls in the application of such methods: (1) the data for the correlations is not available, or (2) the correlations are so poorly based that the use of such information can lead to erroneous results.

Where values of γ and $d\gamma/dT$ are available they are included in the table. The Bruce[53] approach has been assumed valid, as well as the relation between surface tensions and critical temperatures. The critical temperature and multiplicative constant given in Equation (54) have been calculated by the reviewer. It should be noted that the T_c so determined might not be realistic at all. In many cases, it is impossible to measure T_c or to interpret it in classical terms. For example, where compounds dissociate into multiple components, the T_c bears little resemblance to the same quantity referred to with common materials such as water, the noble gases, single-element liquid metals, etc. Therefore, one should not consider derived values of T_c as being highly accurate; they are included merely for illustration and might be useful in the determination of a few other parameters of the system.

The general character of the tables is such as to present what might at first be considered a collection of unrelated data on many different substances. In this connection, it should be pointed out that the purpose of the present report is not only to collect available data on the surface energies of ceramic solids, but also to shed some light on the relative reliability of different techniques (both experimental and theoretical) which can be used in the determination of these values. For many of the materials listed in the table, there is very little information to support or refute the quoted values of surface energies; several individual values must stand alone without benefit of corroboration. In other cases (particularly those of high technical interest, such as alumina, magnesia and the like),

a number of investigations have been carried out using a variety of experimental methods on a variety of materials. It should be obvious, from an inspection of all the data and the discussion throughout the report, that a large number of variables will contribute to the measured values of surface energy and that very few researches have been devoted to a detailed study of these. Under these conditions, it would be normally expected that a variability in results should occur.

For many of the materials reported in the tables, a single value of surface energy has been singled out as being thought of as the most reliable available at the present time. For the most part, however, there is insufficient information available on which to base such a conclusion, and decisions on "best values" have been postponed until further significant research has been completed.

TABLE 6. SOLID SURFACE ENERGIES OF CERAMIC COMPOUNDS

Material	Temperature,[a] C	Material Condition[b]	Surface Energy,[c] dyne per cm	Method	Original Reference	Relevant Discussion in Text Section	Remarks
AgBr	(-273)	Single crystal (100) plane	352	Calculated from elastic constants	31	IV-2.2	-
	(-273)	Single crystal (110) plane	300	Calculated from elastic constants	31	IV-2.2	
AgCl	(-273)	Single crystal (110) and (100) plane	230	Calculated from elastic constants	31	IV-2.2	
Ag_2CrO_4	25	-	575	[illegible]	62	IV-1.3	
AlAs	(-273)	Single crystal (100) plane	[illegible]	Sublimation energy approximation	65	V-2	-
	(-273)	Single crystal (110) plane	[illegible]	Sublimation energy approximation	65	V-2	-
	(-273)	Single crystal (111) plane	[illegible]	Sublimation energy approximation	65	V-2	-
[illegible] or [illegible] (Topaz)	(25)	Natural crystals, coarse	1.95×10^5	Cleaving	37 38 39	IV-2.4	Expected to be much greater than other obtained by other techniques
AlN		Polycrystalline	665	Contact angles	50	IV-3.1, IV-4.2	Single contact liquid, angle measured as function of temperature
Al_2O_3	-	Sapphire (10$\bar{1}$0) plane	See Remarks	Sublimation energy approximation	53	V-2	Minimum value γ_S = 1120 - 0.216T (T = deg C)
	-	Sapphire (10$\bar{1}$0) plane	See Remarks	Sublimation energy approximation	53	V-2	Average value γ_S = 1280 - 0.232T (T = deg C)
	2050	Liquid	580	Sublimation energy approximation	53	V-2	γ_L = [illegible]
	2080	Liquid	690	Sessile drop	84	-	-
	[illegible]	Liquid	[illegible]	Sessile drop	83	V-3	-
	[illegible]	Liquid	577 [illegible]	Sessile drop	85	-	-
	[illegible]	Polycrystalline	[illegible]	Sessile drop	86	-	-
	[illegible]	Polycrystalline	[illegible]	Dihedral angle	87	[illegible]	Analysis includes grain boundary energies
	[illegible]	Sapphire spheres not indicated	[illegible]	Critical angle	40	IV-3.1, IV-4.2	Zisman-Eberhart technique
	[illegible]	Sapphire (10$\bar{1}$0) plane	[illegible]	Sublimation energy approximation	53	V-2	
	25	Polycrystalline	[illegible]	Heat of solution	88	IV-3.1, IV-4.2	Includes interface term
	25	Polycrystalline, 99% Al_2O_3	[illegible] to 30,670	Strain energy release	32	IV-2.3	Analysis by compliance method
	25	Polycrystalline, commercial grade	20 to 34,000	Work of fracture	88	IV-2.3	Includes crack branching and grain boundary terms
	25	Polycrystalline	18,000	Work of fracture	88	IV-2.3, IV-4.4	"Lucalox", 30 μ grain size
	25	Polycrystalline	27,000	Work of fracture	88	IV-2.3, IV-4.4	"Lucalox", 30 μ grain size
	25	Polycrystalline	6,000	Work of fracture	88	IV-2.3, IV-4.4	"Lucalox", 85 μ grain size
	25	Polycrystalline, 95% Al_2O_3	30 to 66,[illegible]	Total work of fracture	32	IV-2.3	-
	25	Powder, 0.95 μ, alpha phase	[illegible]	Heat of immersion	61	IV-3.2, 4.2, 4.3	Immersed in water
	25	Powder, 0.95 μ, alpha phase	[illegible]	Heat of immersion	61	IV-3.2, 4.2, 4.3	Immersed in n-decane
	25	Powder, [illegible]	[illegible]	Heat of immersion	61	IV-3.2, 4.2, 4.3	Immersed in water
	25	Powder, [illegible]	[illegible]	Heat of immersion	61	IV-3.2, 4.2, 4.3	Immersed in n-decane
	25	-	[illegible]	-	89	-	Assumed $d\gamma/dT$ = -0.1 dyne/cm °C
	25	Sapphire spheres not indicated	12,0[illegible]	Work of fracture	69	IV-2.3	Includes kinetic energy terms
	25	Sapphire (10$\bar{1}$1) plane	3 to 8,[illegible]	Work of fracture	90	IV-2.3	-
	[illegible]	Sapphire (11$\bar{2}$0) plane	[illegible]	Work of fracture	91	IV-2.3	-
	[illegible]	Sapphire (11$\bar{2}$0) plane	32,[illegible]	Work of fracture	91	IV-2.3	-
	[illegible]	Sapphire (10$\bar{1}$1) plane	24,[illegible]	Work of fracture	91	IV-2.3	-
	[illegible]	Sapphire (22$\bar{4}$3) plane	15,[illegible]	Work of fracture	91	IV-2.3	-
	273	-	1112 - [illegible]	-	92	-	-
$Al_2O_3 \cdot 2SiO_2 \cdot 2H_2O$ (Kaolinite)	25	-	[illegible]	Work of fracture	93	IV-2.3	Measured at different adsorbate pressure extrapolated to zero pressure
	25	-	[illegible] to [illegible]	Heat of immersion	64	IV-3.2, IV-4.2	Measured in water
	25	-	[illegible]	Heat of immersion	64	IV-3.2, IV-4.2	Measured in ethanol
	25	-	[illegible] to [illegible]	Heat of immersion	64	IV-3.2, IV-4.2	Measured in n-heptane
$Al_2O_3 \cdot 4SiO_2 \cdot H_2O$ (Pyrophyllite)	25	-	[illegible]	Heat of immersion	64	IV-3.2, IV-4.2	Measured in water
	25	-	[illegible]	Heat of immersion	64	IV-3.2, IV-4.2	Measured in ethanol
	25	-	[illegible] to [illegible]	Heat of immersion	64	IV-3.2, IV-4.2	Measured in n-heptane
AlP	(-273)	Single crystal (100) plane	[illegible]	Sublimation energy approximation	65	V-2	-
	(-273)	Single crystal (110) plane	[illegible]	Sublimation energy approximation	65	V-2	
	(-273)	Single crystal (111) plane	[illegible]	Sublimation energy approximation	65	V-2	
AlSb	(-273)	Single crystal (100) plane	[illegible]	Sublimation energy approximation	65	V-2	-
	(-273)	Single crystal (110) plane	[illegible]	Sublimation energy approximation	65	V-2	
	(-273)	Single crystal (111) plane	[illegible]	Sublimation energy approximation	65	V-2, IV-2.5	Difference between A and B faces [illegible] dyne per cm
B_2O_3	[illegible]	Liquid	[illegible]	Sessile drop	84	-	$d\gamma/dT$ = -0.0[illegible] dyne/cm °C
	[illegible]	Liquid	[illegible]	-	83	V-3	$d\gamma/dT$ = -0.0[illegible] dyne/cm °C

Footnotes at end of table.

TABLE 6. (CONTINUED)

Material	Temperature, °C	Material Condition	Surface Energy, dyne per cm	Method	Original Reference	Relevant Discussion in Text Section	Remarks
$BaCl_2$	962	Liquid	171	Maximum value	94		Air atmosphere
BaF_2	195	Single crystal (111) plane	280*	Double cantilever	38	IV-2.1	Reversible cleavage, no plastic relaxation
	273	Single crystal (111) plane	355	Calculated from elastic constants	28	IV-2.1	
	273	Single crystal (111) plane	303.2*	Full theoretical calculation	18,95	V-1	
	273	Single crystal (110) plane	753.0*	Full theoretical calculation	18,95	V-1	-
BaO	273	Single crystal (100) plane	641	Calculated from lattice energy and ionic radii	82	V-3	-
	273		685	Semiempirical correlations	82	V-3	-
	273	Single crystal (100) plane	1087	Elementary calculations	40	V-1	-
BaS	273	Single crystal (100) plane	1261	Elementary calculations	40	V-1	-
	-	Single crystal (100) plane	415	Heat of sublimation	83	V-2	-
BaSe	273	Single crystal (100) plane	1082	Elementary calculations	40	V-1	-
$BaSO_4$	273	Single crystal (100) plane	480	Calculated from elastic constants	29	IV-2.2	-
Barite	25		76		16	IV-3.2	Dispersion force contribution, see also Reference (16)
	25	Powder, particle size 0.3 μ	490	Heat of immersion	61	IV-3.2, IV-4.2	Immersed in water
	25	Powder, particle size 0.3 μ	140	Heat of immersion	61	IV-3.2, IV-4.2	Immersed in benzene
	25		1250	Dislocation	62	IV-3.3	-
BaTe	273	Single crystal (100) plane	772	Elementary calculations	40	V-1	
BeO	-	Single crystal (0001) plane	See Remarks	Sublimation energy approximation	53	V-2	Minimum value γ_s^T = 2140 - 0.321T (T, deg K)
	-	Single crystal (0001) plane	See Remarks	Sublimation energy approximation	53	V-2	Average value γ_s^T = 2400 - 0.357T (T, deg K)
	2547	Liquid	1013	-	53	-	-
	1400	Single crystal (0001) plane	1760	Solid surface energy approximation	53	V-2	-
	25	Polycrystalline, specific gravity = 2.97	15,000	Work of fracture	69	IV-2.3	Includes extraneous nonelastic energy terms
	273		1420	Semiempirical correlations	82	V-3	γ_L^T = 1986 (1 - T/6000)$^{1.2}$
$BiBr_3$	218	Liquid	65.5	-	83	V-3	$d\gamma_L/dT$ = -0.105 dyne/(cm)(K)
$BiCl_3$	271	Liquid	66.2	-	83	V-3	$d\gamma_L/dT$ = -0.13 dyne/(cm)(K); γ_L = 142 (1 - T/1156)[illegible]
C, Diamond	273	Single crystal (100) plane	9400	Calculated from elastic constants	31	IV-2.2	
	273	Single crystal (110) plane	9400	Calculated from elastic constants	31	IV-2.2	
	273	Single crystal (111) plane	3500	Calculated from elastic constants	31	IV-2.2	-
C, Graphite	25	Pile Grade A carbon	100,000	Work of fracture	60	IV-2.3	Includes nonelastic energy terms
	25	Pile Grade A carbon	50,000	Strain energy release	32	IV-2.3	Analysis by compliance method
	25	Pile Grade A carbon	1 to 1.5 x 10^5	Work of fracture	32	IV-2.3	Considerable crack-branching
	25	Carbon	119	Heat of immersion	58	IV-3.2, 4.2, 4.3	Average from immersion in various liquids
	25		123		16	-	Dispersion force contribution
	25	Powder, particle size 0.004 μ	40	Heat of immersion	61	IV-3.2, 4.2, 4.3	Immersed in water
	25	Powder, particle size 0.50 μ	275	Heat of immersion	61	IV-3.2, 4.2, 4.3	Immersed in benzene
	25	Powder, particle size 0.50 μ	122.5	Heat of immersion	61	IV-3.2, 4.2, 4.3	Immersed in n-heptane
$CaCO_3$	25	Calcite	200 to 1250	Work of fracture	93	IV-2.2	Measured at different adsorbate pressures, extrapolated to zero pressure
	25	Coarse powder	50,000	Crushing	37,38,39	IV-2.4	Far too large, due to experimental and interpretative difficulties
	273	Calcite	380*	Calculated from elastic constants	78	IV-2.2	Calculation includes effect of anisotropies in medium
	273	(10$\bar{1}$1) plane of calcite	190	Calculated from elastic constants	79	IV-2.2	Assumes that carbonate units are not intact in cleavage
	273	Aragonite (100) plane	270	Calculated from elastic constants	79	IV-2.2	
	195	Single crystals calcite (1010) plane	230	Double cantilever	78	IV-2.1	Natural crystals of Iceland spar
$CaCO_3 \cdot MgCO_3$, Dolomite or pearl spar		Single crystal (100) plane	See Remarks	Sublimation energy approximation	53	V-2	Minimum value γ_s^T = 2980 - 1.381T (T, deg K)
		Single crystal (100) plane	See Remarks	Sublimation energy approximation	53	V-2	Average value γ_s^T = 2579 - 1.5[illegible]T (T, deg K)
	1400	Single crystal (100) plane	1600	Sublimation energy approximation	53	V-2	
$CaCl_2$	772	Liquid	152		94		

TABLE 6 (CONTINUED)

Material	Temperature (°C)	Method and comments	Surface energy (ergs/cm²)	Method	Degree of confidence	Internal consistency test	Remarks
CaF_2	0		450	Extrapolation	0	no	Wide distribution of values; lack of experimental data
	25	Single crystal (111) plane	450	Double cleavage	2	no	Small amount of plastic deformation
	25	Cleaved powder	0.3 MN/m	Cleaving	1 to 10	no	Up to two steps
	25	Single crystal (111) plane	450*	Powder calorimetry	2	no	Values perfect; average observed
	27	Single crystal (100) plane	450 ± 5*	Fine filament + matrix	10		
	27	Single crystal (111) plane	340 ± 5*	Fine filament + matrix	10		
	27		340		2		See Also Reference 10
	27	Single crystal (111) plane	1180	Calculated from atomic coordinates	1	no	
CaF_2 K_2O P_2O_5 Apatite	1	Cleaved powder	1.30×10^3	Cleaving	1 to 10	no	Expected to be much greater than value obtained by other techniques
CaO		Single crystal (100) plane	See Remarks	Sublimation energy approximation	10		Maximum value γ_s^T [illegible] dyn/cm
		Single crystal (100) plane	See Remarks	Sublimation energy approximation	10		Average value γ_s^T [illegible] dyn/cm
	1577	Liquid	640	Extrapolation from CaO-SiO_2 systems	10		
	1000	Single crystal (100) plane	1575	Sublimation energy approximation	5		
	25	Cleaved powder, pressed out	1130 ± 200*	Heat of solution	5	no	
	25	Single crystal (100) plane	1400	Dissolution calculations	10		Assumed surface ions to retain hydrates positive temperature coefficient
	27	Single crystal (100) plane	1632*	Correlated from silica energy and vapor data	10		
	27	Single crystal (100) plane	975		1	no	
	27		990	Extrapolated value	10		Assumes Δc_p of [illegible] cal/deg/mol over total temp. range; probably poor
	27		870	Semiempirical correlations	10		
	27	Single crystal (100) plane	1630	Dissolution calculations	10		
	27	Single crystal (100) plane	1050		10		
	27	Single crystal (100) plane	1400–1975	Dissolution calculations and correlations	5		Two different values from dissolution calculations
$CaO \cdot MgO \cdot Al_2O_3 \cdot SiO_2$ Gehlenite		Single crystal (001) plane	See Remarks	Sublimation energy approximation	10		Maximum value γ_s^T [illegible] dyn/cm
		Single crystal (001) plane	See Remarks	Sublimation energy approximation	10		Average value γ_s^T [illegible] dyn/cm
	1400 ± T_g	Melting point	670		10		γ_s^T [illegible] dyn/cm
	1400	Single crystal (001) plane	990	Sublimation energy approximation	10		
	1400		1000*		10		
$CaSO_4$	25	Cleaved powder, pressed out	1400 ± 150*	Heat of solution	5	no	
	25	Single crystal (100) plane	1230 ± 250	Dissolution calculations	10		
CaS	25	Single crystal (100) plane	750		10		
	25	Single crystal (110) plane	1400		10		
	25	Single crystal (100) plane	1100	Dissolution calculations	10		
$CaSe$	25	Single crystal (100) plane	1075	Dissolution calculations	10		
$CaSO_4 \cdot 2H_2O$	0		370	Precipitation	5	no	
$CaTe$	25	Single crystal (100) plane	1150	Dissolution calculations	10		
Calcium oxide	25		350	Heat of immersion	10	no	Interpreted in doubt
Calcium [illegible]	25		330 to 350	Heat of immersion	10	no	Interpreted in doubt
	25		330 to 350	Heat of immersion	10	no	Interpreted as diffusion
	25		1150*	Heat of immersion	10	no	Interpreted as a hydrate
$CdCl_2$	600	Liquid			10		Δc_p of [illegible] dyn/cm
							γ_s^T [illegible] dyn/cm
CdO	970 to 1250		700	Capillary rise	10	no	
	25	Fine powder and large pieces in two spectrometers	1000	Heat of solution	5	no	Values can be a bit dependent on [illegible]
	27	Single crystal (100) plane	1300	Correlated from silica energy and vapor data	10		
	27		1150	Semiempirical correlations	10		
CrO_2Cl_2		Single crystal (010) plane	See Remarks	Sublimation energy approximation	10		Maximum value γ_s^T [illegible] dyn/cm
		Single crystal (010) plane	See Remarks	Sublimation energy approximation	10		Average value γ_s^T [illegible] dyn/cm
	1600	Single crystal (010) plane	510	Sublimation energy approximation	5		

TABLE 6 (CONTINUED)

TABLE 4 (CONTINUED)

Material	Temperature °C	State or Condition	Surface Energy ergs per cm	Method	Original Reference	Relevant Discussion in Text Section	Remarks
Ge	[illegible]	Single crystal (111) plane	[illegible]	Cleavage	[illegible]	IV 2.1	
	[illegible]	Single crystal (100) plane	[illegible]	Calculated from (111) value	[illegible]	IV 2.1	
	[illegible]	Single crystal (110) plane	[illegible]	Calculated from (111) value	[illegible]	IV 2.1	
	273	Single crystal (100) plane	[illegible]	Calculated from elastic constants	31	IV 2.2	
	273	Single crystal (110) plane	[illegible]	Calculated from elastic constants	31	IV 2.2	
	273	Single crystal (111) plane	[illegible]	Calculated from elastic constants	31	IV 2.2	
GeO$_2$	[illegible]	Liquid	[illegible]	[illegible]	[illegible]		[illegible]
	25	Particles [illegible]	[illegible]	Heat of solution	61	IV 3.2, 4.2, 4.3	[illegible]
	25	Fine particles, size 225 Å	[illegible]	Heat of solution	61	IV 3.2, 4.2, 4.3	[illegible]
[illegible]	273	Single crystal (100) plane	[illegible]	Sublimation energy approximation	[illegible]	V 2	
	273	Single crystal (110) plane	[illegible]	Sublimation energy approximation	[illegible]	V 2	
	273	Single crystal (111) plane	[illegible]	Sublimation energy approximation	[illegible]	V 2, IV 2.5	Difference between A and B faces [illegible] dyne per cm
[illegible]	273	Single crystal (100) plane	[illegible]	Sublimation energy approximation	[illegible]	V 2	
	273	Single crystal (110) plane	[illegible]	Sublimation energy approximation	[illegible]	V 2	
	273	Single crystal (111) plane	[illegible]	Sublimation energy approximation	[illegible]	V 2	
[illegible]	273	Single crystal (110) plane	[illegible]	Calculated from elastic constants	31	IV 2.2	
[illegible]	273	Single crystal (100) plane	[illegible]	Sublimation energy approximation	[illegible]	V 2	
	273	Single crystal (110) plane	[illegible]	Sublimation energy approximation	[illegible]	V 2	
	273	Single crystal (111) plane	[illegible]	Sublimation energy approximation	[illegible]	V 2, IV 2.5	Difference between A and B faces [illegible] dyne per cm
[illegible]	[illegible]	Liquid	[illegible]		[illegible]	V 1	[illegible]
[illegible]	[illegible]	Liquid	[illegible]	Maximum bubble pressure	[illegible]		
	[illegible]	Single crystal (100) plane	[illegible]	Full theoretical model	[illegible]	V 1	Includes temperature dependence
	273	Single crystal (100) plane	[illegible]	Born-Mayer theory	6	V 1	Surface tension value
	273	Single crystal (110) plane	[illegible]	Born-Mayer theory	6	V 1	
	273	Single crystal (100) plane	[illegible]	Born-Mayer theory	[illegible]	V 1	
	273	Single crystal (110) plane	[illegible]	Full theoretical model	[illegible]	V 1	Surface tension value
	273	Single crystal (100) plane	[illegible]	Calculated from elastic constants	31	IV 2.2	
	273	Single crystal (110) plane	[illegible]	Calculated from elastic constants	31	IV 2.2	
	273	Single crystal (100) plane	[illegible]	Complete Born-Mayer theory	6	V 1	
	273	Single crystal (100) plane	[illegible]	Full theoretical model	[illegible]	V 1	
	273	Single crystal (110) plane	[illegible]	Full theoretical model	[illegible]	V 1	
[illegible]	[illegible]	Liquid	[illegible]	Maximum bubble pressure	[illegible]		[illegible]
	25	Particles [illegible] per g assumed to be (100) bounded cubes	[illegible]	Heat of solution and surface enthalpy	63	IV 3.3, IV 4.3	Suggested to be high due to contribution from high-energy faces
	25	Single crystal (100) plane	[illegible]	Cleavage	[illegible]	IV 2.1	
	[illegible]	Single crystal (100) plane	[illegible]	Full theoretical model	[illegible]	V 1	Includes temperature dependence
	273	Single crystal (100) plane	[illegible]	Elementary electrostatic theory	[illegible]	V 1	
	273	Single crystal (100) plane	[illegible]	Elementary electrostatic theory	[illegible]	V 1	
	273	Single crystal (100) plane	[illegible]	Elementary electrostatic theory including surface polarization	[illegible]	V 1	Values in brackets denote calculations in which ionic polarization and surface relaxation are included
	273	Single crystal (100) plane	[illegible]	Elementary electrostatic theory including surface polarization	[illegible]	V 1	
	273	Single crystal (100) plane	[illegible]	Elementary electrostatic theory including surface polarization	[illegible]	V 1	
	273	Single crystal (100) plane	[illegible]	Born-Mayer theory	6	V 1	
	273	Single crystal (100) plane	[illegible]	Born-Mayer theory	[illegible]	V 1	
	273	Single crystal (100) plane	[illegible]	Quantum-mechanical calculation	[illegible]	V 1	
	273	Single crystal (100) plane	[illegible]	Born-Mayer theory	[illegible]	V 1	
	273	Single crystal (100) plane	[illegible]	Calculated from elastic constants	31	IV 2.2	
	273	Single crystal (110) plane	[illegible]	Calculated from elastic constants	31	IV 2.2	
	273		[illegible]	Extrapolated from liquid measurements	[illegible]		Does not include phase-change effects
	273	Single crystal (110) plane	[illegible]	Born-Mayer theory	6	V 1	Surface tension value
	273	Single crystal (100) plane	[illegible]	Born-Mayer theory	[illegible]	V 1	Surface tension value
	273	Single crystal (100) plane	[illegible]	Full theoretical model	[illegible]	V 1	Surface tension value
	273	Single crystal (100) plane	[illegible]	Full theoretical model	[illegible]	V 1	
	273	Single crystal (110) plane	[illegible]	Full theoretical model	[illegible]	V 1	
[illegible]	[illegible]	Liquid	[illegible]		[illegible]		
[illegible]	[illegible]	Liquid	[illegible]		[illegible]		

TABLE 6. (CONTINUED)

Material	Temperature[a] °C	Material Condition[b]	Surface Energy[c] dyne per cm	Method	Original Reference	Relevant Discussion in Text Section	Remarks
[illegible]	[illegible]	Liquid	[illegible]	Maximum bubble pressure	[illegible]		
	273	Single crystal [illegible] plane	[illegible]	Born-Mayer theory	[illegible]	[illegible]	Surface tension value
	273	Single crystal [illegible] plane	[illegible]	Born-Mayer theory	[illegible]	[illegible]	Surface tension value
	273	Single crystal (111) plane	[illegible]	Born-Mayer theory	[illegible]	[illegible]	
	273	Single crystal [illegible] plane	[illegible]	Elementary calculations	[illegible]	[illegible]	Surface tension value
	273	Single crystal [illegible] plane	[illegible]	Full theoretical model	[illegible]	[illegible]	Surface tension value
	273	Single crystal [illegible] plane	[illegible]	Full theoretical model	[illegible]	[illegible]	
	273	Single crystal [illegible] plane	[illegible]	Full theoretical model	[illegible]	[illegible]	
[illegible]	[illegible] to 273	Liquid	[illegible]	Maximum bubble pressure	[illegible]		[illegible]
	[illegible]	Single crystal [illegible] plane	[illegible]	Full theoretical model	[illegible]	[illegible]	Including temperature dependence
	273	Single crystal [illegible] plane	[illegible]	Calculated from elastic constants	[illegible]	[illegible]	
	273	Single crystal [illegible] plane	[illegible]	Calculated from elastic constants	[illegible]	[illegible]	
	273	Single crystal [illegible] plane	[illegible]	Born-Mayer theory	[illegible]	[illegible]	Surface tension value
	273	Single crystal [illegible] plane	[illegible]	Born-Mayer theory	[illegible]	[illegible]	Surface tension value
	273	Single crystal (111) plane	[illegible]	Born-Mayer theory	[illegible]	[illegible]	Surface tension value
	273	Single crystal [illegible] plane	[illegible]	Elementary calculations	[illegible]	[illegible]	Surface tension value
	273	Single crystal [illegible] plane	[illegible]	Elementary calculations	[illegible]	[illegible]	Surface tension value
	273	Single crystal [illegible] plane	[illegible]	Full theoretical model	[illegible]	[illegible]	
	273	Single crystal [illegible] plane	[illegible]	Full theoretical model	[illegible]	[illegible]	
[illegible] Al_2O_3 $6SiO_2$ [illegible]	25	Single crystal [illegible] plane	[illegible]	[illegible]	[illegible]	[illegible]	[illegible]
	273	Single crystal [illegible] plane	[illegible]	Calculated from elastic constants	[illegible]	[illegible]	
[illegible]	25		[illegible]	Cleavage	[illegible]	[illegible]	[illegible]
	25		[illegible]	Cleavage	[illegible]	[illegible]	[illegible]
	25	Single crystal	[illegible]	Cleavage	[illegible]	[illegible]	In vacuum
	25	Single crystal	[illegible]	Cleavage	[illegible]	[illegible]	In vacuum
	25	Single crystal [illegible] plane	[illegible]	Cleavage	[illegible]	[illegible]	In air
	25		[illegible] to [illegible]	Cleavage	[illegible]	[illegible]	
[illegible]	[illegible]	Liquid	[illegible]		[illegible]	[illegible]	[illegible]
[illegible]	[illegible]	Liquid	[illegible]	[illegible]	[illegible]	[illegible]	
[illegible]	[illegible]	Liquid	[illegible]		[illegible]	[illegible]	[illegible]
[illegible]	273	Single crystal [illegible] plane	[illegible]	Elementary calculations	[illegible]	[illegible]	
	273	Single crystal [illegible] plane	[illegible]	Full theoretical model	[illegible]	[illegible]	[illegible]
	273	Single crystal [illegible] plane	[illegible]	Full theoretical model	[illegible]	[illegible]	[illegible]
	273	Single crystal [illegible] plane	[illegible]	Full theoretical model	[illegible]	[illegible]	Surface tension value
[illegible]	[illegible]	Liquid	[illegible]	Maximum bubble pressure	[illegible]		[illegible]
	273	Single crystal [illegible] plane	[illegible]	Elementary calculations	[illegible]	[illegible]	
	273	Single crystal [illegible] plane	[illegible]	Full theoretical model	[illegible]	[illegible]	[illegible]
	273	Single crystal [illegible] plane	[illegible]	Full theoretical model	[illegible]	[illegible]	[illegible]
	273	Single crystal [illegible] plane	[illegible]	Full theoretical model	[illegible]	[illegible]	Surface tension value
[illegible]	[illegible] to [illegible]	Liquid	[illegible]	Maximum bubble pressure	[illegible]		[illegible]
	25	Single crystal [illegible] plane	[illegible]	Double cantilever	[illegible]	[illegible]	[illegible]
	[illegible]	Single crystal [illegible] plane	[illegible]	Full theoretical model	[illegible]	[illegible]	[illegible]
	[illegible]	Single crystal [illegible] plane	[illegible]	Double cantilever	[illegible]	[illegible]	[illegible]
	[illegible]	Single crystal [illegible] plane	[illegible]	Double cantilever	[illegible]		[illegible]
	[illegible]	Single crystal	[illegible]	Double cantilever	[illegible]	[illegible]	[illegible]
	[illegible]	Single crystal [illegible] plane	[illegible]	Double cantilever	[illegible]	[illegible]	[illegible]
	[illegible]	Single crystal [illegible] plane	[illegible]	Double cantilever	[illegible]	[illegible]	[illegible]
	273	Single crystal [illegible] plane	[illegible]	Elementary calculations	[illegible]	[illegible]	

TABLE 4 (CONTINUED)

Material	Temperature, °C	Nature of Crystal	Surface Energy, dyne per cm	Method	Original Reference	Relevant Discussion in Text Section	Remarks
LiF, Continued	273		[illegible]		[illegible]		
	273	Single crystal, 100 plane	3?0	Calculated from elastic constants	31	IV 2.2	
	273	Single crystal, 110 plane	[illegible]	Calculated from elastic constants	31	IV 2.2	
	273	Single crystal, 100 plane	[illegible]	Fit theoretical model	[illegible]	V 1	Surface tension value
	273	Single crystal, 100 plane	142	Fit theoretical model	[illegible]	V 1	Includes surface relaxation
	273	Single crystal, 100 plane	[illegible]	Fit theoretical model	[illegible]	V 1	Includes surface relaxation
LiI	273	Single crystal, 100 plane	[illegible]	[illegible] calculations	[illegible]	V 1	Surface tension value
	273	Single crystal, 100 plane	545*	Fit theoretical model	[illegible]	V 1	Surface tension value
	273	Single crystal, 100 plane	[illegible]	Fit theoretical model	[illegible]	V 1	Includes surface relaxation
	273	Single crystal, 110 plane	228	Fit theoretical model	[illegible]	V 1	
$LiNO_3$	254	Liquid	1[illegible]		83	V 3	[illegible]
Li_2SO_4	[illegible]	Liquid	2[illegible]		[illegible]	V 3	[illegible]
Li_2SiO_3	1254	Liquid	3[illegible].6		[illegible]		[illegible]
MgO		Single crystal, 100 plane	See Remarks	Sublimation energy approximation	53	V 2	[illegible]
		Single crystal, 100 plane	See Remarks	Sublimation energy approximation	53	V 2	[illegible]
	2800	Liquid	5[illegible]		53		[illegible]
	1400	Single crystal, 100 plane	1[illegible]	Sublimation energy approximation	53	V 2	
	25	Polycrystalline, grain size [illegible] μ	[illegible]	Work of fracture, including kinetic energy terms	69	IV 2.3, IV 4.4	Specific gravity 3.[illegible]
	25	Polycrystalline, grain size [illegible] μ	[illegible]	Work of fracture, including kinetic energy terms	69	IV 2.3, IV 4.4	Specific gravity 3.51
	25	Polycrystalline, grain size [illegible] μ	[illegible]	Work of fracture, including kinetic energy terms	69	IV 2.3, IV 4.4	Specific gravity 3.[illegible]
	25	Polycrystalline, grain size [illegible] μ	[illegible]	Work of fracture, including kinetic energy terms	69	IV 2.3, IV 4.4	Specific gravity 3.[illegible]
	25	Polycrystalline, grain size [illegible] μ	[illegible]	Work of fracture, including kinetic energy terms	69	IV 2.3, IV 4.4	Specific gravity 3.50
	25	Polycrystalline, grain size [illegible] μ	[illegible]	Work of fracture, including kinetic energy terms	69	IV 2.3, IV 4.4	
	25	Polycrystalline, grain size [illegible] μ	[illegible]	Work of fracture, including kinetic energy terms	69	IV 2.3, IV 4.4	
	25	Polycrystalline, grain size [illegible] μ	[illegible]	Work of fracture, including kinetic energy terms	69	IV 2.3, IV 4.4	
	25	Polycrystalline, grain size [illegible] μ	[illegible]	Work of fracture, including kinetic energy terms	69	IV 2.3, IV 4.4	
	25	Polycrystalline, grain size [illegible] μ	[illegible]	Work of fracture, including kinetic energy terms	69	IV 2.3, IV 4.4	
	25	Single crystal	[illegible] to [illegible]	Cleavage	[illegible]	IV 2.1, IV 4.1	[illegible]
	25	Single crystal	[illegible]	Work of fracture, including kinetic energy terms	[illegible]	IV 2.3	[illegible]
	25	Single crystal	[illegible]	Work of fracture, including kinetic energy terms	69	IV 2.3	[illegible]
	25	Single crystal, 100 plane	[illegible]	[illegible] double cantilever	[illegible]	IV 2.1	[illegible]
	25		[illegible]	Double cantilever	[illegible]	IV 2.1	[illegible]
	25		[illegible]	Double cantilever	[illegible]	IV 2.1, IV 4.1	[illegible]
	25		[illegible]	Double cantilever	[illegible]	IV 2.1, IV 4.2	[illegible]
	25		[illegible]	[illegible]	83	V 3	[illegible]
	25	Single crystal, 100 plane	[illegible]	Double cantilever	[illegible]	IV 2.1	[illegible]
	25	Single crystal, 100 plane	[illegible]	Double cantilever	[illegible]	IV 2.1	[illegible]
	[illegible]	Single crystal, 100 plane	[illegible]	Fit theoretical model	[illegible]	V 1	[illegible]
	[illegible]	Single crystal	[illegible]	Double cantilever	[illegible]	IV 2.1	
	[illegible]		[illegible]	Double cantilever	[illegible]	IV 2.1	
	[illegible]	Single crystal, 100 plane	[illegible]	Double cantilever	[illegible]	IV 2.1	
	[illegible]		[illegible]	Cleavage	[illegible]	IV 2.1	[illegible]
	[illegible]	Single crystal, 100 plane	[illegible]	Double cantilever	[illegible]	IV 2.1	
	[illegible]	Single crystal, 100 plane	[illegible]	Calculated from elastic constants	[illegible]	IV 2.2	
	[illegible]	Single crystal, 110 plane	[illegible]	Calculated from elastic constants	[illegible]	IV 2.2	
	[illegible]	Single crystal	[illegible]	Double cantilever	[illegible]	IV 2.1	
	273 to [illegible]		[illegible] to [illegible]	[illegible]	[illegible]	IV 3.3	[illegible]
	273	Single crystal, 100 plane	[illegible]	[illegible] calculations and corrections	[illegible]	[illegible]	[illegible]
	273	Single crystal, 100 plane	[illegible]	Heat of sublimation	83	V 1	

TABLE 6. (CONTINUED)

Material	Temperature[a], K	Material Condition[b]	Surface Energy[c], dyne per cm	Method	Original Reference	Relevant Discussion in Text Section	Remarks
[illegible] Spinel	[illegible]	Single crystal, [illegible] plane	[illegible]	Subroutine energy approximation	53	[illegible]	
		Single crystal, [illegible] plane	See Remarks	Subroutine energy approximation	53	[illegible]	[illegible]
		[illegible]	See Remarks	Subroutine energy approximation	53	[illegible]	Average value [illegible]
	273	Single crystal, [illegible] plane	[illegible]	[illegible] elastic constants	[illegible]	[illegible]	Cleavage assumed [illegible] the [illegible] bond
[illegible]	75	Powders	[illegible]	Heat of solution	83	[illegible]	Comparison of different powder sizes
[illegible]	75	Single crystal, [illegible] plane	[illegible]	Heat of [illegible]	83		
	273	Single crystal, [illegible] plane	[illegible]		[illegible]		
	273	Single crystal, [illegible] plane	[illegible]		[illegible]		
	273	Single crystal, [illegible] plane	[illegible]	Elementary calculations	[illegible]	[illegible]	
[illegible]	273	Single crystal, [illegible] plane	[illegible]	Elementary calculations	[illegible]	[illegible]	
[illegible]	273	Single crystal, [illegible] plane	[illegible]	Calculated from elastic constants	[illegible]	[illegible]	[illegible]
[illegible]	[illegible]	Liquid [illegible]	[illegible]	Extrapolation of values [illegible]	[illegible]		[illegible]
	[illegible]		[illegible]	Extrapolation	[illegible]	[illegible]	
	273	Single crystal, [illegible] plane	[illegible]	Calculated from [illegible] energy and [illegible]	[illegible]	[illegible]	
	273		[illegible]		[illegible]	[illegible]	
[illegible]	273	Single crystal, [illegible] plane	[illegible]	Heat of [illegible]	83	[illegible]	
[illegible]	75	Coarse powder [illegible] and [illegible]	[illegible]	Crushing	[illegible]	[illegible]	Expected to be much greater than value obtained by other techniques
[illegible]	[illegible]	Liquid	[illegible]	[illegible] bubble pressure	[illegible]	[illegible]	Surface tension value
	273	Single crystal, [illegible] plane	[illegible]	Born-Mayer theory	[illegible]	[illegible]	Surface tension value
	273	Single crystal, [illegible] plane	[illegible]	Born-Mayer theory	[illegible]	[illegible]	
	273	Single crystal, 111 plane	[illegible]	Born-Mayer theory	[illegible]	[illegible]	Surface tension value
	273	Single crystal, [illegible] plane	[illegible]	Full theoretical model	[illegible]	[illegible]	
	273	Single crystal, [illegible] plane	[illegible]	Full theoretical model	[illegible]	[illegible]	
	273	Single crystal, [illegible] plane	[illegible]	Full theoretical model	[illegible]	[illegible]	
	273	Single crystal, [illegible] plane	[illegible]	Calculated from elastic constants	[illegible]	[illegible]	
	273	Single crystal, [illegible] plane	[illegible]	Calculated from elastic constants	[illegible]	[illegible]	
	273	Single crystal, [illegible] plane	[illegible]	Elementary theory	[illegible]	[illegible]	Surface tension value
[illegible]	[illegible]	Single crystal, [illegible] plane	See Remarks	Subroutine energy approximation	[illegible]		[illegible]
	[illegible]	Liquid	[illegible]	Maximum bubble pressure	[illegible]		[illegible]
	[illegible]	Liquid	[illegible]		53		Measured in air
	75		[illegible]	Impact cleavage	[illegible]	[illegible]	
	75	Single crystal, [illegible] plane	[illegible]	Heat of solution	[illegible]	[illegible]	
	75		[illegible]	Heat of solution	[illegible]	[illegible]	
	75		[illegible] to [illegible]	Double cantilever	[illegible]	[illegible]	
	75		[illegible]		[illegible]		
	75	Fine powder	[illegible]	Heat of melting	[illegible]	[illegible]	
	75		[illegible]	Subroutine energy approximation	53	[illegible]	
	75	Fine powder	[illegible] to [illegible]	Heat of solution	[illegible]	[illegible]	
	[illegible]	Single crystal, [illegible] plane	[illegible]	Full theoretical model	[illegible]		Including temperature dependence
	[illegible]	Single crystals	[illegible]	Double cantilever	[illegible]	[illegible]	In air [illegible]
	[illegible]	Single crystals	[illegible]	Double cantilever	[illegible]	[illegible]	
	[illegible]	Single crystal, [illegible] plane	[illegible]	Double cantilever	[illegible]	[illegible]	In vacuum
	[illegible]	Single crystal, [illegible] plane	[illegible]	Double cantilever	[illegible]	[illegible]	In liquid nitrogen
	273	Single crystal, [illegible] plane	[illegible]	Lattice energy approximation	53	[illegible]	
	[illegible]	Single crystal, [illegible] plane	[illegible]	Extrapolation	[illegible]	[illegible]	From liquid surface tension, phase change not accounted for
	273	Single crystal, [illegible] plane	[illegible]	Calculated from [illegible] forces	[illegible]	[illegible]	
	273	Single crystal, [illegible] plane	[illegible]	Born-Mayer theory	[illegible]	[illegible]	Surface tension value
	273	Single crystal, [illegible] plane	[illegible]	Born-Mayer theory	[illegible]	[illegible]	Surface tension value
	273	Single crystal, 111 plane	[illegible]	Born-Mayer theory	[illegible]	[illegible]	Surface tension value
	273	Single crystal, [illegible] plane	[illegible]	Full theoretical model	[illegible]	[illegible]	Surface tension value
	273	Single crystal, [illegible] plane	[illegible]	Heat of solution	[illegible]	[illegible]	Surface tension value
	273	Single crystal, [illegible] plane	[illegible]	Full theoretical model	[illegible]	[illegible]	
	273	Single crystal, [illegible] plane	[illegible]	Full theoretical model	[illegible]	[illegible]	
	273		[illegible]	Extrapolation			

TABLE 6. (CONTINUED)

Material	Temperature[a] °C	Nature of Condition[b]	Surface Energy[c] (ergs/cm²)	Method	Original Reference	Relevant Discussion in Text Section	Remarks
[illegible]	[illegible] to [illegible]	Liquid	[illegible]	Maximum bubble pressure	99		
	273	Single crystal, (100) plane	[illegible]	Born-Mayer theory	[illegible]	V.1	Surface tension value
	273	Single crystal, (110) plane	[illegible]	Born-Mayer theory	6	V.1	Surface tension value
	273	Single crystal, (111) plane	[illegible]	Born-Mayer theory	6	V.1	Surface tension value
	273	Single crystal, (100) plane	[illegible]	Full theoretical radii	[illegible]	V.1	Surface tension value
	273	Single crystal, (100) plane	[illegible]	Elementary calculations	[illegible]	V.1	Surface tension value
	273	Single crystal, (110) plane	[illegible]	Full theoretical radii	[illegible]	V.1	
	273	Single crystal, (110) plane	[illegible]	Full theoretical radii	[illegible]	V.1	
[illegible]	651	Liquid	[illegible]	Maximum bubble pressure	99		
	[illegible]	Single crystal, (100) plane	[illegible]	Full theoretical radii	[illegible]	V.1	Including temperature dependence
	273	Single crystal, (100) plane	[illegible]	Born-Mayer theory	6	V.1	Surface tension value
	273	Single crystal, (110) plane	[illegible]	Born-Mayer theory	6	V.1	Surface tension value
	273	Single crystal, (111) plane	[illegible]	Born-Mayer theory	6	V.1	Surface tension value
	273	Single crystal, (100) plane	[illegible]	Full theoretical radii	6	V.1	Surface tension value
	273	Single crystal, (100) plane	[illegible]	Elementary calculations	[illegible]	V.1	Surface tension value
	273	Single crystal, (110) plane	[illegible]	Full theoretical radii	[illegible]	V.1	
	273	Single crystal, (110) plane	[illegible]	Full theoretical radii	[illegible]	[illegible]	
[illegible]	[illegible]	Liquid	116.6	Maximum bubble pressure	114		[illegible]
[illegible]	[illegible]	Liquid	[illegible]		83		
[illegible]	[illegible]	Liquid	[illegible]		83		
[illegible]	25	Powder	[illegible]	Heat of [illegible]	64	[illegible]	[illegible]
[illegible]	25	Powder	[illegible] to [illegible]	Heat of [illegible]	64	[illegible]	[illegible]
	25	Powder	[illegible]	Heat of [illegible]	64	[illegible]	[illegible]
	25	Powder	[illegible] to [illegible]	Heat of [illegible]	64	[illegible]	[illegible]
[illegible]	[illegible]	Liquid	[illegible]	[illegible]	[illegible]		[illegible]
[illegible]	[illegible]		[illegible]	[illegible]	62	[illegible]	
[illegible]	25		[illegible]	[illegible]	62	[illegible]	
PbO	[illegible]	Liquid	[illegible]		83	V.3	[illegible]
	273		[illegible]	Semiempirical correlation		V.3	
PbS (Galena)	273	Single crystal, (100) plane	[illegible]	Calculated from elastic constants	31	[illegible]	
	273	Single crystal, (110) plane	[illegible]	Calculated from elastic constants	31	[illegible]	
	273	Single crystal, (100) plane	[illegible]	[illegible]	83		
[illegible]	[illegible]	Liquid	[illegible]	Maximum bubble pressure	99		
	273	Single crystal, (100) plane	[illegible]	Elementary calculation	[illegible]	V.1	Surface tension value
	273	Single crystal, (100) plane	[illegible]	Full theoretical radii	[illegible]	V.1	Surface tension value
	273	Single crystal, (110) plane	[illegible]	Full theoretical radii	[illegible]	V.1	
	273	Single crystal, (110) plane	[illegible]	Full theoretical radii	[illegible]	V.1	
[illegible]	[illegible]	Liquid	[illegible]	Maximum bubble pressure	99		Surface tension value
	273	Single crystal, (100) plane	[illegible]	Elementary calculation	[illegible]	V.1	
	273	Single crystal, (100) plane	[illegible]	Full theoretical radii	[illegible]	V.1	
	273	Single crystal, (110) plane	[illegible]	Full theoretical radii	[illegible]	V.1	
	273	Single crystal, (110) plane	[illegible]	Full theoretical radii	[illegible]	V.1	
[illegible]	[illegible]	Liquid	[illegible]	Maximum bubble pressure	[illegible]	[illegible]	Surface tension value
	273	Single crystal, (100) plane	[illegible]	Elementary calculation	[illegible]	V.1	
	273	Single crystal, (100) plane	[illegible]	Full theoretical radii	[illegible]	V.1	
	273	Single crystal, (110) plane	[illegible]	Full theoretical radii	[illegible]	V.1	
[illegible]	[illegible]	Liquid	[illegible]	Maximum bubble pressure	99		Surface tension value
	273	Single crystal, (100) plane	[illegible]	Elementary calculation	[illegible]	V.1	Surface tension value
	273	Single crystal, (100) plane	[illegible]	Full theoretical radii	[illegible]	V.1	
	273	Single crystal, (110) plane	[illegible]	Full theoretical radii	[illegible]	V.1	
	273	Single crystal, (110) plane	[illegible]	Full theoretical radii	[illegible]	V.1	
[illegible]	[illegible]	Liquid	[illegible]		[illegible]		
[illegible]	[illegible]	Liquid	[illegible]		[illegible]		

TABLE 6. (CONTINUED)

Material	Temperature,[a] C	Material Condition[b]	Surface Energy,[c] dyne per cm	Method	Original Reference	Relevant Discussion in Text Section	Remarks
[illegible]	25	Powder	[illegible]	Heat of solution	[illegible]	IV 3.3, IV 4.3	Comparison between numbers of various size distributions
[illegible]	25	Single crystal, (111) plane	[illegible]	Cleavage	[illegible]	IV-2.1	
	25	Single crystal, [illegible] plane	[illegible]	Calculated from results on (111) plane, assuming known anisotropies	[illegible]	IV 2.1	
	25	Single crystal, [illegible] plane	[illegible]	Calculated from results on plane, assuming known anisotropies	[illegible]	IV 2.1	
	[illegible]	Single crystal, (111) plane	[illegible]	Double cantilever	[illegible]	IV 2.1	Tendency to crack branching and difficulty in experimental analysis
	273	Single crystal, (111) plane	[illegible]	Calculated from elastic constants	31	IV 2.2	
	273	Single crystal, [illegible] plane	[illegible]	Calculated from elastic constants	31	IV 2.2	
	273	Single crystal, [illegible] plane	[illegible]	Calculated from elastic constants	31	IV 2.2	
[illegible]		Single crystal, [illegible] plane	See Remarks	Sublimation energy approximation	53	V.2	Maximum value γ_s^T = [illegible] (T - deg K)
		Single crystal, [illegible] plane	See Remarks	Sublimation energy approximation	53	V.2	Average value γ_s^T = [illegible] (T - deg K)
	[illegible]	Single crystal, [illegible] plane	[illegible]	Sublimation energy approximation	53	V.2	
[illegible]	25		[illegible]	Work of fracture	[illegible]	IV 2.3	[illegible]
[illegible]		[illegible], [illegible] plane	See Remarks	Sublimation energy approximation	53	V.2	Maximum value γ_s^T = [illegible] (T - deg K)
		[illegible], [illegible] plane	See Remarks	Sublimation energy approximation	53	V.2	Average value γ_s^T = [illegible] (T - deg K)
	[illegible]	Liquid	[illegible]	[illegible]	[illegible]		[illegible]
	[illegible]	Liquid	[illegible]		53	V.2	[illegible]
	[illegible]	[illegible], [illegible] face	[illegible]	[illegible]	53	V.2	
	[illegible]	Liquid alloys	[illegible]	Extrapolation from alloy systems	[illegible]		
	[illegible]	Amorphous films	[illegible]	Film elongation	[illegible]	IV 2.6	[illegible]
	[illegible]	Polycrystalline	[illegible]	Crushing	[illegible]	IV 2.8	
	25		[illegible]	Double cantilever	[illegible]	IV 2.1, IV 4.1	[illegible]
	25		[illegible]	Spreading pressure	[illegible]	[illegible]	[illegible]
	25		[illegible]		[illegible]		
	25		[illegible]	Work of fracture	[illegible]	IV 2.3, IV 4.1	Measured as function of adsorbate pressure
	25	Single crystal, [illegible] plane quartz	[illegible]	Double cantilever	[illegible]	IV 2.1	
	25	Single crystal, [illegible] plane quartz	[illegible]	Double cantilever	[illegible]	IV 2.1	Average value
	25	Single crystal, [illegible] plane quartz	[illegible]	Double cantilever	[illegible]	IV 2.1	
	25	Single crystal, [illegible] plane quartz	[illegible]	Double cantilever	[illegible]	IV 2.1	
	25	[illegible] particle size	[illegible]	Heat of immersion	[illegible]	IV 3.2, IV 4.2	Immersed in water
	25	Amorphous SiO_2, [illegible] particle size	[illegible]	Heat of immersion	[illegible]	IV 3.2, IV 4.2	Immersed in water
	25	Amorphous SiO_2, [illegible] particle size	[illegible]	Heat of immersion	[illegible]	IV 3.2, IV 4.2	Immersed in benzene
	25	[illegible] particle size	[illegible]	Heat of immersion	[illegible]	[illegible]	Immersed in water
	25	[illegible] particle size	[illegible]	Heat of immersion	[illegible]	IV 3.2, IV 4.2	Immersed in [illegible]
	25	[illegible] powder	[illegible]	Crushing	[illegible]	IV 2.8	Far too large, due to experimental and interpretation difficulties
	[illegible]		[illegible]	Heat of solution	[illegible]	IV 3.3	
	[illegible]		[illegible]	Double cantilever	[illegible]	IV 2.1	
	[illegible]		[illegible]	Double cantilever	[illegible]	IV 2.1	
[illegible]	[illegible]	Liquid	[illegible]		[illegible]	[illegible]	[illegible]
[illegible]	25		[illegible]	Spreading pressure	[illegible]	[illegible]	For polar contribution to surface energy see Footnote [illegible]
[illegible]	[illegible]	Single crystal, [illegible] plane	[illegible]	For theoretical model	[illegible]	[illegible]	
	273	Single crystal, (111) plane	[illegible]	Empirical calculations	[illegible]	[illegible]	
[illegible]	273		[illegible]	[illegible]	[illegible]	[illegible]	
	273	Single crystal, [illegible] plane	[illegible]	Empirical calculations	[illegible]	[illegible]	
[illegible]	[illegible]	Single crystal, [illegible] plane	[illegible]	Empirical calculations	[illegible]	[illegible]	
[illegible]	[illegible]		[illegible]	[illegible]	[illegible]	[illegible]	

TABLE 6. (CONTINUED)

Material	Temperature,[a] C	Nature of Condition[b]	Surface Energy,[c] erg per cm	Method	Original Reference	Relevant Discussion in Text Section	Remarks
[illegible]	[illegible]	Single crystal, [illegible] plane	[illegible]	Elementary calculations	[illegible]	[illegible]	
[illegible]	[illegible]	Single crystal, [illegible] plane	[illegible]	Elementary calculations	[illegible]	[illegible]	
TaC	1100		[illegible]	Semiempirical correlations	[illegible]	[illegible]	
ThO_2	[illegible] to [illegible]		[illegible]	Contact angles	[illegible]	[illegible]	
	[illegible]	Single crystal, [illegible] plane	[illegible]	For theoretical model	[illegible]	[illegible]	
	[illegible]		[illegible]	Semiempirical correlations	[illegible]	[illegible]	
TiB_2	[illegible] to [illegible]	Polycrystalline	[illegible]	Contact angle	[illegible]	[illegible]	Sessile liquid contact angle measured as function of temperature
TiC	1100		[illegible]	Semiempirical correlations	[illegible]	[illegible]	
	[illegible] to [illegible]	Polycrystalline	[illegible]	Contact angles	[illegible]	[illegible]	Same method as for TiB_2
TiN	[illegible] to [illegible]	Polycrystalline	[illegible]	Contact angle	[illegible]	[illegible]	Same method as for TiB_2
TiO_2	-	Single crystal, 110 plane	See Remarks	Subsurface energy approximation	[illegible]	[illegible]	[illegible] value [illegible]
		Single crystal, 110 plane	See Remarks	Subsurface energy approximation	[illegible]	[illegible]	Average value [illegible]
	[illegible]	Single crystal, 110 plane	[illegible]	Subsurface energy approximation	[illegible]	[illegible]	
	25		[illegible]	Spreading pressure	[illegible]	[illegible]	Using n-heptane
	25	Anatase, particle size [illegible]	[illegible]	Heat of immersion	[illegible]	[illegible]	Immersed in water
	25	Rutile, particle size [illegible]	[illegible] to [illegible]	Heat of immersion	[illegible]	[illegible]	Immersed in water
	[illegible]		[illegible]	Spreading pressure	[illegible]	[illegible]	Using butane
	[illegible]		[illegible]	Spreading pressure	[illegible]	[illegible]	Use of nitrogen
	[illegible]	Single crystal, 110 plane	[illegible]	Calculated from elastic constants	[illegible]	[illegible]	
UC	[illegible]		[illegible]	Semiempirical correlations	[illegible]	[illegible]	
UO_2	[illegible]	Liquid	[illegible]	Sessile drop			
	[illegible]	Polycrystalline	[illegible]	Contact angles	[illegible]	[illegible]	
	[illegible]		[illegible]	"Contact angles" and extrapolation	[illegible]	[illegible]	
	[illegible]	Single crystal, 111 plane	[illegible]	For theoretical model	[illegible]	[illegible]	
VC	1100		[illegible]	Semiempirical correlations	[illegible]	[illegible]	
$ZnCO_3$			[illegible]		[illegible]	[illegible]	
ZnO	[illegible]	Liquid	[illegible]	Extrapolating from liquid [illegible]	[illegible]	[illegible]	
	[illegible] to [illegible]		[illegible]	Contact angles	[illegible]	[illegible]	
	[illegible]		[illegible]	Work of fracture	[illegible]	[illegible]	
	[illegible]		[illegible]	Semiempirical correlations	[illegible]	[illegible]	This value is obtained assuming [illegible]
ZnS	25	Single crystal, 110 plane	[illegible]	Calculated from elastic constants	[illegible]	[illegible]	
Sphalerite	25	Cubic powder	[illegible]	Crushing	[illegible]	[illegible]	[illegible]
ZrC	1100		[illegible]	Semiempirical correlations	[illegible]	[illegible]	
ZrO_2	[illegible]	Polycrystalline	[illegible]	Semiempirical correlations [illegible]	[illegible]	[illegible]	Includes grain boundary effects
	25	Powder, particle size [illegible]	[illegible]	Heat of immersion	[illegible]	[illegible]	Immersed in water
	25	Powder, particle size [illegible]	[illegible]	Heat of immersion	[illegible]	[illegible]	Immersed in benzene
	[illegible]		[illegible]	Semiempirical correlations	[illegible]	[illegible]	Assumed [illegible]

Footnotes on following page.

Footnotes for Table 6

(a) The temperatures in parentheses are presumed to be the temperatures of the determination, as indicated by the method used

(b) The surface tension of some molten ceramics (fused salts) at or near their melting point is included, where no other information is available or where the relation to solid surface energy might be of interest. See also Appendix C, Table C-1

(c) Values marked with an asterisk (*) are believed to be particularly accurate for the experimental conditions, where this judgment has, for the most part, been made by other investigators. The absence of a value so designated should not be interpreted as meaning that no value is reliable

(d) The dihedral angle measurement usually involves the geometry shown in the accompanying figure, in which a grain boundary is taken as perpendicular to the surface. The ψ, can develop, in which case the solid surface energy is taken to be $\gamma_S = 2\,\gamma_{SA} \cos \psi/2$. γ_{SA} is the interface energy between the solid and the appropriate atmosphere (liquid, vapor, or gas).

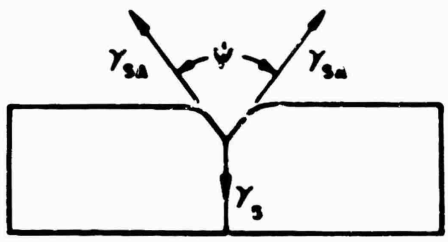

FIGURE 22. DIHEDRAL ANGLE GEOMETRY

(e) The somewhat lower value given here is not completely representative of the system under consideration, inasmuch as the composition quoted by King[51] is said to be $CaO\text{-}Al_2O_3\text{-}SiO_2$. The argument given states, in effect, that the lower value is the result of migration of a low-energy component in this liquid species. It is also noteworthy that the absence of the MgO component would not necessarily achieve the same end, since the liquid MgO has a surface tension not too dissimilar from that quoted in this citation. Of course, since MgO has a higher melting point, the inclusion of MgO in the mineral gehlenite is expected to raise the surface tension. Hence, qualitative arguments would suggest that the absence of MgO would, on the average, produce a material with lower surface tension at a given temperature

VI-2. The Surface Energy of Glasses

In the preceding tabulation and discussion of the surface energy of solids, we have purposely omitted consideration of the properties of glasses. At this point, it is well to consider some of the difficulties that might be expected, not so much in the measurement of surface energy but in the interpretation of experimental results. One basic difference between glasses and crystalline materials relates to the comparative difficulties in such measurement and interpretation. For the most part, glasses are elastically isotropic and, over the temperature range where they are brittle, lend themselves to a straightforward phenomenological analysis of fracture energies, surface energies, etc. However, the structure of glass, on an atomic scale, is such that no fundamental calculations are possible on the basis of atomic arrangements, lattice distortion near the surface, and similar considerations.

On the other hand, while crystalline materials may be investigated rigorously (as was the case with Benson's theoretical work[18], certain difficulties are encountered in the analysis of experimental work where crystalline anisotropies must be taken into account.

Two particular aspects of the surface energies of glasses should be touched upon; namely, the surface energies of solid glasses and the surface tension of liquid glasses. The first of these has been covered in some detail by the recent work of Wiederhorn[17], who included considerable review work along with his recent original findings. This contribution should be coupled with the paper by Mould[9], who discussed many details of the fracture of glass. Inasmuch as these other papers are fairly self-contained, we shall not discuss solid glasses further at this point, but will include, on the following pages, representative samples of data on various glass systems.

The second point, the surface tensions of liquid glasses, should be mentioned briefly here, and further reference will be made in the following table. There is a considerable body of data available on the surface tensions and contact angles of a number of different glasses, many of these being mixtures of many (perhaps five or more) different compounds, such as SiO_2, B_2O_3, Na_2O, P_2O_5, K_2O. In addition, much work has been done on the surface tension and viscosity of the liquid phases used in enameling, where these are similarly composed of multiple compounds. Such data can be of exceeding importance in correlative studies of the surface energies of solids if sufficient reliable information is available for these comparisons. One of the more useful tools (if it is, indeed, applicable) lies in the use of Bruce's correlations[24] of the liquid surface tension, the critical temperature, the surface energy at absolute zero and the temperature coefficient of the surface energies of both the liquid and solid state. The use of this technique depends, of course, on the degree to which one can define and use the critical temperature as a meaningful parameter particularly when applied to a mixture of liquids and on the availability of reliable data on the temperature dependence of the liquid surface tension.

For single liquid oxides, such data can be obtained from the literature (in some cases) by extrapolation of the results reported for mixtures, thereby achieving relatively reliable end-point values of surface tensions as a function of temperature.

The data collected for the surface tensions of liquids and their mixtures also has great applicability in the use of the Zisman-Eberhart technique for determining the

surface energy of selected solids, particularly at temperatures where more "conventional" liquids cannot be used.

Table 7 lists the surface energies of various glasses. Surface energy is best characterized in soda-lime glass, particularly because of the work of Wiederhorn[25], who undertook a rather thorough study on the surface energy of it. He investigated, in some detail, the effects of various atmospheres on crack velocities and acceleration, using the relations defined in Equations (27) and (28). The most probable value, as measured by crack propagation techniques at -196 C, is given as 3200 dyne per cm, as measured in a nitrogen atmosphere.

TABLE 7. SURFACE ENERGIES OF VARIOUS GLASSES

Type of Glass	Temperature, C	Surface Energy, dynes per cm	Method	Reference	Remarks
Plate Glass	25	3400-5200	Modified edge crack bend specimen	34	Similar to experiments by Wiederhorn[117]
High Lead Glass	25	3500	Double cantilever	117	Corning 0041
	-196	4110	Double cantilever	117	Corning 0041
Borosilicate Glass	25	4750	Double cantilever	117	Corning 7740
	-196	4800	Double cantilever	117	Corning 7740
Aluminosilicate Glass	25	4650	Double cantilever	117	Corning 1720
	-196	5210	Double cantilever	117	Corning 1720
Lead Disilicate Glass	400 to 700	210	Fiber elongation	2, 123	Vacuum environment
	20	1210	Crack propagation	123	Vacuum environment
	20	290	Crack propagation	123	H_2O environment
"Glass"[a]		1214	--	29	Unspecified conditions of experiment and composition of materials; early works referenced in Reference (23)
		540	--	29	
	1000	310	--	83	$Na_2Si(O)_3$ glass (liquid)
	1300	218.4	--	83	Liquid, NBS lead glass (F 750/27.7)
	1300	310.6	--	83	Liquid, NBS barium glass (BaC 617/55.0)
	1300	251.6	--	83	Liquid, NBS soda borate glass (LC 5125/60.5), $d\gamma_L/dT$ = -0.05 dyne per cm
Vycor	25	4000	Double cantilever	117	Corning 7913
	-196	4170	Double cantilever	117	Corning 7913
Soda-lime Glass	25	3820	Double cantilever	117	Nitrogen atmosphere
	-196	4530	Double cantilever	117	--
	-60	4380	Double cantilever	117	--
	25	4060	Double cantilever	38	In vacuum; see Wiederhorn[116] for specifics
	25	7000	Strain energy release	32	--
	25	9800	Compliance	32	--
	25	4-6000	Work of fracture	32	--
	25	3000	--	117	
	450 to 700	315	Fiber stress	2	Soda-lime-silica glass. No effect observed with H_2, N_2, He, or dry air atmosphere; CO_2 lowers energy slightly; SO_2 and H_2O have marked effect

(a) The entry "glass" is used in the broadest sense here in referring to materials which are, generically glasses but for which no further specifications are available, except as noted

VII. CONCLUSIONS

In the text and tables, we have attempted to summarize the available information on the surface energies of ceramics, and have found that much research is needed in order to provide a reasonably definitve collection of ceramic surface energy data.

Among the possible routes for advancement in this field, the following are recommended:

(1) Crack propagation experiments. The methods that have been developed and expanded by Gilman[20] and Westwood[21] et al., are presently applicable to a large number of materials over a temperature range where the specimens are brittle. However, where a certain degree of plasticity is involved, such as with either mobile or maneuverable dislocations, the analysis used by these authors breaks down. There are, quite generally, several different though related factors that must be included in the criterion as to whether brittle fracture occurs, among which one of the more important is consideration of the dislocation velocity along selected crystallographic planes at a given temperature. In those cases where the crack tip velocity is much greater than the dislocation velocity (either in normal glide or in climb), the material can be considered brittle and the standard analysis may be used. However, this condition may not be reached under controlled conditions at higher temperatures. It is then necessary to either develop improved experimental techniques for effecting high-speed fracture, or to develop more nearly exact theories of fracture that will accomodate ductile materials. One must use caution, however, in expending too great an effort at attempting to define and derive the necessary correction factors, inasmuch as one may rapidly reach the point where the resultant surface energy is inaccurately determined as a small difference between large terms.

(2) Thermodynamic interface experiments. It is well to recall the general problem of the use and interpretation of experiments that rely upon the properties of the solid surface in question in contact with a different phase or material. Earlier, the point was raised that the total surface energy is a summation of contributions from different types of interactions, i.e., coulombic forces, dispersion forces, metallic and ionic bonding, hydrogen bonding, and the like. Both Weyl and Fowkes have given qualitative arguments that suggest that, in the interaction between two distinct species, each having different degrees of several of these components, the total interaction will depend only upon the degree to which similar components are present. That is to say, if one material has a surface energy which is totally a result of dispersion and metallic forces and if the other is a result of dispersion and ionic forces, then the total interaction between these two would depend only upon the interaction of dispersion forces; the remaining contributions to the surface energy would be unaffected by juxtaposition.

As of the present writing, there has been no distinct quantitative argument forwarded to support this hypothesis. However, one can go somewhat further in the qualitative analysis by considering a simplified model for electronic interactions between, for example, a metal and a (defect) ceramic. In the case where the metal is situated in a vacuum, the surface energy will be a total of contributions from dispersion forces and the metallic bonding forces which are inherent to the material, in addition to any component deriving from the free (conduction) electrons. The juxtaposition of a highly insulating material provides other atoms and/or molecules which will interact via dispersion forces, however, there are no corresponding metallic-force electrons or conduction electrons available for additional interactions and the placement of the

insulator does not materially affect the electron cloud distributions of the metal, the former being essentially no different from the vacuum state. Hence, one would not expect significant interactions between the two materials over those due only to dispersion forces.

On the other hand, as the defect concentration of the insulator increases (toward the semiconducting state), free electrons are made available in a density corresponding to the defect concentration. Fermi levels, temperature, etc., which can interact with the free electrons of the metal. Hence, the electronic contribution to interfacial phenomena will increase. (It is noted, of course, that defects in sufficient density will reduce the dispersion force component of the total surface energy, so that one can expect an inflection in a hypothetical plot of total interaction energy versus defect concentration. Similarly, interdiffusion of components will be a function of the defect concentration of the insulator material and one should expect a time dependence for the total interaction energy. To this author's knowledge, no detailed investigation of these phenomena has been undertaken.)

Generally speaking, the most serious limitation to the use of thermodynamic property measurements for surface energy determinations lies in the paucity of information on the various contributions to the total surface energy. It is suggested that selected experiments can be performed where, through appropriate choices of well-characterized materials, one may be able to measure or reduce the individual components of the surface energy.

More specifically, the use of "homologous series" of liquids for the performance of the Zisman-Eberhart experiments should be evaluated. It is apparent that this technique offers considerable promise for the measurement of surface energies provided that the materials chosen conform rigidly to the constraints that must be imposed. Since there is already a vast amount of data available on the surface tensions of binary and higher order liquid mixtures as functions of composition and temperature, it seems most natural that this would provide an excellent starting point for the determination of critical surface tensions, and the concomitant derivation of the surface energy of the subetrate, particularly at "high" temperatures. This is especially attractive as a tool for the further study of surface energies at temperatures where ductility nature of the material precludes the application of the cleavage technique.

(3) Empirical Approaches. Although the semi-empirical techniques, as accredited to Bruce[53], are seriously lacking in fundamental justification, it is apparent that they may be quite useful in estimating surface energies of a number of untested materials, provided that sufficiently accurate data may be obtained on the physical properties which enter the analysis. In addition, there is an obvious need for continuing effort on the development of meaningful correlation; not only those that seem to give approximate answers but also those in which a reasonable phenomenological basis for the correlation can be established on theoretical grounds.

REFERENCES

(1) For a review of work on the critical angles of wetting, see Zisman, W. A., "Influence of Constitution on Adhesion", Ind. Eng. Chem., 55, 19 (1963).

(2) Parikh, N. M., "Effect of Atmosphere on the Surface Energy of Glass", J. Am. Ceram. Soc., 41, 18 (1956).

(3) Morey, G. W., Properties of Glass, Second Edition, American Chemical Society Monograph No. 124, Reinhold Publishing Company, New York (1954).

(4) Boni, R. E. and Derge, G., "Surface Tension of Silicates", J. Metals, 8, 53 (1956).

(5) Kantro, D. L. Brunauer, S., and Copeland, L. E., "BET Surface Areas - Methods and Interpretations", in The Gas-Solid Interface, Edited by E. A. Flood, Marcel Dekker, Inc., New York (1967), p 413 ff.

(6) Shuttleworth, R., "The Surface Tension of Solids", Proc. Phys. Soc. (London), A63, 444 (1950).

(7) Johnson, R. E., Jr., "Conflicts Between Gibbsian Thermodynamics and Recent Treatments of Interfacial Energies in Solid-Liquid-Vapor Systems", J. Phys. Chem., 63, 1655 (1959)

(8) Gregg, S. J., The Surface Energy of Solids, Reinhold Publishing Co., New York (1961).

(9) Mould, R. E., "The Strength of Inorganic Glasses", in Fundamental Phenomena in the Materials Sciences, Volume IV: Fracture, Edited by L. J. Bonis, J. J. Duga, and J. J. Gilman, Plenum Press, New York (1967), p 119 ff.

(10) Stokes, R. J., "Fracture of Ceramics", in Fundamental Phenomena in the Material Sciences, Volume IV: Fracture, Edited by L. J. Bonis, J. J. Duga and J. J Gilman, Plenum Press, New York (1967), p 151 ff.

(11) Sharpe, L. H., and Schonhorn, H., "Surface Energetics, Adhesion, and Adhesive Joints", Advan. Chem. Ser., 43, 189 (1964).

(12) See, for example, Bikerman, J. J., The Science of Adhesive Joints, Academic Press, New York (1961), p 125 ff.

(13) Weyl, W. A., "Partial Surface Energies, the Key to Adhesion", Bull. Am. Ceram. Soc., 45, 433 (1966).

(14) Fowkes, F. M., "Dispersion Force Contributions to Surface and Interfacial Tensions, Contact Angles, and Heats of Immersion", Advan. Chem. Ser., 43, 99 (1964); also "The Relation of the Attractive Forces at Interfaces to Wetting, Spreading, Adsorption, and Long-Range Attractive Forces", in Fundamental Phenomena in the Materials Sciences, Volume II: Surfaces, Edited by L. J. Bonis and H. H. Hauser, Plenum Press, New York (1965), p 139 ff.

(15) Fowkes, F. M., "Intermolecular and Interatomic Forces at Interfaces", in Surfaces and interfaces I, Edited by J. J. Burke, N. L. Reed and V. Weiss, Syracuse University Press, Syracuse, New York (1967), Chapter 8.

(16) Partington, J. R., An Advanced Treatise on Physical Chemistry, Volume III, Longmans, Green & Co., London (1952), p 242 ff.

(17) Bikerman, J. J., "Surface Energy of Solids", Phys. Stat. Solidi, 10, 3 (1965).

(18) Benson, G. C. and Yun, K. S., "Surface Energy and Surface Tension of Crystalline Solids", in The Gas-Solid Interface, Edited by E. A. Flood, Marcel Dekker, Inc., New York (1967), pp 203-269.

(19) Obreimoff, J. W., "The Splitting Strength of Mica", Proc. Roy. Soc. (London), A127, 290 (1930).

(20) Gilman, J. J., "Direct Measurements of the Surface Energies of Crystals", J. Appl. Phys., 31, 2208 (1960).

(21) Westwood, A. R. C. and Hitch, T. T., "Surface Energy of {100} Potassium Chloride", J. Appl. Phys., 34, 3085 (1963).

(22) Gillis, P. P., "Surface Energy Determinations by Cleavage", J. Appl. Phys., 36, 1374 (1965).

(23) Westwood, A. R. C. and Goldheim, D. L., "Cleavage Surface Energy of {100} Magnesium Oxide", J. Appl. Phys., 34, 3336 (1963).

(24) Berry, J. P., "Some Kinetic Considerations of the Griffith Criterion for Fracture. I. Equations of Motion at Constant Force.", J. Mech. Phys. Solids, 8, 194 (1960).

(25) Wiederhorn, S. M., "Fracture Surface Energy of Soda-Lime Glass", in Materials Science Research, Volume III: The Role of Grain Boundaries and Surfaces in Ceramics, Edited by W. W. Kriegel and H. Palmour, III, Plenum Press, New York (1966), pp 503-528.

(26) Orowan, E., "The Tensile Strength of Mica and the Problem of the Technical Strength", Z. Physik., 82, 235 (1933).

(27) Bryant, P. J., Taylor, L. H., and Gutshall, P. L., "Cleavage Studies of Lamellar Solids in Various Gas Environments", in Transactions of the Tenth National Vacuum Symposium (1963), pp 21-26.

(28) Gregg, S. J., "The Surface of Solids and its Significance for Industry and in the Laboratory", Silicates Ind., 25, 283 (1960).

(29) Brace, W. F. and Walsh, J. B., "Some Direct Measurements of the Surface Energy of Quartz and Orthoclase", Amer. Mineralogist, 47, 1111 (1962).

(30) Bowden, F. P., "The Nature and Topography of Solid Surfaces and the Study of Von Der Waals Forces in Their Immediate Vicinity: The Surface Decomposition of Solids", in Fundamentals of Gas-Surface Interactions, Edited by H. Saltzberg, J. N. Smith and M. Rogers, Academic Press, New York (1967), p 12.

(31) Gilman, J. J., "Cleavage, Ductility, and Tenacity in Crystals", in Fracture, Edited by B. L. Averbach, et al., Technology Press, MIT, and John Wiley & Sons, New York (1960), pp 193-225.

(32) Davidge, R. W. and Tappin, G., "The Effective Surface Energy of Brittle Materials", J. Mater. Sci., 3, 165 (1968).

(33) Srawley, J. E. and Brown, W. F., "Fracture Toughness Testing and its Application", NASA, TMX-52030 (1964).

(34) Nakayama, J., "Direct Measurement of Fracture Energies of Brittle Heterogeneous Materials", J. Am. Ceram. Soc., 48, 583 (1965).

(35) Berdennikov, W. P., "Messung der Oberflachenspannung von Festern Korpern", Soviet Phys. Z. S., 4, 397 (1933); Summary by Kuznetsov, Reference (35); Corrections in Reference (25).

(36) Kuznetsov, V. D., Surface Energy of Solids, Her Majesty's Stationary Office, London (1957).

(37) Kwong, J. N. S., Adams, J. T., Jr., Johnson, J. F., and Piret, E. L., "Energy - New Surface Relation in the Crushing of Solids: I. Application of Permeability Methods to an Investigation of the Crushing of Some Brittle Solids", Chem. Eng. Prog., 45, 508 (1949).

(38) Adams, J. T., Jr., Johnson, J. F., and Piret, E. L., "Energy - New Surface Relation in the Crushing of Solids: II. Application of Permeability Measurements to an Investigation of the Crushing of Halite", ibid., p 655.

(39) Johnson, J. F., Axelson, J., and Piret, E. L., "Energy - New Surface Relation in the Crushing of Solids: III. Application of Gas Adsorption Measurements to an Investigation of the Crushing of Quartz", ibid., p 708.

(40) Maringer, R. E., "Etch Pitting on Single Crystal InSb", J. Appl. Phys., 29, 1261 (1958).

(41) Gatos, H. C., Finn. M. C., and Lavine, M. C., "Antimony Edge Dislocations in InSb", J. Appl. Phys., 32, 1174 (1961).

(42) Gatos, H. C., "Dangling Bonds in III-V Compounds", ibid., p 1232.

(43) Gatos, H. C., Strauss, A. J., Lavine, M. C., and Harmon, T. C., "Impurity Striations in Unrotated Crystals of InSb", ibid., p 2057.

(44) Faust, J. W., Jr., Private Communication.

(45) Cahn, J. W. and Hanneman, R. E., "(111) Surface Tensions of III-V Compounds and Their Relationship to Spontaneous Bending of Thin Crystals", Surface Sci., 1, 387 (1964).

(46) Fiun, M. C. and Gatos, H. C., "Spontaneous Bending of Thin (111) Crystals of III-V Compounds", Surface Sci., 1, 361 (1964).

(47) Udin, H., Shaler, A. J., and Wulff, J., "The Surface Tension of Solid Copper", J. Metals, 1, 186 (1949).

(48) Nicolson, M. M., "Surface Tension in Ionic Crystals", Proc. Roy. Soc., 228A, 490 (1955).

(49) Eberhart, J. G., "The Critical Surface Tension of Sapphire", J. Phys. Chem. 71, 4125 (1967).

(50) Rhee, S. K., "Surface Tension and Interactions of Liquid Aluminum With Ceramics", Bull. Am. Ceram. Soc., 47, 745 (1968).

(51) King, T. B., "The Surface Tension and Structure of Silicate Slags", Trans. Soc. Glass Tech., 35, 241 (1951).

(52) Konskowitch, P., "Surface Tension and Viscosity of Artificial Slags", Rev. Met. (Paris), 46, 505, 572 (1949).

(53) Bruce, R. H., "Aspects of the Surface Energy of Ceramics: I. Calculation of Surface Free Energies; II. Calculation of the Average Surface Free Energy and the Effects of Some Variables", in Science of Ceramics, Volume 2, Edited by G. H. Stewart, Academic Press, London (1965), pp 359, 368.

(54) Mitra, S. S. and Sanyal, N. K., "Surface Tension-Temperature Relationship", J. Chem. Phys., 23, 1737 (1955).

(55) Bowden, S. T., "Variation of Surface Tension and Heat of Vaporization With Temperature", J. Chem. Phys., 23, 2454 (1955); see also Reference (54).

(56) Berghausen, P. E., Good, R. J., Kraus, G., Podolsky, B., and Soller, W., "Fundamental Studies of the Adhesion of Ice to Solids", WADC-TR-55-44 (1955).

(57) Lester, G. R., "Contact Angles of Liquids at Deformable Solid Surfaces", J. Coll Sci., 16, 315 (1961).

(58) Good, R. J., Girifalco, L. A., and Kraus, G., "A Theory for Estimation of Interfacial Energies. II. Application to Surface Thermodynamics of Teflon and Graphite", J. Phys. Chem., 62, 1418 (1958).

(59) Girifalco, L. A. and Good, R. J., "A Theory for the Estimation of Surface and Interfacial Energies. I. Derivation and Application to Interfacial Tension", J. Chem. Phys., 61, 904 (1957); "III. Estimation of Surface Energies of Solids From Contact Angle Data", ibid., 64, 561 (1960).

(60) Fowler, R. and Guggenheim, Statistical Thermodynamics, Cambridge University Press, Cambridge (1949), p 445 ff.

(61) Zettlemoyer, A. C., "Immersional Wetting of Solid Surfaces", Ind. Eng. Chem., 57 (2), 27 (1965).

(62) Freundlich, H., Kapillarchemie, Volume 1, Fourth Edition, Akademische Verlagsgesellschaft M. B. H., Leipzig (1930), p 218.

(63) Balk, P. and Benson, G. C., "Calorimetric Determination of the Surface Enthalpy of Potassium Chloride", J. Phys. Chem., 63, 1009 (1959).

(64) Brooks, C. S., "Free Energies of Immersion for Clay Minerals in Water, Ethanol, and n-Heptane", J. Phys. Chem., 64, 532 (1960).

(65) deBruyn, P. L., "Some Aspects of Classical Surface Thermodynamics", in Fundamental Phenomena in the Material Sciences, Volume III: Surface Phenomena, Edited by L. J. Bonis, P. L. deBruyn, and J. J. Duga, Plenum Press, New York (1966), pp 1-3[illegible].

(66) Hirschfelder, J. O., Curtiss, C. G., and Bird, R. B., Molecular Theory of Gases and Liquids, John Wiley & Sons, New York (1954), p 351.

(67) Marian, J. E., "Surface Texture in Relation to Adhesive Bonding", ASTM Materials Science Series - 4, ASTM Special Publication No. 340, p 122 (1963).

(68) Gutshall, P. L., and Gross, G. E., "Observations and Mechanisms of Fracture in Polycrystalline Alumina", in Proceedings of the National Symposium on Fracture Mechanics, Lehigh University (1967), to be published.

(69) Clarke, F.J.P., Tattersall, H. G., and Tappin, G., "Toughness of Ceramics and Their Work of Fracture", Brit. Ceram. Soc. Proc., 6, 163 (1966).

(70) Lennard-Jones, J. E. and Dent, B. M., "Cohesion at a Crystal Surface", Proc. Roy. Soc. (London), A121, 247 (1928).

(71) Huggins, M. L. and Mayer, J. E., "Interatomic Distances in Crystals of the Alkali Halides", J Chem Phys , 1, 643 (1933)

(72) Zadumkin, S. N. and Khulamkhanov, V. Kh., "A Simple Method of Calculating the Surface Energy of Ionic Crystals", Soviet Phys. -Solid State, English Transl., 5, 31 (1963).

(73) Walton, A. G., "Calculation of Ionic Crystal Surface Energies From Thermodynamic Data", J. Am. Ceram. Soc., 48, 151 (1965).

(74) See, for example, the recent review by Morabito, J. M. and Somorjai, G. A., "Low Energy Electron Diffraction: The Techniques and Its Application to Metallurgical Science", J. Metals, 20 (5), 17 (1968).

(75) See, for example, Weyl, W. A., in Structure and Properties of Solid Surfaces, Edited by R. Gomer, and C. S. Smith, University of Chicago Press, Chicago (1953), pp 147-184.

(76) Fowkes, F., "Attractive Forces at Interfaces", Ind. Eng. Chem., 56 (12), 40 (1964).

(77) Friedel, J., Cullity, B. D., and Crussard, C., "The Surface Tension of a Grain Boundary in a Metal as a Function of the Orientation of the Two Grains Which the Boundary Separates", Acta Met., 1, 79 (1953).

(78) McLeod, D. B., "On a Relation Between Surface Tension and Density", Trans. Faraday Soc., 19, 38 (1923).

(79) Siuta, V. P. and Belicki, M., "Development of a Corrosion Resistant Magnesium Alloy. Part II. Surface Tension Data of Elements", WADC Technical Report 57-241 (1957).

(80) Sikorski, M. E., "Correlation of the Coefficient of Adhesion With Various Physical and Mechanical Properties of Metals", J. Basic Eng., 85, 279 (1963).

(81) Sikorski, M. E. and Courtney-Pratt, J. S., "Adhesion of Rare Earth Metals", Amer. Soc. Lub. Engrs. Preprint 63 LC-16 (1963).

(82) Livey, D. T. and Murray, P., "Surface Energies of Solid Oxides and Carbides", J. Am. Ceram. Soc., 39, 363 (1956).

(83) Bondi, A., "The Spreading of Liquid Metals on Solid Surfaces", Chem. Rev., 52 (2), 417 (1953).

(84) Kingery, W. D., "Surface Tension of Liquid Oxides and Their Temperature Coefficients", J. Am. Ceram. Soc., 42, 6 (1959).

(85) Kingery, W. D., "Role of Surface Energies and Wetting in Metal-Ceramic Sealing", Bull. Am. Ceram. Soc., 35, 108 (1956).

(86) Perkins, R. N., Armour Research Foundation (IITRI), Report ASD-TR-61-628, Part II (April, 1963).

(87) Kingery, W. D., "Metal-Ceramic Interactions: IV. Absolute Measurement of Metal-Ceramic Interfacial Energy and the Interfacial Adsorption of Silicon From Iron-Silicon Alloys", J. Am. Ceram. Soc., 37, 42 (1954).

(88) Fricke, R., "Uber die Feinstruktur von Festkorpern mit Bauelementen kolloider Grosse und Deren Physikalische und Chemische Eigenschaften", Kolloid-Z, 96, 213 (1941).

(89) Ryshkewitch, E., Oxide Ceramics: Physical Chemistry and Technology, Academic Press, New York (1960), p 169.

(90) Wiederhorn, S. M. (Unpublished).

(91) Petch, N. J., Congleton, J., Hardie, D., and Perkins, R. N., "Study of the Brittle Behaviour of Ceramic Materials: Effect of Surface Energy", Technical Documentary Report No. ASD-TR-61-628, Parts I, II, and III (1961).

(92) Robins, D. A., "Bonding in Carbides, Silicides, and Borides", Powder Met., 1/2, 172 (1958).

(93) Bronsall, P. C., Dollimer, D., and Dollimer, J., "The Selective Effect of Adsorption on the Strength of Compacts of Various Oxides and Salts", Brit. Ceram. Soc. Proc., 6, 61 (1966).

(94) Handbook of Chemistry, 10th Edition, Edited by N. A. Lange, McGraw-Hill Book Company, New York (1961), p 1648.

(95) Benson, G. C. and Claxton, T. A., "Calculation of the Surface Energy of the {110} Face of Some Crystals Possessing the Fluorite Structure", Canad. J. Phys., 41, 1287 (1963).

(96) Brunauer, S., Kantro, D. L., and Weise, C. H., "The Surface Energies of Calcium Oxide and Calcium Hydroxide", Canad. J. Chem., 34, 729 (1956).

(97) Fricke, R., "Struktur und Verteilungsart Realer Festkorper und Katalysatoren Sowie Deren Untersuchungsmethoden", in Handbuch der Katalyse, Volume IV, Edited by G. M. Schwab, Springer Verlag, Vienna (1943), p 1; also "On the Fine Structure of Solid Substances With Colloidal-Sized Particles and Their Physical and Chemical Properties", Koll. z., 96, 211 (1941).

(98) G. E. Boyd, in Surface Chemistry, Edited by F. R. Moulton, Amer. A soc. Adv. Sci. Publication No. 21 (1943), p 128 ff.

(99) Jaeger, F. M., "Temperature Variation of Molar Surface Free Energy of Liquids in the Temperature Range 80 to 1650 C", Z. Anorg. Allgem. Chem., 101, 1 (1917).

(100) Jaccodine, R. J., "Surface Energy of Germanium and Silicon", J. Electrochem. Soc., 110, 524 (1963).

(101) Born, M. and Stern, O., "The Surface Energy of Crystals and Its Influence on Crystal Form", Sitzber. Preuss. Akad. Wiss., 48, 901 (1919).

(102) Lennard-Jones, J. E. and Taylor, P. A., "Some Theoretical Calculations of the Physical Properties of Certain Crystals", Proc. Roy. Soc. (London), A109, 476 (1925).

(103) Dent, B. M., "The Effect of Boundary Distortion on the Surface Energy of a Crystal", Phil. Mag., 8, 533 (1929).

(104) van Zeggeren, F. and Benson, G. C., "Calculation of the Surface Energies of Alkali Halide Crystals", J. Chem. Phys., 26, 1077 (1957).

(105) van Zeggeren, F. and Benson, G. C., "The Quantum Mechanical Calculation of the Surface Energy of Sodium Chloride - A First Approximation", Canad. J. Phys., 34, 985 (1956).

(106) Benson, G. C., "Recalculation of the Surface Energies of Alkali Halide Crystals", J. Chem. Phys., 35, 2113 (1961).

(107) Shockey, D. A. and Groves, G. W., "Effect of Water on Toughness of MgO Crystals", J. Am. Ceram. Soc., 51, 299 (1968).

(108) Gutshall, P. L. and Gross, G. E., "Clevage Surface Energies of NaCl and MgO in Vacuum", J. Appl. Phys., 36, 2459 (1965).

(109) Jura, G. and Garland, C. W., "The Experimental Determination of the Surface Energy of Magnesium Oxide", J. Am. Chem. Soc., 74, 6033 (1952).

(110) Boyd, G. E., "Some Aspects of the Properties of Solid Surfaces", in Surface Chemistry, Edited by F. R. Moulton, American Adv Sci. Pub No 21 (1943), p 128 ff.

(111) Benson, G. C., Schreiber, H. P., and van Zeggeren, F., "Experimental Determination of the Surface Enthalpy of Sodium Chloride", Canad. J. Chem., 34, 1553 (1956).

(112) Lipsitt, A. G., Johnson, F. M. G., and Maas, O., J. Am. Chem. Soc., 49, 1940 (1927); also ibid., 50, 2071 (1928); see also Harkins, W. D., "Energy Relations of the Surface of Solids. I. Surface Energy of the Diamond", J. Chem. Phys. 10, 268 (1942); Benson, G. C. and Benson, G. W., "Surface Energy of the Alkali Halides", Canad. J. Chem., 33, 232 (1955).

(113) Ryazantsev, P. P. and Shcherbakov, L. M., "The Effect of Comminution on the Solubility and the Heat of Solution", Kolloid-Z., 21, 464 (1959).

(114) Adamson, A. W., Physical Chemistry of Surfaces, Interscience, New York (1967), p 57.

(115) Parikh, N. M., "Effect of Atmosphere on the Surface Tension of Glass at Low Temperature", Sc. D. Dissertation, Massachusetts Institute of Technology (1953).

(116) Schellinger, A. K., "Solid Surface Energy and Colorimetric Determinations of Surface-Energy Relationships for Some Common Minerals", Mining Eng., 4, 369 (1952).

(117) Wiederhorn, S. M., "Fracture of Ceramics", Mechanical and Thermal Properties of Ceramics, Edited by J. D. Wachtman, Jr., Natl. Bur. Std. Special Publication No. 303 (1969), p 217.

(118) Boyd, G. E. and Livingston, H. K., "Adsorption and the Energy Changes at Crystalline Solid Surfaces", J. Am. Chem. Soc., 64, 2483 (1942).

(119) Basford, P. R., Harkins, W. D., and Twiss, S. B., "Effect of Temperature on the Adsorption of n-Decane on Iron", J. Phys. Chem., 58, 307 (1954).

(120) Jura, G. and Harkins, W. D., "Surfaces of Solids: XI. Determination of the Decrease of Free Surface Energy of a Solid by an Adsorbed Film", J. Am. Chem. Soc., 66, 1356 (1944).

(121) Eberhart, J. G., "The Critical Surface Tension of Uranium Dioxide", J. Nucl. Mater., 25, 103 (1968).

(122) Livey, D. T. and Murray, P., "The Wetting Properties of Solid Oxides and Carbides by Liquid Metals", in Plansee Proceedings, 1955, Edited by F. Benesovsky, Pergamon Press, Ltd., London (1956), p 375 ff.

(123) Humenik, M. and Whalen, T. J., "Physicochemical Aspects of Cermets", in Cermets, Edited by J. R. Tinklepaugh, Reinhold Publishing Co., New York (1960), p 6 ff.

(124) Beimuller, J., Z Physik, 38, 759 (1936)

(125) Glauberman, A. E., 'Theory of the Surface Energy of Heteropolar Crystals", Zh. Fiz. Khim, 23, 124 (1949).

APPENDIX A

APPLICATION OF TECHNIQUES

Table A-1 lists the various materials measured by the most commonly used experimental methods for determining solid surface energy. Table A-2 gives a similar listing for the use of theoretical methods.

TABLE A-1 PRIMARY EXPERIMENTAL TECHNIQUES AND THE MATERIALS MEASURED BY THEM

Technique	Materials Measured		
Maximum bubble pressure and similar experiments on liquids	Al_2O_3	KBO_2	NaCl
	B_2O_3	KBr	NaF
	$BiBr_3$	KCl	NaI
	$BiCl_3$	KF	$NaNO_3$
	$CdCl_2$	KI	$NaPO_3$
	CsBr	KOP_3	Na_3SO_4
	CsCl	La_2O_3	P_2O_5
	CsF	$LiBO_3$	RbBr
	CsI	LiCl	RbCl
	Cs_2SO_4	LiF	RbF
	$CsNO_3$	$LiNO_3$	RbI
	GeO_2	Li_2SO_4	$SnCl_2$
		NaBr	
Solubility and heat of solution	Ag_2CrO_4	$CaSO_4\ 2H_2O$	NaCl
	Al_2O_3	CdO	PbI_2
	$BaSO_4$	CuO	PbF_2
	CaF_2	Fe_2O_3	Sb_2O_3
	CaO	KCl	SiO_2
	CaOH	MgO	$SrSO_4$
		$Mg(OH)_2$	
Heat of immersion	Al_2O_3	NaCl	
	$Al_2O_3\ 2SiO_2\ 2H_2O$	Sodium Illite	
	$Al_2O_3\ 4SiO_2\ H_2O$	Sodium Montmorillonite	
	$BaSO_4$	SiO_2	
	C (graphite)	SnO_2	
	Calcium Illite	TiO_2	
	Calcium Montmorillonite	ZrO_2	
	GeO_2		
Work of fracture, cleavage	Al_2O_3	$K_2O\ Al_2O_3\ 6SiO_2$	
	$Al_2O_3\ 2SiO_2\ 2H_2O$	$K_2O\ 3Al_2O_3\ 6SiO_2\ 2H_2O$	
	BaF_2	LiF	
	C (graphite)	MgO	
	$CaCO_3$	NaCl	
	CaF_2	Si	
	Ge	SiO_2	
	KCl	ZnO	
Contact angles	AlN	Sapphire	TiC
	Al_2O_3	ThO_2	TiN
	CdO	TiB_2	UO_2
			ZnO

TABLE A-2. MAJOR THEORETICAL TECHNIQUES AND SOLID SURFACE ENERGIES CALCULATED BY THEM

Technique	Materials Determined		
Atomistic calculation	BaF_2	KBr	NaCl
	BaO	KCl	NaF
	BaS	KF	NaI
	BaSe	KI	RbBr
	BaTe	LiBr	RbCl
	CaF_2	LiCl	RbF
	CaO	LiF	RbI
	CaS	LiI	SrF_2
	CaSe	MgS	SrS
	CaTe	MgSe	SrSe
	CsF	NaBr	SrTe
Elastic constants	AgBr	Ge	$MgO\ Al_2O_3$
	AgCl	InS	Mg_2SiO_4
	$BaSO_4$	KBr	NaBr
	C (diamond)	KCl	NaCl
	$CaCO_3$	KI	PbS
	CaF_2	$K_2O \cdot Al_2O_3 \cdot 6SiO_2$	Si
	Fe_2O_3	LiF	TiO_2
	FeS_2	MgO	ZnS
Sublimation energy	AlAs	Cr_2O_3	InP
	Al_2O_3	FeO	InSb
	AlP	Fe_2O_3	MgO
	AlSb	Fe_2O_3-CaO	MnS
	BaS	Fe_3O_4	NaCl
	BeO	GaAs	PbS
	$CaCO_3 \cdot MgCO_3$	GaP	β-SiC
	CaO	GaSb	TiO_2
	$CaO \cdot MgO \cdot Al_2O_3 \cdot SiO_2$	InAs	
Empirical calculations	BaO	KBO_3	ThO_2
	BeO	KCl	TiC
	CaO	KF	UC
	CdO	KI	UO_2
	CsBr	MnO	VC
	CsCl	PbO	ZnO
	CsF	SrO	ZrC
	CsI	TaC	ZrO_2
	FeO		

APPENDIX B

CLASSES OF MATERIALS STUDIED

Since it is seen of value to study trends within different classes of materials, the compounds that have been studied and reported in this work are categorized into different groups. It should be noted that comparisons among different materials within a group can be misleading and caution is urged in attempting to draw correlations between values of surface energy for various members of the groups. Table B-1 lists materials by class, while Table B-2 provides a minerals cross-reference. It should be pointed out that the tables of Appendix C list materials by alphabetical order in their chemical symbols.

TABLE B-1. MATERIALS STUDIED BY PRIMARY CLASSES

Materials Class	Materials Studied		
Elements	C (graphite) C (diamond) Germanium Silicon		
Halides	AgBr	CsI	NaF
	AgCl	KBr	NaI
	BaF_2	KCl	PbI_2
	$BiBr_3$	KF	PbF_2
	$BiCl_3$	KI	RbBr
	CaF_2	LiBr	RbCl
	$CdCl_2$	LiCl	RbF
	CsBr	LiF	RbI
	CsCl	LiI	$SnCl_2$
	CsF	NaBr	SrF_2
		NaCl	
Simple oxides	Al_2O_3	Fe_2O_3	Sb_2O_3
	B_2O_3	Fe_3O_4	SiO_2
	BaO	GeO_2	SnO_2
	BeO	La_2O_3	SrO
	CaO	MgO	ThO_2
	CdO	MnO	TiO_2
	Cr_2O_3	P_2O_5	UO_2
	CuO	PbO	ZnO
	FeO		ZrO_2
Mixed oxides	Ag_2CrO_4	$K_2O \cdot Al_2O_3 \cdot 6SiO_2$	
	$Al_2O_3 \cdot 2SiO_2 \cdot 2H_2O$	$K_2O \cdot 3Al_2O_3 \cdot 6SiO_2 \cdot 2H_2O$	
	$Al_2O_3 \cdot 4SiO_2 \cdot H_2O$	KPO_3	
	$CaO \cdot MgO \cdot Al_2O_3 \cdot SiO_2$	$LiBO_3$	
	Calcium Illite	$MgO \cdot Al_2O_3$	
	Calcium Montmorillonite	Mg_2SiO_4	
	Fe_2O_3-CaO	$NaPO_3$	
	KBO_2	Sodium Illite	
		Sodium Montmorillonite	
Chalcogenides	BaS	MgS	
	BaSe	MgSe	
	BaTe	MnS	
	CaS	PbS	
	CaSe	SrS	
	CaTe	SrSe	
	FeS_2	SrTe	
	InS	ZnS	
III-V semiconductors	AlAs	GaP	
	AlN	GaSb	
	AlP	InAs	
	AlSb	InP	
	GaAs	InSb	

TABLE B-1. (Continued)

Materials Class	Materials Studied		
Carbonates, nitrates, sulphates	$BaSO_4$	$CsNO_3$	$NaNO_3$
	$CaCO_3$	$CsSO_4$	Na_2SO_4
	$CaCO_3 \cdot MgCO_3$	$LiNO_3$	$SrSO_4$
	$CaSO_4 \cdot 2H_2O$	Li_2SO_4	$ZnCO_3$
Miscellaneous	CaOH	TaC	UC
	$Mg(OH)_2$	TiB_2	VC
	β-SiC	TiC	ZrC
	Si_3N_4	TiN	

TABLE B-2. THE COMPOSITION OF MINERALS LISTED IN THE TEXT, TABLE 6[a]

Mineral	Chemical Formula
Anatase	TiO_2
Apatite	$CaF_2 \cdot 3Ca_3P_2O_8$
Barite	$BaSO_4$
Calcite	$CaCO_3$
Calcium Illite	$CaCO_3$
Calcium Montmorillonite	$CaCO_3$
Diamond	Carbon
Dolomite	$CaCO_3 \cdot MgCO_3$
Forsterite	Mg_2SiO_4
Galena	PbS
Gehlinite	$CaO \cdot MgO \cdot Al_2O_3 \cdot SiO_2$
Graphite	Carbon
Hematite	Fe_2O_3
Kaolinite	$Al_2O_3 \cdot 2SiO_2 \cdot 2H_2O$
Labradorite	$NaAlSi_3O_8 : CuAl_2Si_3O_8$
Mica	$K_2O \cdot 3Al_2O_3 \cdot 6SiO_2 \cdot 2H_2O$
Orthoclase	$K_2O \cdot Al_2O_3 \cdot 6SiO_2$
Pearl Spar	$CaCO_3 \cdot MgCO_3$
Potassium feldspar	$K_2O \cdot Al_2O_3 \cdot 6SiO_2$
Pyrite	FeS_2
Pyrophyllite	$Al_2O_3 \cdot 4SiO_2 \cdot H_2O$
Rutile	TiO_2
Sapphire	Al_2O_3
Sphalerite	ZnS
Spinel	$MgO \cdot Al_2O_3$
Sodium Illite	--
Sodium Montmorillonite	--
Topaz	$(AlF)_2SiO_4$ or $Al(F_2OH)_2SiO_4$

(a) For the most part, minerals are identified in the table of surface energy (Table 6) under their chemical formulae. There are however, some minerals listed by common name

APPENDIX C

SURFACE TENSION OF SELECTED FUSED SALTS AS A FUNCTION OF TEMPERATURE

Values for surface tension of various fused salts over a broad temperature range are available at selected temperatures from The Handbook of Chemistry[91]. The values given in the handbook have been approximately fitted here to the general relation $\gamma_L^T = k\,(1 - T/T_c)^{1.2}$, which is used widely. The constants k and T_c were calculated and tabulated in Table C-1. Note that these may be somewhat different from similar calculations listed under "Remarks" in Table 6; this discrepancy is related to the wider temperature ranges employed here.

It should be emphasized that the values of T_c are calculated only from experimental data and are not presumed to have intrinsic significance as the critical temperature (since dissociation and other effects may perturb interpretation).

TABLE C-1. CONSTANTS FOR THE EQUATION $\gamma_L^T = k(1 - T/T_c)^{1.2}$ FOR VARIOUS FUSED SALTS

Material	k	Critical Temperature, (T_c), k	Atmosphere
AgCl	175	2194	Air
$BiCl_3$	112	1161	Nitrogen
CsBr	120	2522	Nitrogen
CsCl	138	2297	Nitrogen
CsF	151	2804	Nitrogen
CsI	110	2401	Nitrogen
$CsNO_3$	128	2130	Nitrogen
$C \cdot {}_2SO_4$	163	3576	Nitrogen
KBr	135	2487	Nitrogen
KCl	147	2664	Nitrogen
$K_2Cr_2O_7$	154	6600	Nitrogen
KF	206	3141	Nitrogen
KI	116	2504	Nitrogen
KNO_3	145	2359	Nitrogen
KPO_3	220	3431	Nitrogen
K_2SO_4	201	4070	Nitrogen
$LiBO_2$	336	4472	Nitrogen
LiCl	161	3178	Nitrogen
LiF	340	3686	Nitrogen
$LiNO_3$	138	2796	Nitrogen
Li_2SO_4	275	5163	Nitrogen
NaBr	159	2683	Nitrogen
NaCl	164	3018	Nitrogen
NaF	290	3539	Nitrogen
NaI	120	2917	Nitrogen
$NaNO_3$	145	2916	Nitrogen
$NaPO_3$	249	4522	Nitrogen
Na_2SO_4	238	5502	Nitrogen
$PbCl_2$	186	2522	Air
RbBr	134	2519	Nitrogen
RbCl	154	2354	Nitrogen
RbF	191	2789	Nitrogen
RbI	124	2294	Nitrogen
$RbNO_3$	138	2313	Nitrogen
Rb_2SO_4	179	4404	Nitrogen
$SnCl_2$	132	1884	Nitrogen

Unclassified

Security Classification

DOCUMENT CONTROL DATA - R&D

(Security classification of title, body of abstract and indexing annotation must be entered when the overall report is classified)

1. ORIGINATING ACTIVITY (Corporate author) Defense Ceramic Information Center Battelle Memorial Institute Columbus Laboratories, 505 King Avenue, Cols., Ohio 43201	2a. REPORT SECURITY CLASSIFICATION UNCLASSIFIED 2b. GROUP

3. REPORT TITLE

SURFACE ENERGY OF CERAMIC MATERIALS

4. DESCRIPTIVE NOTES (Type of report and inclusive dates)

Special DCIC Report

5. AUTHOR(S) (Last name, first name, initial)

Dr. Jules J. Duga, Battelle Memorial Institute, Columbus Laboratories

6. REPORT DATE	7a. TOTAL NO. OF PAGES	7b. NO. OF REFS
June 1969	93	125

8a. CONTRACT OR GRANT NO.	9a. ORIGINATOR'S REPORT NUMBER(S)
F33615-69-C-1493 b. PROJECT NO.	DCIC Report 69-2
c. d.	9b. OTHER REPORT NO(S) (Any other numbers that may be assigned this report)

10. AVAILABILITY/LIMITATION NOTICES

[redacted]. Unlimited distribution

11. SUPPLEMENTARY NOTES	12. SPONSORING MILITARY ACTIVITY
	Air Force Materials Laboratory Materials Support Division (MAAM) Wright-Patterson Air Force Base, Ohio 45433

13. ABSTRACT

The concepts, experimental techniques, and theoretical analyses of the surface energy of solid ceramic materials are reviewed with the aim of condensing a large mass of unrelated data into a concise form for comparison and evaluation. It is shown that various experimental methods can be applied to the measurement of surface energy, but, that each of these has certain limitations which are often unstated. Furthermore, it is shown that theoretical analyses and empirical correlations, while sometimes rather imprecise, can be used to approximate surface energies, particularly as functions of temperature. While a few materials have been discussed in considerable detail (such as MgO, Al_2O_3 and some alkali halides), a review of the literature notes that there is a great paucity of information on the surface energies of many solids of interest. Improvements and extensions of experimental and empirical techniques are suggested that will help to fill the voids in the present understanding of ceramic solid surfaces, and specific analyses of experimental methods are forwarded. It is shown in the report that the proper use of thermodynamic techniques offers considerable potential for the measurement and interpretation of solid surface energies of a large number of materials that are poorly understood at present. In addition, the further development of thermodynamic methods presents an opportunity to investigate solid surface energies of nonbrittle materials, thus overcoming one of the basic limitations of the use of mechanical methods.

DD FORM 1473

Security Classification

Unclassified
Security Classification

14 KEY WORDS	LINK A		LINK B		LINK C	
	ROLE	WT	ROLE	WT	ROLE	WT
Ceramic materials						
Experimental techniques						
Glass						
Measurement						
Mechanical Properties						
Physical Properties						
Surface tension						
Surfaces, energy						
Theoretical calculations						

Security Classification